THE UNIVERSITY OF BIRMINGHAM

Department of Electronic, Electrical and Computer Engineering

Software Based Solutions for Mobile Positioning

By Sadek Hamani

PHD Thesis

June 2012

Supervisors: Dr Mourad Oussalah and Pr Peter Hall.

Abstract:

This thesis is concerned with the development of pure software-based solutions for cellular positioning. The proposed self-positioning solutions rely solely on the available network infrastructure and do not require additional hardware or any modifications in the cellular network. The main advantage of using RSS rather than timing measurements is to overcome the need for synchronisation between base stations. By exploiting the availability of RSS observations, the self-positioning methods presented in this thesis have been implemented as mobile software applications and tested in real world positioning experiments. The well-known Extended Kalman Filter can be used as a static positioning process while modeling the uncertainty in signal strength observations. The range estimation is performed using an empirical propagation model that has been calibrated using RSS measurements in the same trial areas where the positioning process is applied. In order to overcome the need for a priori maps of the GSM network, a novel cellular positioning method is proposed in this thesis. It is based on the concept of Simultaneous Localisation And Mapping (SLAM) which represents one of the greatest successes of autonomous navigation research. By merging target localisation and the mapping of unknown base stations into a single problem, Cellular SLAM allows a mobile phone to build a map of its environment and concurrently use this map to determine its position.

Table of Contents

List Of Figures

List Of Tables

Abbreviations

A-FLT	Advanced Forward Link Trilateration
AGV	Autonomous Guided Vehicle
AMF	Absolute Map Filter
AOA	Angle-Of-Arrival
AUV	Autonomous Underwater Vehicle
AVG	Autonomous-Guided Vehicle
AVL	Automatic Vehicle Location
BIM	BTS Initialization Model
BTS	Base-Transceiver Stations
CCS	Constrained Cellular SLAM
CDMA	Code Division Multiple Access
CID	Cell Identity
CPS	Cambridge Positioning System
DCM	Database Correlation Method
EKF	Extended Kalman Filter
E-OTD	Enhanced-Observed Time Difference
FCC	Federal Communication Commission
FDMA	Frequency Division Multiple Access
GIS	Geographic Information Systems
GLONASS	Global Navigation Satellite System
GPS	Global Positioning System
GTD	Geometric Time Difference
IMS	Initial Mapping Stage
IMS	Initial Mapping Stage
LBS	Location-Based Service

LDE	Landmark Database Entry
LMU	Location Measurement Units
MT	Mobile Terminal
NLF	Network Localisation Filter
NLS	Network Localisation Stage
NMR	Network Measurement Report
OTD	Observed Time Difference
PDA	Personal Digital Assistant
PMR	Private Mobile Radio
RDF	Radio Direction Finder
RP	Remote-Positioning
RSS	Received Signal Strength
RTT	Round Trip Time
SLAM	Simultaneous Localisation And Mapping
SP	Self-Positioning
TA	Timing Advance
TDMA	Time Division Multiple Access
TDOA	Time-Difference-of-Arrival
TOA	Time-of-arrival
TTF	Time-To-Fix
VOR	VHF Omnidirectional Ranging
WLAN	Wireless Local Area Networks
WSN	Wireless Sensor Networks

Chapter 1 - Introduction

Localisation is the process of finding the spatial location of a target. From ancient times to the modern era, the localisation problem was part of the art of navigation, one of the earliest subjects of scientific research. Navigation determines the position of the target as well as the course and distance it has travelled. For thousands of years, sailors relied on maps, landmarks and celestial bodies like the sun, the moon and navigational stars to navigate their ships. Instruments like the astrolabe and the compass have ancient roots and were used for early navigation methods such as celestial navigation and dead reckoning. The development of these instruments throughout medieval times and the invention of the marine chronometer[1] accelerated the Age of Discovery. Lasting from the 15th to the 17th century, this important period in the history of navigation is also known as the Age of Great Navigation as it enabled the global mapping of the world and the transition to the modern era.

The emergence of wireless communication in the end of the 19th century revolutionised the art of navigation. By exploiting the propagation properties of electromagnetic waves, the first radio direction finders appeared. During the 1930's and 1940's, more advanced radiolocation systems were developed such as Radar, VOR, Loran and Decca which were

[1] A technological breakthrough which allowed navigators to determine longitude for the first time.

used for aerial and naval navigation. With the start of space exploration, satellite-based radiolocation systems were developed beginning with TRANSIT during the 1960's followed by the Global Positioning System (GPS) and the Global Navigation Satellite System (GLONASS) during the 1970's. Nowadays, GPS is the most widely used navigation system as it made obsolete other terrestrial systems including VOR, Loran and Decca.

1.1 Radiolocation

Radiolocation systems use measurements on radio signals travelling between the target and reference stations or beacons of well-known location. Strictly speaking, the spatial locations of the target and the reference stations are points in the Euclidean space each expressed by a vector of coordinates based on a well-defined reference system. The positioning process can be applied once the geometrical relationships linking the target position to the reference points are derived from the measurements. These spatial relationships consist of range and angle parameters, which are typically estimated using signal processing techniques. Angle or bearing parameters consist of angle-of-arrival (AOA) measurements obtained using direction finding techniques. The Radio Direction Finder (RDF) was the first radiolocation system to be developed and was the primary navigation system used until the fifties when it was replaced by a more advanced bearing-based system known as the VHF Omnidirectional Ranging[2] (VOR). On the other hand, there are two types of range-based relationships:

- Absolute range relationship between the target and a single reference point, which can be derived from time-of-arrival (TOA) or received signal strength (RSS) measurements.

[2] Achieving accuracies between 100 and 500 metres, VOR became the standard navigation system used by aircrafts and is still in use today by some airports.

For instance, GPS is a TOA-based system whereas Radar uses a combination of TOA and RSS measurements.

- Relative range difference relationship linking the target to a pair of reference points, which can be derived from time-difference-of-arrival (TDOA) measurements. Typical TDOA-based systems are Loran-C and Decca.

Localisation methods using range-based and angle-based measurements are generally referred to as lateration and angulation methods respectively. This classification is based on an intuitive interpretation of the geometrical relationships rather than the specific method of computation adopted as the location estimation process. A geometrical interpretation of an absolute range relationship between a reference point and the target is a locus, which can be circular in 2-D space or spherical in 3-D space, centred at the reference point with radius equal to the range value. Trilateration is the process of finding the intersection of three circles given range measurements with respect to three reference points. Figure 1.1 illustrates trilateration in a radiolocation scenario with RF transmitters used as reference points to determine the position of the target receiver. The latter measures the signal received from the transmitters to estimate the absolute range relationship, which is biased due to measurement errors. In fact, the circles do not intersect at a single point but rather at several points which represent estimates of the target position.

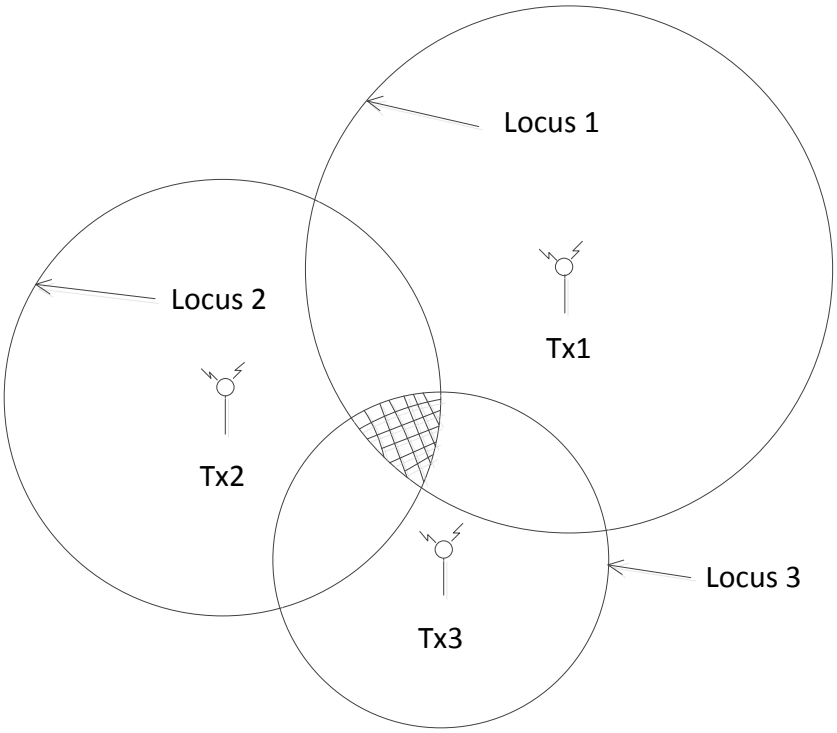

Figure 1.1 Trilateration in a radiolocation scenario

On the other hand, a range difference relative to a pair of reference points defines a hyperbola whose foci are denoted by these two reference points. In order to estimate the target position, the intersection of at least two hyperboloids is required resulting from at least three reference points. This is known as hyperbolic lateration. In Figure 1.2, two hyperboloids resulting from three transmitters are depicted. Hyperbola (1,2) is produced from a range difference measurement taken by the target receiver relative to Tx1 and Tx2, while hyperbola (2,3) is produced from a range difference measurement relative to Tx2 and Tx3.

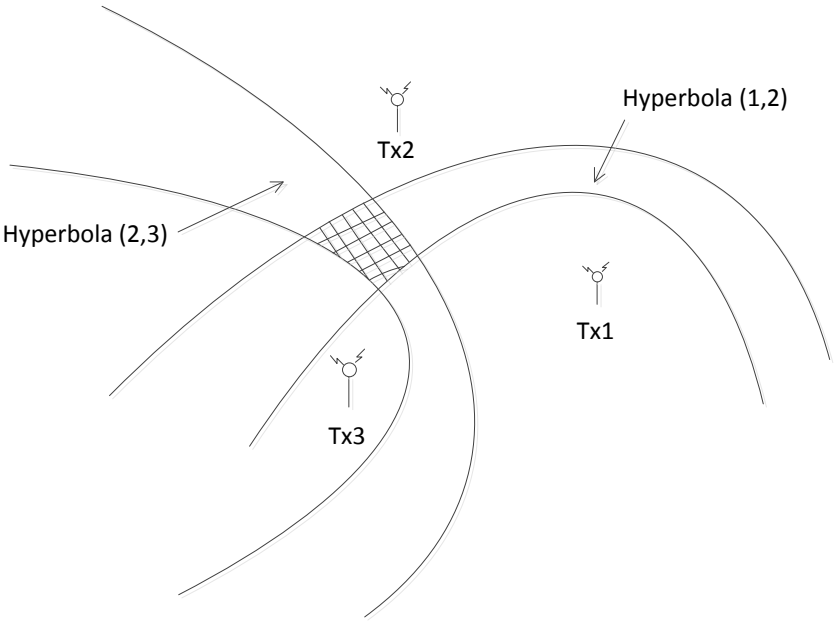

Figure 1.2 Hyperbolic lateration in a radiolocation scenario

Angle-based relationships are defined by line of bearing or radials linking the location of the target to the reference station locations. The angulation requires at least two reference points to produce two radials intersecting at the target position, as shown in Figure 1.3.

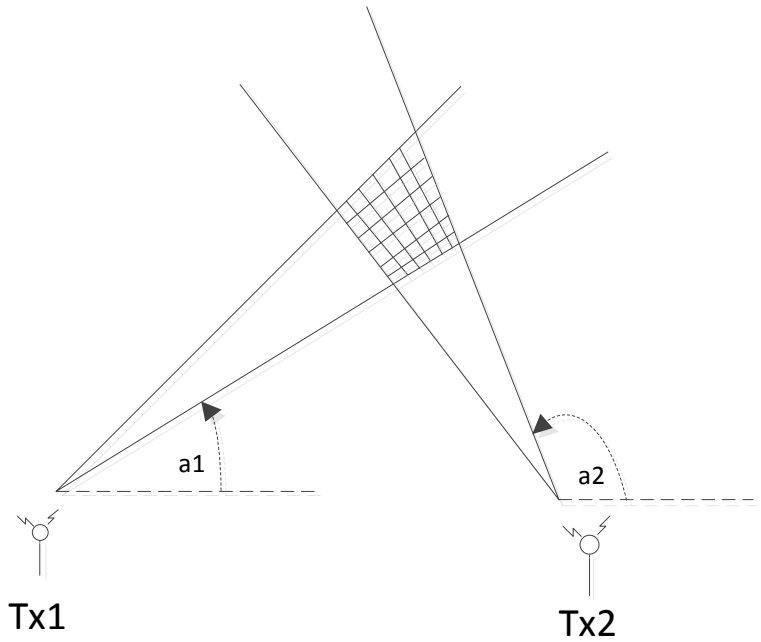

Figure 1.3 Angulation

In order to compute the target position mathematically, the measured range and/or angle values are used to solve the nonlinear equations defined by the given geometrical relationships between the target and each reference point. However, it is well known that the propagation of radio signals is subject to multipath effects, especially in non-line-of-sight situations, which corrupt all types of radio measurements. With large errors in the estimated spatial relationships simple geometrical techniques and close-form solutions are deemed inadequate for the location estimation process [Gus05][Sir07]. For this reason, radiolocation systems such as GPS [GXu03], Loran-C [Web99] and many others employed statistical methods such as least squares to solve the nonlinear equations iteratively while taking into account the errors in the measurements.

Another important aspect which can be used to classify radiolocation systems is the system's topology or architecture, which concerns where measurements are taken and processed to compute the position of the target. Two broad classifications exist: self-positioning (SP) and remote-positioning (RP) systems [Dra98]. In self-positioning systems such as GPS, Loran-C and Decca, the target includes a wireless device which receives signals from reference transmitters, performs the measurements and computes the position. In remote-positioning systems like Radar however, the processing of measurements are not performed at the target but rather at a remote location. The ability to remotely determine the location of the target expanded the domain of the localisation problem which became no longer restricted to navigation purposes but also to remote location monitoring and location-based services. In effect, remote positioning systems were used for Automatic Vehicle Location (AVL) which emerged after the advancement of radio communication technology in the mid-twentieth century.

1.2 The Emergence of Cellular Positioning

Technological breakthroughs in the mid-twentieth century such as the transistor, the integrated circuit and the microprocessor later enabled the creation of more compact, power-efficient and low-cost wireless equipment. These advancements in micro-electronics revolutionised wireless communication on one hand and boosted the research in radiolocation on the other. Parallel to the evolution of navigation systems, mobile telephony evolved from closed-group Private Mobile Radio systems (PMR) in the 1930's to high-capacity cellular networks in the 1980's. Motivated by law enforcement in the late sixties, radiolocation methods were applied for land vehicles by Automatic Vehicle Location systems (AVL) [Rit77]. As mobile terminals during the analogue era of cellular networks were mounted on vehicles, research in AVL led to the emergence of cellular positioning. The latter is defined in this thesis as the process of determining the position of a mobile terminal (MT) within a cellular network. The positioning process is applied using measurements on signals travelling between the mobile terminal and the Base-Transceiver Stations (BTS), which represent the well-known reference points.

1.2.1 AVL Origins

With the emergence of digital maps and improved Geographic Information Systems (GIS), various AVL applications were deployed in the 1980's such as fleet management, rapid response and intelligent transportation systems. A typical AVL system consists of a wireless communication system which allows a central control station to monitor the location of several vehicles in order to apply a certain decision making process. Depending on the application, AVL systems can employ either a self-positioning or remote-positioning

radiolocation system. In the former case, the localisation process is performed by a device installed on the vehicles which transfer the location information to the central control. In the latter case, the localisation process is performed by the central control using signals transmitted from the vehicles.

When GPS was made available for civilian use, the high accuracy of the positioning service was reserved to the US military. Moreover, GPS devices require clear views of the sky to receive at least four satellite signals and produce a position fix. As a result, GPS was clearly not adequate for use for AVL application at the time[3]. As a result, most AVL systems had to rely on dead reckoning measurements and some sort of radiolocation method to correct the incremental errors of dead reckoning. Some AVL companies deployed dedicated radiolocation infrastructures which were expensive, while others used existing Loran-C and Decca infrastructures, which had limited coverage and accuracy in urban areas [Sco93]. The successful deployment of analogue cellular networks in the eighties attracted the researchers within the AVL community who realised the cost-saving advantages of exploiting the nationwide cellular coverage [Sag93][She91]. In addition to providing means for voice and data communication, cellular networks also provided AVL systems with the infrastructure for implementing radiolocation techniques. As a result, AVL research linked radiolocation to mobile telephony giving birth to the field of cellular positioning, which is the main concern of this thesis.

[3] GPS was widely adopted by AVL systems when selected availability is turned off in the year 2000.

1.2.2 Wireless Enhanced-911

Inspired by radiolocation techniques implemented by radio navigation systems and AVL applications, the first cellular positioning techniques emerged as experimental systems in the early nineties. They were classified as mobile-based and network-based methods referring to self-positioning and remote-positioning methods respectively [Wan00][Dra98]. Due to the increasing number of emergency calls made from mobile phones, the Federal Communication Commission (FCC) issued the wireless Enhanced-911 mandate which required network operators in the United States to provide emergency call centres with the location of wireless callers. Accurate positioning of calls would improve response time for life threatening situations and maximise resources to handle multiple calls [ABI11]. After consulting with the wireless industry, the FCC announced that E-911will be implemented in two phases: the first required the location of the cell tower connecting the call while the second imposed strict accuracy requirements for each of mobile-based and network-based methods [Bul09]. E-911 has become the main driving force of the research and the telecommunications industry began working towards the standardisation of cellular positioning methods for both TDMA and CDMA networks. The first phase of E911 was met using the cell identification method which simply consisted of fetching the location of the base station serving the call and sending it to the emergency answering point. Due to necessary modifications either in the network or the handsets or both, the second phase was not implemented by the required deadline and was postponed many times [ABI05].

Since AOA techniques required expensive antenna arrays to be installed in base stations, TDOA techniques received the most attention among researchers [Mot01]. In order to achieve accurate positioning however, TDOA requires precise synchronisation between

base stations, accurate time delay estimation and error mitigation of multipath effects [Dra98]. As they are synchronised, CDMA networks had an advantage over GSM networks which required the installation of new network elements called Location Measurement Units to perform the timing synchronisation between base stations. By 1999, TDOA-based techniques for both CDMA and GSM networks were standardised allowing the implementation of E-911 to progress further [Mot01]. In the same time, a hybrid system called Wireless Assisted-GPS emerged as an important contender for standardisation. As it required signal reception from at least four satellites, conventional GPS suffered from long Time-To-Fix (TTF) and interrupted service in poor signal situations like in dense urban areas, indoors or under foliage. A-GPS combines TOA measurements from GPS satellites and cellular base stations in order to improve coverage and latency of conventional GPS [Sol00].

By 2009, the second phase E-911 is implemented across almost the entire United States with standardised handset-based method and network-based methods applied by CDMA and GSM networks respectively [Bul09]. Handset-based methods used by the CDMA carriers Sprint and Verison Wireless include A-GPS and the TDOA-based technique known as Advanced Forward Link Trilateration (A-FLT). Network-based methods adopted by the GSM carriers AT&T Mobility and T-Mobile USA include U-TDOA and Cell Identification [Bul09]. Despite the challenges facing its practical implementation, E-911 has been saving lives by providing rapid response to medical emergencies and stopping crimes as soon as they are reported. The main challenge consists of achieving high positioning accuracies in all types of environments. According to E-911 trials, A-GPS fails to meet the accuracy requirements indoors and in urban canyons. TDOA-based techniques perform well in all types of

environments except in rural areas where only one or two base stations can be used for positioning [ABI11].

In the same spirit as E-911, the European Community officially confirmed the use of 112 as a common emergency number and started to work towards the establishment of location-enhanced emergency services known as E-112. Unlike E-911, the E-112 project is not only faced with the cost of deploying positioning systems but also by the diversity of emergency services in the member states [Van05]. After assessing the issues facing the implementation of E-112 project, accuracy requirements were only proposed as the EU was unwilling to impose a financial burden on mobile operators and preferred waiting for GSM standards bodies to adopt a common location technology [ABI05]. Despite the standardisation of the Enhanced-Observed Time Difference[4] (E-OTD) technique through a common effort of phone manufacturers Nokia and Ericsson with Cambridge Positioning System, a bigger obstacle remained which is the cost upgrading emergency response centres throughout Europe. There is however an on-going EU project based on E112 called eCall, which aims to provide rapid assistance to motorists involved in serious accidents within the EU. A device equipped with a GPS receiver will be installed in all vehicles that will automatically dial 112 at the moment of the accident and wirelessly send impact sensor information along with the GPS position to the emergency call centre [Fil11].

[4] E-OTD was developed as a possible GSM positioning system for E-911. Due financial issues and failure to satisfy the FCC accuracy requirements, E-OTD was abandoned and the more accurate U-TDOA was adopted instead as the main method for GSM carriers.

1.3 Mobile Location-Based Services

E-911 represents the first large-scale implementation of a Location-Based Service (LBS) for mobile phones. LBS can be defined as the real-time localisation process of a mobile device in order to provide a service based on the returned location information. LBS applications which had been gaining fast popularity since the mid-nineties were telematics. Benefitting from decades of research in AVL, GIS and wireless telephony, automobile manufacturers developed telematics systems which provided customers with emergency services and navigation information based on GPS location and cellular communication.

1.3.1 Early Commercial LBS

On the other hand, the growth of commercial LBS for mobile phones had to wait for the evolution of cellular networks towards the third generation systems as well as hardware and software improvements of the mobile devices. In fact, the growth of the Internet during the nineties pushed wireless telephony to achieve high data rates and allowed GIS vendors to make digital maps available to the public as Internet-based services. In the same time, personal digital assistants (PDA's) have become capable of displaying rich colour maps and integrating a GPS unit. Deployed by the Japanese operator NTT DoCoMo in 2000, DokoNavi was the first commercial LBS which offered high accuracy positioning based on the A-GPS technology. This system consisted of a cellular mobile phone connected to a PDA with built-in A-GPS chipset which displayed the position of the user on a map [Gul03]. The refinements of wireless technology which followed shortly after enabled the creation of smartphones with enough computational power and memory to integrate GPS receivers. In the USA, while cellular network operators were implementing the positioning systems standardised for E-

911, iDEN[5] carrier Nextel[6] began offering an A-GPS system and became the leading operator offering LBS [ABI05].

In 2005, few years after introducing A-GPS phones to its customers with E-911 in mind, CDMA operator Sprint deployed a location-based service which provided customers with A-GPS phones with turn-by-turn navigation instructions from a live operator after dialling 411 [ABI05]. As for GSM networks, only AT&T deployed commercial LBS which adopted the basic cell identification technique since the more accurate network-based method U-TDOA required the installation of LMU's needed for timing synchronisation. In Europe also, CID was also the most widely used technique among GSM operators to provide LBS functionality to third-party LBS vendors such as ChildLocate and other online mobile tracking services [ABI05].

1.3.2 Software-Based Solutions

In order to compensate for the lack of accuracy of commercial cellular positioning systems and the lack of indoor or dense urban coverage of GPS, new software-based solutions emerged such as Skyhook's WPS and Intel's Placelab. These solutions exploit the expanding coverage of WLAN networks and are based on previous work in WLAN indoor localisation, also known as location fingerprinting. This concept consists of linking signal strength measurements to ground-truth location forming tuples known as fingerprints, which will be stored in a database. The fingerprinting process is performed offline in a calibration phase so

[5] iDEN is a TDMA-based technology developed by Motorola in the early nineties which lies at the intersection of trunked radio system and cellular networks network.
[6] Software developers within Nextel developed the first Java Location API's which were later published to the developer community.

that the resulting database will be used during the location estimation phase. The latter is the online phase in which the mobile terminal measures the received signal strength and searches the database for the best-matching fingerprint, whose position determines the solution. In 2001, Laitinen introduced the Database Correlation Method (DCM) which applies the fingerprinting concept for cellular networks. By exploiting the availability of RSS measurements, DCM overcomes the need for accurate timing synchronisation while coping with multipath propagation effects [Lai01].

1.3.3 The Smartphone Era

What really boosted the popularity of location-based services is the emergence of user friendly and high performance smartphones in the last half-decade. In 2007, the computing giant Apple revolutionised the smartphone industry with the release of the iPhone which was the first smartphone with a multi-touch interface. A year later, the iPhone 3G allowed the user to download mobile applications directly from the Apple AppStore via a Wi-fi internet connection or a 3G cellular network [She10]. Google later introduced Android, the first open-source operating system for smartphones which attracted several phone manufacturers ending the long domination of Symbian OS[7]. In 2008, Apple used Skyhook and Google Maps as a location-based service which combined GPS, Cellular and Wi-fi positioning[8] [Zan09]. Skyhook is currently one of the leading LBS vendors with a database including millions of Wi-fi access points and cellular base stations used as reference points for positioning [Vau09].

[7] The leadership of Symbian OS lasted since the release of the Nokia Communicator which was the first device that was called "smartphone" as it combined the functionalities of PDA's and mobile phones.
[8] Currently Apple are using their own databases for cellular and Wifi positioning, accessible by third party LBS applications.

The database is constructed through the so-called "war driving" which refers to the calibration phase of location fingerprinting and database correlation methods. The Cell Identity of cellular base stations and the MAC address of Wifi access points are associated with GPS samples gathered whilst driving.

Moreover, Software Development Kits made available to third-party developers led to the creation of a plethora of LBS applications such as turn-by-turn navigation, nearby points of interests, real-time transport information and many more [Hub09]. Some LBS application developers use databases maintained by LBS vendors while others use smaller and less accurate databases maintained by developers within the open-source LBS community using data collected by the smartphone users themselves [Ofc10]. Open source databases such as OpenSignal were created in order to enable third-party developers to access cellular network information that is not publically available, namely the location of base stations and the CID codes identifying individual transmitters.

1.4 Research Scope

Nowadays, 80% of smartphone users have LBS-type applications installed on their devices and the LBS market is predicted to exceed $12 billion by 2014 mainly from increasing application sales and mobile advertising [She10]. Despite the increasing popularity of smartphones in the last few years, they are still significantly more expensive than standard mobile phones which are referred to nowadays as feature phones [Hub09]. In addition to the high cost, the diverse functionality of smartphones comes at the cost of higher power consumption, making them less adequate for long talk times than standard mobile phones. As a result, feature phones are still being sold in higher numbers [But11].

As far as location-based services are concerned, low-cost feature phones must rely on cellular positioning alone as they are not designed to have GPS and Wifi capabilities. As a result, the need for GPS-free methods for cellular positioning is still present especially for emergency services. While the E-911 emergency services are implemented in almost the entire US territory regardless of the type of cellular handset used, Europe and other parts of the world are still not benefitting from this important public safety LBS. While not as important for smartphones, cellular positioning is the only solution available to commercial LBS for feature phones. According to Ofcom, the adopted cellular positioning method in the UK is Cell Identification which is the most basic and less accurate technique [Ofc11]. As the more accurate time-based techniques such as Uplink Time Difference Of Arrival (U-TDOA) and Enhanced Observed Time Difference (E-OTD) require the installation of expensive network elements, they have seldom been implemented by cellular network operators in Europe. As a result, new cellular positioning techniques which do not require modifications in the network infrastructure are needed, which is the main motivation driving this research.

1.4.1 Main Focus

This thesis is concerned with the development of pure software-based solutions for cellular positioning. The proposed self-positioning solutions rely solely on the available network infrastructure and do not require additional hardware or any modifications in the cellular network. Among the observable information that is inherently available within the GSM network is the Cell Identity code (CID) and the received signal strength (RSS). The former identifies the BTS antenna communicating with the mobile terminal while the latter can be used to estimate the range between the mobile terminal and the BTS. The main advantage of using RSS rather than timing measurements is to overcome the need for synchronisation

between base stations. By exploiting the availability of RSS observations, the self-positioning methods presented in this thesis have been implemented as mobile software applications and tested in real world positioning experiments.

1.4.2 Positioning Methodology

It is well known that the range between the mobile receiver and the base station transmitter can be estimated using a propagation model given signal strength measurements. As the positioning outcome depends on the accuracy of the range estimation, the errors in RSS measurements due to multipath propagation have to be taken into account by both the propagation model and the positioning process. As demonstrated by the Author in [Ham06], [Ham07] and [Ham08], the well-known Extended Kalman Filter (EKF) can be used as a static positioning process[9] which models the uncertainty in signal strength observations. Different generic propagation models were used to predict the MT-BTS range and a comparative experimental evaluation has been conducted. In the current research however, the range estimation is performed using an empirical propagation model that has been calibrated using RSS measurements in the same trial areas as the positioning experimental setup. In fact, it will be shown through experimental evaluation in this thesis that the use of the EKF with a calibrated propagation model improves the accuracy of the RSS-based estimation process as opposed to using generic models. Two static EKF models[10] are presented in Chapter 3: one using range observations and the other using range and bearing observations. Using prior knowledge of the sectorisation setup of base stations, the relative bearing angle between the

[9] The EKF model is defined here as a static positioning process meaning that the mobile terminal target is not moving while measurements are taken and the computation is performed. The process model of the EKF is in fact static.
[10] Static EKF models refer to EKF models each having a static process model.

BTS and the mobile is quantified and integrated into the EKF estimation process with the RSS-derived range observation. Without relying on Angle-Of-Arrival measurements, the angle relationship between the mobile and the BTS is approximated and deduced from the knowledge of the sectorisation setup of the BTS.

In order to be applied in real-world experimentation, these static positioning systems were implemented as a mobile software application we refer to as the "GSM Mobile Locator". Running on the Windows Mobile platform, this application applies the positioning process and displays the result on a map downloaded from the Microsoft MapPoint web service. It stores well-known BTS details on a database and allows the user to input the signal strength measurements with respect to the BTS used during the positioning experiment. RSS measurements are then translated to distance measurements using the selected propagation model among different generic models such as the Hata model and the Walfisch-Ikegami model. Chapter 5 provides the software design of the "GSM Mobile Locator" application while Chapter 6 presents the positioning experiments conducted using the application.

As they represent the positioning reference points, BTS locations must be known a priori and identified according to their associated Cell Identity Codes. In this work, BTS locations were retrieved from Ofcom's Sitefinder database[11] [Ofc12]. However, this database does not include the CID codes associated with each transmitter as such information is still restricted by mobile operators. As a result, extensive surveys[12] have been conducted to identify base stations using their associated CID codes. As the Sitefinder website is not

[11] Sitefinder is the most reliable database available to the public in the UK as the data is provided by the network operators themselves.
[12] Data collection surveys consisted of monitoring CID in the vicinity of known BTS locations and building the databases required by the software applications.

updated regularly and may not contain all transmitter locations, the CID identification of known transmitters was a laborious task particularly in dense urban areas. In fact, it is the lack of a complete and accurate map of identifiable base stations which boosted the need to extend the proposed EKF-based localisation methodology to perform the mapping of BTS locations as well as the localisation of the target mobile terminal.

1.4.3 Main Contribution

In order to overcome the need for a priori maps of the GSM network, a novel cellular positioning method is proposed in this thesis. It is based on the concept of Simultaneous Localisation And Mapping (SLAM) which represents one of the greatest successes of autonomous navigation research [Cso97][New99][Bai02][Dur06]. By merging target localisation and the mapping of unexplored environments into a single problem, SLAM allows an autonomous guided vehicle (AGV) to build a map of its environment and concurrently use this map to determine its position. The AVG can therefore be deployed without the need for an offline survey of the environment which can be a lengthy and costly process [Bai02].

The proposed cellular positioning method adopts the fundamental EKF-SLAM formalism to build a map of the cellular network and then uses this map to estimate the position of the mobile station. Similarly to feature-based SLAM methods, the term 'map' is defined in this thesis as a set of observable and identifiable landmarks or features. In the cellular network, landmarks are represented by BTS locations which are identified by the CID code allocated to each transmitter. BTS landmarks can be related to the position of the mobile terminal through relative range observations, which are derived from signal strength measurements.

In the literature, the SLAM applications for tracking mobile phones in unknown environments are based on visual tracking using images taken by built-in phone cameras [Kle09]. To the best of our knowledge, the SLAM methodology has not been applied for cellular positioning using measurements on downlink BTS signals. This is the case mainly because the problem of locating a mobile phone without BTS location information is encountered only by third party LBS developers who do not have access to restricted network information. As a result, the proposed Cellular SLAM solution for mobile phones represents the main contribution of this thesis.

Moreover, SLAM has been applied for RF-based localisation such as robot navigation problems using unknown sensor nodes in WSN [Dju05][Men09][Pat05] and localisation using unknown RFID beacon locations [Kur04] [Dju08]. These methods are known as range-only SLAM because bearing measurements are not available in their respective frameworks. Compared to range-bearing or bearing only SLAM, range-only SLAM has not been studied extensively [Kur04][Ols04]. The similarity of our approach with other range-only SLAM applications in the literature lies in the RSS-based observation model as well as the EKF-SLAM formalism of state augmentation. What characterises the proposed range-only SLAM method is that it does not rely on dead reckoning measurements like typical SLAM applications. As it implements a SLAM approach constrained by the lack of motion sensing capability, this methodology is referred to in this thesis as the Constrained Cellular SLAM (CCS). The constrained approach consists of performing the SLAM process after the initialisation of base station locations. Instead of relying on dead reckoning measurements as prior knowledge for the mobile state prediction stage of the Kalman Filter, a location

fingerprinting two-stage approach is adopted consisting of an Initial Mapping Stage (IMS) followed by a Network Localisation Stage (NLS).

The IMS is a data collection process which is performed by conducting a survey of the area surrounding each base station. The initialisation of BTS positions relies on absolute knowledge of the position of the mobile terminal as well as range measurements taken from the MT relative to the serving base station. Mobile position data can be measured using GPS while the MT-BTS range data is deduced from signal strength measurements. The IMS is similar to the calibration stage of location fingerprinting techniques as it associates with each surveyed BTS a set of mobile location fingerprints. The aim of this fingerprinting process is to enable the system to model the dynamics of the target mobile terminal during the Network Localisation Stage. The NLS is the online stage which performs the EKF-SLAM process of tracking the movement of the mobile terminal while simultaneously updating the map of base stations. In order to evaluate the performance of the proposed methodology, the CCS system has been implemented as a smartphone application running on a Symbian OS platform. The design of the software is outlined in Chapter 5 and the experimental evaluation of the system is presented in Chapter 6.

1.5 Thesis Overview

The next chapter will begin with a comparative survey of different cellular positioning techniques some of which have been standardised following the E-911 mandate. Section 2.3 will provide a brief literature review of signal strength-based radiolocation techniques which appeared in Automatic Vehicle Location research before they were applied for cellular positioning. Section 2.4 will describe the propagation model which has been adopted by the

proposed positioning systems to link the mobile terminal target estimate to the received signal strength measurements. Section 2.5 will introduce the subject of Simultaneous Localisation and Mapping and briefly describe its application in radiolocation systems.

Chapter 3 will present the static positioning system proposed in this thesis which is characterised by the use of a static Extended Kalman Filter model. The latter adopts the calibrated propagation model as the range-based observation model, as described in Section 3.3. In Section 3.4, a new approach is presented to derive bearing measurements from the sectorisation setup of GSM/UMTS base stations, which is applied by the proposed range-bearing EKF model.

Chapter 4 presents the Constrained Cellular SLAM system, which represents the main contribution of this thesis as it tackles the cellular positioning problem from a new perspective, namely mobile location estimation using unknown BTS locations. Firstly, an overview of the SLAM-based approach is described in Section 4.2. The adopted observation model which is also based on the calibrated signal strength model is described in Section 4.3. The BTS Initialisation Model responsible for initializing landmarks during the Initial Mapping Stage is described in Section 4.4, while the Network Localisation Filter responsible for applying the EKF-SLAM process during the Network Localisation Stage is described in Section 4.5.

Chapter 5 is concerned with the design of the "GSM Mobile Locator" and the Constrained Cellular SLAM mobile software applications which were used to perform the positioning trials for each of the static positioning system and the Constrained Cellular SLAM system respectively.

Chapter 6 is concerned with the experimental evaluation of the positioning systems presented in this thesis. It begins with outlining the preparation stages required to perform the positioning trials, namely the BTS identification and propagation model fitting in Section 6.2 and Section 6.3 respectively. The performance analysis of the static positioning system and the Constrained Cellular SLAM system is presented in Section 6.4 and Section 6.5 respectively. Defined in terms of positioning accuracy, the performance of the proposed systems is evaluated against other cellular positioning methods, which has been used in real life E-911 emergency services.

Finally, Chapter 7 will give concluding remarks, present possible improvements to the CCS solution and future research directions.

Chapter 2 – Background

2.1 Introduction

The problem of locating mobile terminals is inherent in the design of cellular networks. As far as mobile telephony is concerned, the location of the mobile terminal user within the network is required for mobility management procedures such as channel assignment and handover [Fren10]. The required location information is not the exact geographical location of the terminal but a set of network parameters indicating the terminal's location relative to the base stations. These parameters include the cell identity code identifying the BTS antenna, signal strength and timing measurements which are sent between the mobile terminal and nearby base stations in the form of messages. Unlike mobility management, cellular positioning aims at determining the geographical position of the mobile stations as accurately as possible in order to perform a certain decision making process [Kup05]. Using network parameters to define the geometrical relationship between the target mobile station and a set of reference base stations, different radiolocation techniques can be adopted for cellular positioning depending on the application. Multipath propagation is the greatest challenge faced by cellular positioning techniques as it corrupts the measurements producing ambiguous and inaccurate position estimates [Bla02][Fig10]. Error mitigation of multipath effects has been

studied extensively in the literature to identify multipath signals using different signal processing techniques [Ven04] [AUP06].

This chapter begins with a description of the cellular positioning techniques that have been standardised by telecommunications bodies to implement the E-911 mandate in the US. Techniques adopting cell identification, TDOA and GPS have been standardised whereas AOA and signal strength-based techniques have not been standardised due to deployment cost and performance issues respectively. While accurate AOA-based localisation requires expensive antenna arrays installed in each base station, RSS localisation depends on accurate propagation models to derive accurate estimates of the range relationship between the mobile target and reference base stations.

Applying TOA, TDOA or AOA techniques without multipath error mitigation leads to ambiguous positioning outcomes. Similarly, applying signal strength-based localisation without an appropriate empirical propagation model produces an even more ambiguous outcome due to the high variability of signal strength measurements caused by multipath effects such as fading and shadowing [Bla02]. On the other hand, the so-called location fingerprinting techniques seem to cope well with multipath propagation and the variability of RSS measurements [Lai01] [Hil00]. These techniques have been developed in the literature not only for cellular positioning but in other RF-based localisation frameworks such as WLAN and RFID [Mut09]. In fact, they are the most suitable and accurate techniques for indoor localisation [Kae05]. As discussed in Section 2.4, location fingerprinting is characterised by a two-phase approach to radiolocation, which consists of building a database of RSS measurements in an offline calibration phase before using this database to estimate location in

real-time. A brief literature review of signal strength techniques used in cellular positioning will be provided in Section 2.3.

As mentioned in the introductory chapter, this work is focused on the development of software-based solutions to cellular positioning without relying on the infrastructure required by TOA, TDOA or AOA measurements. In the same spirit as other RF-based localisation applications, the positioning methodologies proposed in this thesis take advantage of the inherent availability of RSS observations in cellular networks. An important motivation factor driving the research is the growing interest in location-based services in light of the recent technological advancement in wireless communications. Current 3G cellular networks and state-of-the-art smartphones boosted the popularity of LBS applications as they are attracting an increasing number of software developers in both the professional and amateur worlds.

The software positioning solution presented in this thesis uses an empirical propagation model to define the range relationships between the target MS and reference base stations as accurately as possible. The path loss equation of the propagation model is calibrated using real RSS measurements taken prior to the positioning process in each trial area of the positioning experimental setup. In fact, it will be demonstrated in Chapter 6 that using a calibrated propagation model as an observation model of an Extended Kalman Filter will produce more accurate positioning results as opposed to using generic propagation models. Section 2.4 introduces propagation modeling and shows how the calibrated path loss equation is derived.

As introduced previously, the main contribution of this work consists of a new solution to cellular positioning which allows third-party developers who do not have access to base station location information to perform the mapping of the cellular network prior to the

positioning process. Instead of relying on a database from a commercial LBS vendor or unreliable third-party databases, the proposed methodology allows the LBS developer to build his own map of base stations. The methodology is based on an important research subject within the robotics community known as Simultaneous Localisation And Mapping (SLAM). While chapters 4 and 5 describe the proposed Constrained Cellular SLAM system in detail, this chapter introduces the SLAM concept in Section 2.5.

2.2 Standard Cellular Positioning Methods

The first cellular positioning methods emerged in the late nineties after decades of research in Automatic Vehicle Location. Cellular networks were analogue FDMA systems at the time and most mobile terminals were mounted on vehicles. In 1989, an American AVL company TrackMobile developed one of the first AVL systems using the AMPS cellular network infrastructure as means for localisation [She91]. This system called Hawk-3000 consisted of an alarm system which automatically tracks the position of a stolen vehicle. As it provided an anti-theft service to the vehicle owner, Hawk-3000 can be considered as one of the first location-based services for vehicle-mounted cellular phones.

The phenomenal increase in the number of cellular subscribers in the eighties boosted the need for digital cellular networks mobile positioning. In 1990, the IS-54 standard, also known as D-AMPS emerged as a digital TDMA system which considerably increased capacity. In the same year, Swales et Al demonstrated the use of antenna arrays and direction finding techniques to collect Angle of Arrival measurements and triangulate the position of the mobile station [Swa90]. Following Swales's work a year later, the American company KSI conducted the first trials of the AOA positioning technique using two D-AMPS base stations

[Swa99]. Also in 1990, a year after Qualcomm demonstrated the first CDMA cellular system to mobile operators, William Sagey from Hughes Aircraft Company filed his patent entitled "Cellular telephone service using spread spectrum transmission" [Sag93]. Sagey was previously involved in the development of satellite-based AVL systems and realised the cost-saving advantage of integrating location capability into existing cellular networks based on spread spectrum technology. As the deployment of CDMA cellular networks seemed far from reach, Sagey proposed the installation of spread spectrum processors in AMPS base stations to perform the messaging required for accurate TDOA-based localisation. However, Qualcomm succeeded in standardising CDMA under the name IS-95 few years later. A cellular network based on CDMA technology is time synchronised with GPS downlink satellite signals enabling accurate timing measurements which can in turn be used for TOA/TDOA cellular positioning. FDMA and TDMA networks are not synchronised and therefore need additional network elements as initially proposed by Sagey. In 1991, the advantages of determining the position of a mobile phone were discussed by Paton et al [Pat91] and H. Hashemi [Has91]. In addition to providing AVL-like dispatch applications such as law enforcement, fleet management and emergency services, they pointed out that cellular positioning would provide solutions to mobility management issues of newly deployed TDMA networks as well as future CDMA networks.

Due to the increasing number of emergency calls made from mobile phones[13] in 1994, the FCC ordered cellular carriers to provide the emergency call centre with the geographic position of 911 wireless callers. After consulting the wireless industry, the FCC issued the

[13] In the United States, an average of 50,000 emergency calls per day were made from mobile phones in 1994.

enhanced 911 mandate (E911) in 1996 requiring operators to implement the wireless emergency service in two phases. Phase 1 consisted of providing the local Public Safety Answering Point with the caller's number as well as the coordinates of the serving base station connecting the call. Phase 2, however, consisted of improving the positioning accuracy to 125 m 67% of the time. Most of the cellular positioning methods which existed at the time were network-based methods which used Cell Identification (CID), AOA, TDOA techniques for two main reasons:

- They evolved from remote-positioning AVL systems which monitor the target from a central location.
- They were designed to work with existing handsets without making hardware modifications.

During the late nineties, the E-911 boosted the research in cellular positioning and led to the creation of mobile-based techniques which used downlink signals transmitted from the base stations to the mobile station such as Enhanced Observed Time Difference (E-OTD), Advance Forward Link Trilateration (A-FLT) and Wireless Assisted-GPS (A-GPS). As a result, the FCC revised the accuracy requirements in 1999. The accuracy required for network based methods was within 100m for 67% of the calls and 300m for 95% of the calls. For handset-based methods, the required accuracy was within 50m for the 67th percentile and 150m for the 95th percentile. E-OTD, A-FLT and OTDOA are TDOA-based methods which were standardised for TDMA (GSM, iDen), CDMA (Cdma2000) and WCDMA (UMTS) networks respectively. A-GPS however could be used across all types of networks. The methods mentioned above have been standardised for E-911 and are described next.

2.2.1 Cell Identification

Each base station transmitter in the cellular network is allocated a Cell Identity Code, or CID, in order to identify the cell area covered by the transmitter. Sectored base stations contain more than one directional antenna each with a unique CID. As its name suggests, cell identification is the process of determining the cell in which the mobile terminal is located, which is known as the serving cell. Similarly to radiolocation methods based on proximity sensing, the location of the base station illuminating the serving cell indicates the approximate location of the mobile terminal In fact, CID represents the simplest cellular positioning method as it is based solely on proximity sensing. As it does not require any modifications in the network infrastructure, CID has been used by mobile carriers in the USA to comply with the first phase of E-911, which only required the location of the serving cell[14]. The accuracy of CID as a proximity sensing method is inversely proportional to the size of the serving cell. The accuracy varies between a few tens of metres in urban areas to several kilometres in rural areas.

In order to improve the accuracy of the CID method, the gain pattern of directional base station transmitters and the Timing Advance (TA) parameter can be used. The antenna gain pattern indicates the approximate azimuth angle between the mobile and the BTS reducing the cell area covered by the BTS and thus improves the accuracy. TA, also known as adaptive frame synchronisation, is used in TDMA networks such as GSM to synchronise the transmission time of uplink signals from different mobile stations to the same serving base station [Kup05]. The aim of this technique is to ensure that uplink signals arrive at the BTS

[14] The location of the serving BTS can be determined by consulting the coverage database at the serving mobile location centre SMLC.

without overlapping with one another while minimizing the duration of guard times[15]. The technique is called timing advance as the MS advances its time of transmission according to the Round Trip Time (RTT) of the signal transmitted from the BTS to the MS and back to the BTS. The RTT is measured by the BTS which converts it to a TA value and sends the latter to the MS. According to the GSM specification, the TA value is represented by a 6 bits integer code between 0 and 63 (2^6-1). The minimum value of 0 means no timing advance while 63 refers to the maximum RTT of 233 Nano-seconds. The TA bit period is therefore 3.698 μs which corresponds to an approximate BTS-MS range of 554 metres assuming free-space propagation. Table 2.1 shows the relationship between TA values, RTT and BTS-MS range.

TA value	0	1	2	3	4
RTT (μs)	0	3.7	7.4	11.1	14.8
BTS-MS Range (m)	0-554	554-1108	1108-1662	1662-2216	2216-2770

Table 2.1 TA values and their corresponding RTT and BTS-MS range

As it provides an indication of the range between the serving BTS and the mobile terminal, the TA value can be used as a positioning method in conjunction with Cell Identification. In fact, 3GPP standardised CID+TA in 1999 in order to be used by GSM carriers in the USA for E-911 localisation [Tay05]. Due to its poor accuracy, it is currently used as a fall-back technique for E-911 when the more accurate U-TDOA technique fails to return a position estimate [Bul09]. ID+TA is the most widely adopted positioning method for commercial location-based services such as Google MyLocation, Child Locate, Trace a Mobile …etc.

[15] TDMA systems avoid interference by inserting between adjacent time slots guard times in which transmission is disallowed.

2.2.2 Enhanced Observed Time Difference (E-OTD)

Similarly to TA, the Observed Time Difference (OTD) is another parameter in the GSM specifications which can be used for cellular positioning [Sil96]. In GSM, OTD can be used to perform an optional pseudo-synchronisation procedure which improves the handover process from a serving BTS to a neighbour BTS. As GSM networks are unsynchronised, base stations do not transmit in the same time resulting in a difference of transmitting times between the serving BTS and each neighbour BTS called the Real Time Difference (RTD). When pseudo-synchronisation is supported, the mobile is constantly monitoring the OTD by measuring the time differences of bursts arriving from the serving BTS (used as reference) and neighbour base stations one of which will become the serving BTS after the handover. Before the latter is initiated, the pseudo-synchronisation allows the mobile to predict the propagation delay relative to a future serving BTS without requiring the latter to perform a Timing Advance measurement. In order to do so, the mobile requires the time difference due to the relative geometrical displacements between the mobile and the serving BTS and between the mobile and a neighbour BTS. This time difference is called the Geometric Time Difference (GTD) and is defined as the difference between the OTD and the RTD times as follows:

$$GTD=OTD-RTD \tag{2.1}$$

For synchronised networks like CDMA, base stations transmit at the same time so there is no RTD and thus GTD coincides with OTD. GTD can be considered as a TDOA measurement for unsynchronised networks as it produces a range difference between the target MS and a pair of reference base stations and thus defines a hyperbolic relationship between the target and the reference points. As the case with TA, the time resolution of 1 bit coincides with 554 metres of propagation distance. The OTD as a hyperbolic positioning method was

investigated by Nokia following the E-911 mandate. After conducting trials in 1998, the positioning accuracy of 125 metres required for E-911 was not met mainly due to the low accuracy in the timing measurement.

However, an improvement to the OTD method was standardised in 1999 under the name Enhanced-OTD, based on a system developed by the Cambridge Positioning System (CPS) called the Digital Cursor system [Duf96]. E-OTD consists of installing extra receivers within the network called the Location Measurement Units (LMU) in order to contribute to the location estimation process and overcome the need to process TDOA measurements (or OTD in the case of GSM) at the mobile station. Instead, E-OTD relies on synchronised LMU's capable of accurately measuring the Time-Of-Arrival of signals transmitted from different base stations. Consider a base station n (BTS_n) communicating with both the mobile terminal and a single Location Measurement Unit (LMU_m). Let T_L be a TOA measurement taken against the internal clock of LMU_m with bias ε_L, T_B be the broadcast transmission time from BTS_n and c as the speed of light, the range between BTS_n and LMU_m, denoted here by R_{BL} reads as:

$$R_{BL} = c\,(T_L - T_B + \varepsilon_L) \qquad (2.2)$$

Let T_M be the TOA measurement taken by the mobile terminal against its internal clock with bias ε_M on the signal transmitted by the same base station BTS_n at time T_B. This second TOA measurement results in a second range relationship between the mobile target and BTS_n defined by R_{BM} as follows:

$$R_{BM} = c\,(T_M - T_B + \varepsilon_M) \qquad (2.3)$$

Taking the range difference by subtracting (2.2) and (2.3) cancels out the broadcast transmission time T_B and results in a common synchronisation error Ɛ as follows:

$$R_{BM} - R_{BL} = c\,(T_M - T_L + \mathcal{E}) \qquad (2.4)$$

In the range difference expression (2.4), only the position of the mobile target and the synchronisation error are unknown. Given at least 3 range difference equations for 3 base stations and a single LMU, a 2-d position can be computed by trilateration.

After the successful trials of the CPS Digital Cursor system in 1996, the E-OTD method attracted wireless manufacturers including Ericsson, Nokia and Siemens to implement the required software changes in the handsets and GSM network operators in the USA, namely Cingular (currently AT&T Mobility) and T-Mobile to adopt E-OTD as the standard method for E-911 Phase II. Despite reasonable accuracies achieved during several trials, E-OTD suffered from the need for compatible handsets which delayed the implementation of E-911. As a result, the largest GSM carriers abandoned the method by the end of 2003 [ABI05] and adopted the network-based method developed by TruePosition known as Uplink-TDOA, which is described next.

2.2.3 U-TDOA

Delivering more accurate positioning than E-OTD without requiring handset modifications, the Uplink-TDOA has been standardised by 3GPP for use by GSM carriers in the USA to comply with Phase 2 of the E-911 mandate [Tay05]. Since its first deployment by the LBS vendor TruePosition, U-TDOA has been used as the primary method for positioning the 911 call and in case of failure, the CID+TA is used as a fall back method [Bul09]. As its name suggests, U-TDOA uses the uplink signals transmitted from the mobile phone and received by

synchronised Location Measurement Units which are typically installed at the base transceiver stations. Using the serving BTS as reference, cross correlation techniques are applied to measure TDOAs between pairs of receiving LMU's. The TDOA measurements are sent to a processor which converts them into range differences and applies a hyperbolic multi-lateration algorithm to determine the position of the target MS. U-TDOA proved to satisfy the accuracy requirements of E-911 Phase 2 and represents the success of GSM positioning in the USA as it saved many lives according to real-life E-911 case studies. Its major drawback in terms of accuracy and availability is the so-called hearability problem encountered in rural areas where less than the required three base stations are within reach of the mobile terminal resulting in poor GDOP.

2.2.4 Advanced Forward Link Trilateration

This method is the fallback method used by CDMA-based networks for E-911 when A-GPS fails to return a position fix or is unavailable in case the handset is not equipped with an A-GPS chipset. A-FLT has been standardised by the CDMA standard Committee as a handset-based method in 1999 [Tay05]. The location estimation is performed by the mobile terminal using the downlink signals transmitted from CDMA base stations which are synchronised using GPS reference time. The inherent synchronisation allows for accurate TDOA measurements between pairs of base stations, which define the range differences required for hyperbolic localisation.

2.2.5 Assisted-GPS

Before selective availability was turned off in 2000, the conventional GPS satellite navigation system available for civilian use suffered from low accuracy, limited availability and low

latency (long time-to-fix). In the late 1980's, the British security company Securicor[16] developed their own localisation system known as Datatrak[17] to monitor cash-in-transit fleets [Ban89]. Using a network of low frequency transmitters operating on a TDMA arrangement, Datatrak applied TDOA-based hyperbolic localisation which achieved accuracies between 20 and 50 metres. Being more accurate than the restricted GPS service at the time, Datatrak became popular in the 1990's and was offered to British emergency services including the police, ambulances and fire services [Ban91].

Motivated by E-911 and the refinements in the GPS chipset design in the mid-nineties, American company based in California called Snaptrack developed a hybrid technology called Wireless Assisted GPS. In order to improve the performance of the GPS service available for civilian use, A-GPS combines TOA measurements on signals transmitted from GPS satellites with TOA measurements on signals transmitted from cellular base stations. After processing the measurements, the wireless device equipped with an A-GPS chipset sends the information to a server within the cellular network which is responsible for the location estimation process. As the server is equipped with a powerful computer, the network assistance reduces the time-to-fix (TTF). However, the location estimation can also be performed by the handset similarly to conventional GPS, at the expense of increased battery consumption and TTF.

Snaptrack's novel technology attracted Motorola and Texas Instruments as equity investors and was put to trial by US carriers as a potential E-911 Phase 2 solution and by other

[16] In 1985, Securicor helped BT build the first cellular network in Britain (TACS).
[17] Siemens took over Securicor's Datatrak division in the year 2000 and have since been providing the Datatrak system to telematics companies such as Aplicom [SAR00].

operators and LBS vendors in the USA, Europe and Japan. Using A-GPS enabled PDA's made by Denso and after extensive field tests since 1997, the largest Japanese cellular network NTT DoCoMo launched the world's first high performance[18] location-based service in 2000 called "DokoNavi" [Gul03]. While conventional GPS was performing poorly in Tokyo's urban areas, DokoNavi allowed the user to see the estimated location on a map displayed on the PDA within 20 metre of the true position. In the same year, Snaptrack became a Qulacomm subsidiary and selective availability was turned off by the US government further improving the accuracy of A-GPS, which became known under Qualcomm's trade name 'GpsOne'. After the first mobile phones with built-in A-GPS capability were produced, CDMA carriers adopted A-GPS as the main method to comply with E-911 Phase 2 requirements. As A-GPS may fail in indoor environments, A-FLT is used as a fallback technique to return the position of the emergency call.

2.3 Signal Strength-Based Techniques

As introduced previously, TrackMobile developed the first AVL system which used cellular base stations as reference transmitters for radiolocation in 1989. In order to avoid any changes in the network infrastructure[19] required for timing measurements, this vehicle alarm system implemented a positioning method based on RSS measurements on the downlink signals from the base stations to the mobile terminal mounted inside the vehicle. Upon intrusion, the latter sends RSS measurements relative to at least four base stations to a central computer which

[18] Only a handful of commercial location-based services were available at the time, most of them using basic cell identification for positioning [ABI05].
[19] The major network deployed in the USA at the time was the analogue FDMA-based AMPS network.

converts them to ranges and applies a circular lateration algorithm. The latter is a simple geometrical method which uses the intersection of at least four circles to determine the target position. The range estimation is based on the simple inverse-square law formula [She91]. Without taking into account the large errors in the RSS measurements due to multipath propagation, the positioning outcome was deemed very inaccurate [Hil00].

In 1994, Frederick Leblanc adopted the concept of storing RSS measurements taken at different distances and directions relative to the base station in a database in order to model the coverage of the BTS as a "scaled contour shape" [Leb96]. In order to determine the location of the mobile terminal, LeBlanc proposed matching real-time RSS measurements relative to base stations with their corresponding contours and finding their intersection. The concept of linking ground-truth location with RSS measurements and storing the information in a database dates back to 1969, when Figel et Al presented an Automatic Vehicle Location system based on signal attenuation [Fig69]. This concept would later become known as location fingerprinting and become extensively used in both cellular and Wi-fi positioning. Typically, location fingerprinting methods are based on a two-phase approach.

- A calibration phase is conducted offline to collect all the data necessary to form the so-called fingerprints and store them in a database. The fingerprints include at least RSS measurements taken next to ground-truth and may contain other signal characteristics such as the ID of the reference beacons.
- A location estimation phase applies some sort of correlation algorithm to associate real-time RSS measurements and other signal characteristics to the fingerprints in the database in order to determine the target location.

After the E-911 mandate was issued, Oliver Hilsenrath and Mati Wax from U.S Wireless Corp. developed a network-based location fingerprinting system called RadioCamera. While other time-based techniques aim at identifying and removing multipath signals before applying the positioning process, RadioCamera uses signal characteristics including multipath patterns to determine the target position [Hil00]. The location estimation process of RadioCamera is based on the correlation of real-time signal characteristics with signal signatures or fingerprints stored in the database during the calibration phase of the system. A single base station is required for location estimation but needs to have an antenna array installed. The fingerprints are collected by the BTS which receives the signal transmitted from the mobile phone inside a vehicle while driving the roads within the coverage area of the BTS. This would later become known as war-driving, although using the downlink signals instead of the uplink signals. In 1998, U.S Wireless tested their system in the Baltimore area demonstrating that it meets and exceeds the FCC accuracy requirements for E-911 Phase 2. However, this location fingerprinting method was not standardised mainly due to the need for installing expensive antenna arrays, which is the same problem the AOA technique faced despite the fact that it was one of the earliest of all cellular positioning techniques.

In around the same time in Japan, LBS vendor Locus Corp deployed the so-called personal locator systems for PHS cellular networks. The method they adopted was known as Enhanced Signal Strength due to the fact that it is more robust than standard RSS based lateration methods in the sense that they cope with multipath propagation effects. The database of fingerprints is collected using a propagation prediction tool which uses terrain information, antenna characteristics and a propagation model to simulate the coverage of base

stations. Enhanced Signal Strength worked both indoors and outdoors achieving mean accuracies of 40-50 metres [Kos00].

In 2001, Laitinen et Al introduced the Database Correlation Method (DCM), a location fingerprinting method which estimates the position of a GSM mobile phone using RSS measurements on the downlink signals [Lai01]. The fingerprint database was constructed using real RSS measurements in a dense urban environment (Helsinki, Finland). A correlation algorithm is used to extract the best matching fingerprint, whose position is taken as the estimate, based on the nearest neighbour data association method. The latter consists of comparing the real time measurements against the calibrated measurements using the Euclidean Norm as a metric to find the closest fingerprint in signal strength space[20]. The accuracy achieved by DCM as mentioned in [Lai01] is shown in table 2.2.

Table 2.2 DCM accuracy

Environment	**Rms 67%**	**Rms 90%**
Urban	44 m	90 m
Suburban	74 m	190 m

Given the signal strength measurement Y taken by the mobile terminal and one of the fingerprints belonging to the ith BTS p_{r_i}, the Euclidean distance function d_{yi} is defined as:

$$d_{yi} = \sqrt{\left(Y - p_{r_i}\right)^2} \qquad (2.5)$$

[20] A WLAN localisation system known as RADAR adopted a similar correlation algorithm to find the best matching fingerprint [Rad00].

The accuracy of the DCM method depends on the resolution of the fingerprint database and performs better in indoor and dense urban areas [Lai01]. The resolution refers to the spread of fingerprint samples across the trial area which depends on the sampling frequency of the fingerprinting process. In order to achieve the high accuracies Laitinen relied on an extensive calibration phase which collected thousands of fingerprints in a relatively small areas.

DCM caught the attention of other researchers in the cellular positioning community who usually use the acronym DCM to refer to location fingerprinting applied to cellular positioning as opposed to WLAN fingerprinting for instance.

2.4 Propagation Modelling

Location estimation based on signal strength measurements depends on propagation models to derive range relationships between reference base stations and the target mobile station. As they predict the propagation properties of radio signals, propagation models have been used by cellular network operators to predict the coverage of base stations and plan the network layout. The main parameter predicted by propagation models which provides an indication on the distance between a transmitter and a receiver is the path loss. The latter measures the signal attenuation or the amount of signal strength reduction while travelling from the transmitter to the receiver. Expression (2.6) describes the path loss L as the ratio of the transmitted power P_t to the received power P_r using the logarithmic scale.

$$L(dB) = 10log\left(\frac{P_t}{P_r}\right) = P_t(dB) - P_r(dB) \qquad (2.6)$$

As shown in expression (2.6), when P_t and P_r are expressed in decibels, the path loss is simply their difference. Typically, the well-known power law model, also known as the log-distance

model, is used to describe the path loss in terms of the distance between a transmitter and a receiver as follows:

$$L = 10\alpha log(d) + \beta \quad (2.7)$$

Where:

- L is the path loss measured in decibels.
- d is the BTS-MS distance measured in kilometres.
- α is known as the path loss exponent which is found empirically to depend on antenna heights and other environmental parameters.
- β is the model's intercept which consists of the predicted loss at the reference distance of 1 km. It is also referred to as the absolute loss value.

Expression (2.7) is the simplest form of the propagation model function with only two parameters in addition to the distance, namely the path loss exponent α and the absolute loss intercept β. Other generic models however define these two parameters using functions of other environmental parameters such as frequency, antenna heights and multipath attenuation factors.

Generic empirical propagation models such as Hata-Okumura, Walfish-Ikegami and many others were developed by conducting extensive path loss measurements in different environments [Sau07]. An appropriate path loss function based on the log-distance model is tuned to the measurements using least squares-based parameter estimation techniques. As far as network rollout is concerned, path loss model calibration is typically the starting point, whether in a new frequency band or in a new environment, before they are integrated within network planning tools [Sau07]. The path loss fitting process minimises the mean and

standard deviation of the error between the path loss measurements and their predicted counterparts produced by the calibrated model function. In fact, the goodness of the fitting process is typically assessed using the path loss error standard deviation of the differences between the measured and predicted path loss values. According to Saunders and Aragon-Zavala in [Sau07], a well-fitted path loss model for macrocell base stations may achieve an error standard deviation of between 3 and 8 decibels. [Sau07] also discusses the impact of measurement inaccuracies on the path loss fitting process.

As introduced previously, the positioning systems proposed in this thesis employ EKF-based algorithms, in which the range-based observation model handle received signal strength measurements. The observation model link RSS observations to the position of the mobile terminal using a propagation model expressed in log-distance form as follows:

$$P_r = P_t - \beta - 10\alpha log(d) \qquad (2.8)$$

As the transmitted power P_t varies from a base station site to another, it is considered by the adopted propagation model as part of the absolute loss value parameter β and thus expression (2.8) is rewritten as:

$$P_r = \beta - 10\alpha log(d) \qquad (2.9)$$

Expression (2.9) represents the RSS-based model function to be calibrated. The following outline describes the least squares process which fits the model described in (2.9) to RSS and BTS-MT distance measurements.

Given a dataset obtained by collecting i data sample pairs (d_i, P_{ri}) comprising of the distance as the independent variable $d_i$and the signal strength as the dependent variable P_{ri}, the least square fitting process computes the parameters α and β as follows:

$$\binom{\beta}{\alpha} = (H^T H)^{-1} H^T s \tag{2.10}$$

Where:

- s is the vector of signal strength measurements of the form
  - $s = \begin{pmatrix} P_{r1} \\ P_{r2} \\ \vdots \\ P_{ri} \end{pmatrix}$ (2.11)
- H is the Jacobian matrix of the model function (2.8) which is expressed below:
  - $H = \begin{bmatrix} 1 & -10\log(d_1) \\ 1 & -10log(d_2) \\ \vdots & \vdots \\ 1 & -10log(d_i) \end{bmatrix}$ (2.12)

As the Walfish-Ikegami model resulted in the most accurate distance estimation in [Ham06], it has been used here to initialise the path loss exponent α and absolute loss intercept β before the least squares fitting process is applied. The experimental procedure to collect the measurement dataset and the results of the fitting process are outlined in Section 6.3.

2.5 Simultaneous Localisation And Mapping:

Simultaneous Localisation And Mapping, or SLAM is one of the greatest successes of robotics research. In fact, SLAM represents the key to achieve autonomous navigation as it makes an Autonomous-Guided Vehicle (AVG) truly autonomous. SLAM applications exploit the sensor fusion of using internal sensors to predict the target vehicle's motion and external sensors to

take measurements relative to surrounding landmarks and update the predicted target position. The position of each observed landmark is estimated using the AVG's position in order to build a map of the environment. The position estimates of the target and surrounding landmarks are updated simultaneously.

The EKF is the most common mathematical tool used to implement the SLAM process [Dur06]. EKF-SLAM consists of maintaining the state of the AVG and the map of estimated landmark states as part of a joint state vector. A typical AVG retrieves deduced reckoning measurements from internal sensors to estimate its position. The uncertainty in the estimation increases over time with the error accumulation of motion measurements. The SLAM process consists of the data fusion of these deduced reckoning measurements with absolute observations relative to reference points in the environment, known as landmarks or features [Bai02]. Absolute measurements relative to landmarks are taken using external sensors and consist of range and/or bearing measurements. As they are initially unknown, landmark locations must be estimated using the AVG's pose[21] and absolute measurements. When they are observed for the first time, landmarks are typically initialised using range and bearing observations and their locations are integrated into the state vector which represents the map. This process is known in the SLAM literature as landmark registration [Bai02] or Landmark extraction [Wil01][Kim04]. Correct data association is required to identify future observations associated with registered landmarks, whose positions have already been initialised and integrated into the state vector. In fact, when they are associated with landmarks that are already registered in the map, new measurements are used in the EKF update step to improve

[21] In robotics, the pose of a target consists of its position and orientation.

the AVG pose estimate and thus reduce the uncertainty accumulated from incremental motion measurements.

In 1990, Smith, Self and Cheesman introduced the notion of the *stochastic map* which later became the foundation of what is known as the EKF-SLAM method [Dur06]. In their landmark paper [SSC90], Smith et Al proposed the use of the Kalman Filter as a state space model to estimate the stochastic map. The latter consists of a state vector containing the robot's pose augmented with the locations of landmarks and its associated covariance matrix maintaining the uncertainties of the estimates and their correlations. They argued that observations are taken as nominal values with errors that can be estimated and thus can be assumed to be Gaussian distributed. As spatial relationships are in practice non-linear, they proposed the use of the extended Kalman filter to model the motion of the robot and integrate measurements taken relative to surrounding landmarks.

In the full EKF-SLAM approach, also known as the Absolute Map Filter [New99], the entire map of landmarks maintained in the state vector will also be updated which increases the correlations between the error estimates maintained in the covariance matrix. Moreover, the covariance update step of the EKF increases the complexity and computational effort of the estimation process as more landmarks are integrated into the state vector. With increasing correlations and computation times, it was initially assumed that the estimated landmark errors within the covariance matrix would not converge and researched focused on reducing or eliminating the correlations between them [Dur06]. However, these correlations were proven to be crucial for the consistency as well as the accuracy of the estimation [Cso97]. As a result, researchers turned to reducing the computational effort of the state covariance matrix update step and many methods were proposed [Wil01][Kim04][Gui02].

In 2002, Kantor and Singh proposed a range-only SLAM method for robot navigation using radio beacons as landmarks [Kan02]. In typical range-bearing SLAM applications, the robot can estimate the position of a landmark using a single measurement from its sensors combining the range and bearing observations relative to the landmark. In range-only SLAM however, a single range observation results in a circular locus around the mobile robot and thus the landmark cannot be accurately initialised and registered within the map. The range-only SLAM problem has seen an increasing interest in wireless sensor networks in the last decade. In order to cope with the lack of bearing measurements, different landmark initialisation methods have been proposed in the literature. Some of these approaches use delayed initialisation of landmarks, which rely on batch processing to estimate the position of the radio beacon after the wireless device has travelled a certain distance. An example of delayed landmark initialisation is the sliding batch technique adopted by Dereth Kurth in [Kur04]. The latter combines the EKF-SLAM approach with non-linear optimisation of the beacon landmark estimate based on the Gauss-Newton algorithm. Another range-only SLAM method using non-linear least–squares approach has been implemented by Newman and Leonard for a Sub-Sea SLAM application which allows an autonomous underwater vehicle (AUV) to navigate using submerged transponders with no prior knowledge of their locations [New03]. On the other hand, more advanced techniques have been proposed which achieve un-delayed beacon initialisation in which landmarks are initialised from the very first range measurement. For instance, Merino et Al adopted a multiple hypothesis approach which represents the non-Gaussian probability distribution of the beacon landmark state using Gaussian Mixtures Models [Mer10].

CHAPTER 3 - Static Cellular Positioning Using EKF Models

3.1 Introduction

As introduced previously, this work is focused on using the available infrastructure to estimate the position of the target mobile terminal without any modifications in the GSM network. As described in Chapter 2, an empirical propagation model has been developed to estimate the distance between the BTS transmitter and the mobile receiver using the available received signal strength (RSS) measurement. As BTS positions are the reference points in the cellular positioning process, RSS observations taken at the mobile are translated to range observations relative to the base stations. This chapter is concerned with the use of the Extended Kalman Filter (EKF) for static cellular positioning using a known map of base stations and signal strength measurements. Similarly to a recursive least squares algorithm, a static EKF model is adopted for the estimation of the mobile terminal position. Due to the nonlinear nature of RSS measurements, the EKF provides an optimal estimation technique

which models the uncertainty of the observation and reduces the mean square error of the estimate. The advantage of using an EKF based approach compared to other nonlinear optimization techniques is to recursively estimate the position of the mobile terminal each time a new measurement becomes available. Moreover, RSS observations can be processed individually to improve the performance of the EKF in terms of computation time and robustness. In fact, the proposed positioning system consists of a sequential Kalman Filter with a static process model and a nonlinear observation model.

In order to evaluate the performance of the proposed positioning method, real-world experiments have been conducted and they are presented in Chapter 6. Extensive surveys have been conducted as part of this work to create a database storing the details of several base stations including the position, the CID and the transmitted power level. This database is used by the "GSM Mobile Locator" software application implementing the static positioning method presented in this chapter. Using this mobile application in the experimental setup described in Chapter 6, the localisation process is activated from a reference location measured using GPS in order to evaluate the result. All network observations relative to surrounding base stations are taken from the trial reference position by monitoring the history of the network measurement report. Once the BTS is identified using the CID code, the application extracts its position coordinates from the database and applies the positioning process. Like any radiolocation method, the accuracy of the positioning result depends on the number of measurements taken from distinct base stations.

This chapter presents two versions of the proposed static EKF method. The first adopts a range-only observation model whereas the second expands the observation model to take into account bearing measurements. In this discussion, the former is referred to as the

range-only model and is presented in Section 3.3 while the latter is referred to as a hybrid range-bearing model and is presented in Section 3.4. Both positioning systems share the same static process model, which is presented in Section 3.2. They both also rely on the path loss model described in Section 2.4 to relate RSS measurements to the state of the mobile terminal. In order to obtain bearing information from the mobile terminal relative to the BTS position, the hybrid range-bearing EKF relies on the knowledge of the sector configuration of the observed BTS.

As stated in Section 2.1, Angle of Arrival measurements require modifications in the GSM network and thus they are not used in this framework. Recall that sectorisation consists of installing multiple directional antennas at the base stations. Each antenna represents a sector, which is assigned a unique Cell Identity code for identification. According to our surveys, network operators allocate similar CID codes to sectors belonging to the same base station. This similarity can be noticed, for instance, when only one digit of the CID differs between neighbouring sectors. As a result, the observed CID allows us to identify which sector is communicating with the mobile. If the orientation of each BTS sector is known, one can deduce an approximate bearing measurement relative to the BTS. Rather than relying on the knowledge of the exact orientation of BTS sectors, we will rely on a common sectorisation setup used by network operators in urban areas to derive the bearing measurement.

3.2 The Static EKF Model

The static model of the Extended Kalman Filter presented in this section is based on the Author's work presented in [Ham06] and [Ham08]. In this thesis however, the state of mobile terminal is parameterised by Cartesian coordinates rather than geodetic coordinates (latitude and longitude) in order to reduce the non-linearity of the observation model. In [Ham05] and [Ham06], different generic path loss models were used by the EKF positioning process. The Walfish-Ikegami model produced range estimations which led to the most accurate positioning results. In this work however, the calibrated propagation model described in Section 2.4 is adopted by two EKF models as a range-based observation model. In both EKF models, the path loss observation is integrated directly into the EKF algorithm, whereas the positioning systems in [Ham06] and [Ham08] require the intermediate step of converting the path loss into a range observation. This intermediate step is deemed necessary due to the complex path loss equation of empirical models such as the Hata model or the Walfish-Ikegami model [Sau07]. As it provides a simplified path loss expression, the calibrated propagation model is adopted by the EKF models presented in this chapter in order to predict the path loss measurement using the estimated range between the MT and the BTS. In order to improve the accuracy of the range estimation, the adopted path loss model has been calibrated using RSS measurements prior to the positioning trials. The model fitting campaigns were conducted in the same areas as the positioning trials. It will be demonstrated in Chapter 6 that the use of a calibrated path loss model as an observation model of an EKF estimation process improves the accuracy of the measurement prediction and consequently the positioning result.

This section outlines the structure of the static EKF methodology which is shared by both the range-only model and the range-bearing model presented in sections 3.3 and 3.4 respectively.

Let $X_m(k)$ be the true state of the mobile terminal at any time instant *k*. Using some global reference frame *F*, the MT and all the base stations used in the positioning process are parameterised in Cartesian coordinates. At time k, the estimate of the mobile state has the form:

$$\hat{X}_m(k) = \begin{pmatrix} \hat{x}_m(k) \\ \hat{y}_m(k) \end{pmatrix} \tag{3.1}$$

Where $\hat{x}_m(k)$ and $\hat{y}_m(k)$ are the easting and northing coordinates respectively with respect to the reference frame F. The mobile terminal is assumed to be stationary while observing surrounding base stations. Thus, the EKF employs a stationary process model of the form:

$$\hat{X}_m^-(k) = \hat{X}_m^+(k-1) \tag{3.2}$$

As shown in expression (3.2), the prediction step takes the previous a posteriori estimate $\hat{X}_m^+(k-1)$ as the current a priori estimate $\hat{X}_m^-(k)$. Consequently, the propagation of the state covariance matrix is:

$$P_m^-(k) = P_m^+(k-1) \tag{3.3}$$

Because of the static nature of the process model, the operation of the EKF is synchronized with the measurements taken from the mobile position relative to the base stations. The time increment k is therefore synchronized with the input of a new measurement which triggers the EKF update cycle to produce the a posteriori estimate of the state. The measurement innovation is the only contribution in the EKF estimation process as the prediction stage has

no effect on the state. The next prediction cycle, as shown by expressions (3.2) and (3.3), will simply take the updated state and its covariance as a priori estimates.

Let n be the number of base stations hearable from the position of the mobile to be estimated. The measurement associated with each BTS consists of the tuple (CID,RSS) which is retrieved from the network measurement report received by the MT. The CID identifies each base station and allows the system to extract its position and transmitter power. For sectored base stations, the sector used for communication is supposed to be known.

A rational application of the principle of insufficient reason consists of initializing the state of the mobile terminal using a convex combination[22] of the BTS locations. In most cases, when the mobile terminal is communicating with three or more base stations, its position lies within the area surrounded by the base stations (within the convex hull of the points representing the BTS positions). Given the position of the i^{th} base station in easting and northing coordinates x_b^i and y_b^i relative to the frame *F*, the state can be initialised as follows. If the base stations are chosen to contribute equally to the initialization of the state, then the mean of all base station locations is taken as the initial estimate *X(0)*, that is:

$$X(0) = \begin{pmatrix} \frac{1}{n}\sum_{i=1}^{n} x_b^i \\ \frac{1}{n}\sum_{i=1}^{n} y_b^i \end{pmatrix} \qquad (3.4)$$

[22] Defined in convex geometry as a linear combination of points where all coefficients are non-negative and sum up to 1. For example, the centre of gravity of a polygon is a convex combination of the polygon's vertices where all coefficients are equal. The area formed by the polygon can be formally defined as a convex hull of the vertices, that is, the smallest convex set containing the polygon's vertices.

In this case, the initial estimate of the mobile position $X(0)$ in expression (3.4) coincides with the centre of gravity of the polygon formed by the points representing the BTS locations. More formally, $X(0)$ is a convex combination of the BTS positions (x_b^i, y_b^i), where all coefficients are equal to $\frac{1}{n}$.

Alternatively, the state can be initialised using a weighted mean of the BTS locations. We can follow the strong trend that the mobile terminal is closer to the base station yielding the smallest path loss. In this respect, the state can be initialised as follows:

$$X(0) = \begin{pmatrix} \frac{1}{\sum_i^n w_i} \sum_{i=1}^{n} w_i x_b^i \\ \frac{1}{\sum_i^n w_i} \sum_{i=1}^{n} w_i y_b^i \end{pmatrix} \qquad (3.5)$$

The weight w_i in (3.5) for the i[th] BTS position can be the inverse of its associated path loss measurement L_i taken at the mobile terminal, that is $w_i = \frac{1}{L_i}$.

As the errors on the x and y coordinates are initially uncorrelated, the initial covariance matrix associated with the state estimate is the following diagonal matrix:

$$P(0) = \begin{bmatrix} \sigma_{x(0)}^2 & 0 \\ 0 & \sigma_{y(0)}^2 \end{bmatrix} \qquad (3.6)$$

The error in the initial state estimate is assumed to be the typical error of the Cell Identity proximity sensing method. Recall from Chapter 2, that this method consists of retrieving the position of the serving BTS and use it as the target location estimate. The error associated with the estimate is relative to the size of the cell coverage area of the base station. Depending on the environment and the type of antenna communicating with the MT, this error can vary

from a few tens of metres to hundreds of metres in urban environments and to kilometres in rural environments. As the experimental setting of the proposed system is within an urban environment of medium density, a standard deviation of 500 metres is used to initialize the state covariance matrix.

Once the state and its associated covariance are initialised, the EKF algorithm iterates through the list of n base stations and sequentially updates the state estimate using the measurement associated with a single BTS at a time. The observation model used in the update step of the proposed static EKF model has the form:

$$Y_i(k) = h\big(X_m(k)\big) + w(k) \qquad (3.7)$$

Where:

- $Y_i(k)$ is the true measurement associated with the ith observed BTS taken at time k from the true position of the mobile terminal $X_m(k)$.
- h is a nonlinear model function which links the true state $X_m(k)$ to the true measurement so that it can be used to predict the measurement $\hat{Y}_i(k)$ given an estimate of the state $\hat{X}_m(k)$.
- $w(k)$ accounts for the error pervading the real measurement $Y_i(k)$ as well as the error of the observation model h predicting the measurement $\hat{Y}_i(k)$. It is assumed to be Gaussian distributed with mean zero and known covariance matrix R.

Note that the observation model described in (3.7) is a generic expression of the observation shared by both EKF models presented in this Chapter. It is used for the purpose of outlining the EKF update cycle of the proposed positioning method. In the range-only EKF described in Section 3.3, expression (3.7) describes the path loss measurement. In the range-bearing EKF

described in S ection 3.4 however, the term $Y_i(k)$ in expression (3.7) consists of the measurement vector containing both the path loss and bearing observations.

When the observation of the i[th] base station is retrieved at time k, the function h predicts the measurement using the current mobile estimate $\hat{X}_m^-(k)$ and the BTS position B_i as follows:

$$\hat{Y}(k) = h\left(\hat{X}_m^-(k), B_i\right) \tag{3.8}$$

As the case of the Kalman filter, the prediction of the measurement is based on the assumption that the measurement noise w_k is Gaussian distributed with mean zero and known covariance matrix R. The difference between the real measurement (3.7) and its predicted counterpart (3.8) defines the measurement innovation *v(k),* that is:

$$v(k) = \hat{Y}(k) - Y(k)$$

In order to update the state and its associated covariance, the EKF relies on the linear approximation of the observation model around the current state estimate $\hat{X}_m^-(k)$. The underlying Jacobian matrix has the form:

$$H(k) = \frac{\partial h}{\partial \hat{X}_m^-(k)} = \left[\frac{\partial \hat{Y}(k)}{\partial \hat{x}_m^-(k)} \quad \frac{\partial \hat{Y}(k)}{\partial \hat{y}_m^-(k)}\right] \tag{3.9}$$

The constructed Jacobian matrix is then used to compute the innovation covariance $S(k)$ and the filter gain $K(k)$ as shown below:

$$S(k) = H(k)P_m^-(k)H(k)^T + R(k) \tag{3.10}$$

$$K(k) = P_m^-(k)H(k)^T S(k)^{-1} \tag{3.11}$$

The EKF model uses the measurement innovation and the Kalman Filter gain to update the state and its associated covariance as follows:

$$X_m^+(k) = X_m^-(k) + K_m(k)v(k) \quad (3.12)$$

$$P_m^+(k) = (I - K(k)H(k))P_m^-(\mathrm{k}) \quad (3.13)$$

3.3 Range-Only EKF model

This section is concerned with the range-only EKF model which relies on received signal strength measurements (RSS) and the propagation model described in Section 2.4 to estimate the state of the mobile terminal. As stated previously, the measurement update cycle proceeds sequentially to process the measurement relative to one BTS antenna at a time. The RSS measurement is therefore a scalar measurement which can be expressed as follows:

$$Y_r(k) = p_r^i = h_r\big(X_m(k)\big) + v_r(k) \quad (3.14)$$

Where:

- p_r^i is the received signal strength observed by the mobile terminal relative to the i^{th} base station denoted by $\mathrm{BTS}^{\mathrm{i}}$.
- h_r is the range-only observation model which consists of the path loss equation (2.8) from the adopted propagation model.
- $v_r(k)$ is the zero-mean Gaussian noise pervading the signal strength measurement.

Using the range between the known BTS position B_i and the current estimate of the mobile state $\hat{X}_m^-(k)$, the nonlinear function h_r predicts the path loss measurement according to the adopted propagation model as follows:

$$\hat{Y}_r(k) = h_r\left(\hat{X}_m^-(k), B_i\right) = \beta - 10\alpha\ log\left(\sqrt{\left(x_b^i - \hat{x}_m^-\right)^2 + \left(y_b^i - \hat{y}_m^-\right)^2}\right) \qquad (3.15)$$

α and β in expression (3.15) are the propagation model parameters denoted in (2.8). α represents the path loss exponent while β represents the absolute loss value which takes into account the loss at the reference distance of 1 km as well as the transmitted power of the BTS.

The innovation representing the contribution of the path loss measurement to the estimation of the state at time k reads as:

$$v_r(k) = \hat{Y}_r(k) - Y_r(k) \qquad (3.16)$$

The Jacobian matrix of the measurement prediction function h_{ro} is constructed as follows:

$$H_r(k) = \frac{\partial h}{\partial \hat{X}_m^-(k)} = \left[\frac{\hat{Y}_r(k)}{\partial \hat{x}_m^-(k)} \quad \frac{\hat{Y}_r(k)}{\partial \hat{y}_m^-(k)}\right] \qquad (3.17)$$

The partial derivatives of the predicted loss with respect to the mobile's easting and northing coordinates are computed below:

$$\frac{\partial \hat{Y}_r(k)}{\partial x_m} = \frac{c\,(x_b - x_m)}{(x_b - x_m)^2 + (y_b - y_m)^2} \qquad (3.18)$$

$$\frac{\partial \hat{Y}_r(k)}{\partial y_m} = \frac{c\,(y_b - y_m)}{(x_b - x_m)^2 + (y_b - y_m)^2} \qquad (3.19)$$

The constant c in expressions (3.18) and (3.19) is denoted below:

$$c = \frac{\beta}{\ln(10)}$$

The sequential operation of the EKF treats measurements as scalars and therefore avoids matrix inversion during the computation of the filter gain (3.11) as the innovation covariance is also a scalar. The latter is in fact the variance of the path loss measurement which is expressed in (3.10). The model then proceeds to the state update and covariance update equations expressed in (3.12) and (3.13) respectively.

3.4 Range-Bearing EKF Model

The system presented in this section is an improvement of the range-only model described in the previous section. As it expands the observation model to take into account bearing measurements, this model performs better in terms positioning accuracy as it will be shown in chapter 6. Similarly to the range-only EKF model, this hybrid positioning system is a sequential Kalman Filter which reads range and bearing measurements from one BTS antenna at a time to estimate the state of the mobile terminal. Let h_{rb} be the observation model linking the true state of the mobile terminal to the hybrid range-bearing measurement as follows:

$$Y_{rb}(k) = \begin{pmatrix} Y_r(k) \\ Y_\theta(k) \end{pmatrix} = h_{rb}\big(X_m(k)\big) + v_{rb}(k) \qquad (3.20)$$

In expression (3.20), the real measurement vector is decomposed into the path loss measurement $Y_r(k)$ and the bearing measurement $Y_\theta(k)$. Thus, the measurment noise $v_{rb}(k)$ is also a vector comprising the error associated with the path loss measurement $v_r(k)$ as well as the error associated with the bearing measurement $v_\theta(k)$, that is:

$$v_{rb}(k) = \begin{pmatrix} v_r(k) \\ v_\theta(k) \end{pmatrix} \qquad (3.21)$$

The two noise components in (3.21) are uncorrelated and assumed to be Gaussian distributed with mean zero. Hence, the measurement noise $v_{rb}(k)$ has a covariance matrix of the form:

$$R(k) = \begin{bmatrix} R_r(k) & 0 \\ 0 & R_\theta(k) \end{bmatrix} \quad (3.22)$$

Where $R_r(k)$ and $R_\theta(k)$ represent the variance-covariance attached to the range and bearing measurements, respectively.

Therefore the hybrid observation model h_{rb} of 3.20 encompasses the path loss model function h_r and the bearing model function h_θ as follows:

$$Y_r(k) = h_r(X_m(k)) + v_r(k) \quad (3.23)$$

$$Y_\theta(k) = h_\theta(X_m(k)) + v_\theta(k) \quad (3.24)$$

Note that the path loss observation model h_r is exactly the same as the observation model adopted by the range-only EKF expressed in (3.14) and defined by the propagation model function of (3.15). The second part of the measurement, denoted by $Y_\theta(k)$ with subscript θ, is the bearing measurement whose dynamics are modeled by the nonlinear function h_θ. As described in (3.24), the function h_θ predicts the bearing measurement assuming that the associated error is Gaussian distributed with mean zero. In order to define the bearing observation model h_θ, we will first explain how bearing information can be inferred from the knowledge of the sectorisation setup of base stations. Section 3.4.2 will then outline how the bearing measurement is fused with the path loss measurement and integrated into the EKF positioning process. As the latter relies on the linear approximation of both the range and bearing observation models, the underlying Jacobian matrix has the form:

$$H_{rb}(k) = \begin{bmatrix} H_r(k) \\ H_\theta(k) \end{bmatrix} = \begin{bmatrix} \frac{\partial h_r}{\partial X(k)} \\ \frac{\partial h_\theta}{\partial X(k)} \end{bmatrix} \quad (3.25)$$

The submatrix $H_r(k)$ is the result of the linear approximation of the path loss model h_r with respect to the current mobile state estimate. $H_r(k)$ is in fact the Jacobian of the range-only observation model described in the previous section, which is constructed in expression (3.17) and computed in (3.18) and (3.19)). On the other hand, $H_\theta(k)$ is the Jacobian of the bearing observation model function h_θ and is computed in section 3.4.3.

3.4.1 Sectorisation-based bearing measurement:

Instead of using the AOA technique, we propose a method which relies on the knowledge of the sectorisation setup of the observed BTS to induce bearing measurements relative to the mobile terminal. As the BTS-MT bearing cannot be measured directly, the only available information pointing to the relative BTS-MT displacement is the orientation of the BTS sector. Assuming that the observed base station has the common configuration illustrated in Figure 3.1, we can deduce an approximate bearing observation once we identify which sector is communicating with the mobile terminal.

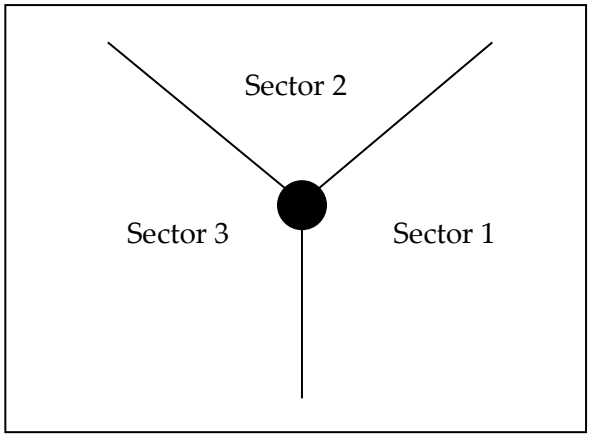

Figure 3.1 BTS sectorisation setup

Since the available bearing information is the identified sector itself, a practical approach to quantify the bearing measurement is to create a ternary representation of the base station. In fact, the actual bearing measurement used in the EKF estimation process can be described as a vector containing three variables representing the 3-sectored BTS. Thus, the bearing observation model described in (3.24) is rewritten as:

$$Y_\theta(k) = \begin{pmatrix} I_1(k) \\ I_2(k) \\ I_3(k) \end{pmatrix} = h_\theta(X_m(k)) + v_\theta(k) \qquad (3.26)$$

I_i *(with i=1 to 3)* represent the sector indicator variables with subscript 'i' denoting the number of the sector communicating with the mobile as shown in Figure 3.1. The adopted ternary representation consists of allocating each indicator variable one of the following ternary set of values: {0, 0.5, 1}. As it will be described in Section 3.4.2, these values are chosen to coincide with the values of the Heaviside step function in order to allow the observation model h_θ to predict the measurement. The following outline explains how the bearing measurement is derived from the observed CID codes and the history of the network measurement report (NMR).

Recall that the network measurement report lists all the communication channels sorted according to the value of the received signal strength. The BTS antenna transmitting the strongest signal is the first in the NMR list and is chosen as the serving BTS. The first task needed to obtain a bearing measurement is to identify the sectored base stations communicating with the mobile using the observed CID. The omnidirectional BTS antennas are not taken into account by this hybrid positioning system. Once sectored base stations are identified in the NMR, the second task consists of observing the channels pointing to sectors of the same BTS site by recognising the similarity between the CID codes. If the NMR

contains only a single sector from each BTS site, inferring the bearing measurement for each BTS is straight forward. In this case, each BTS will have a bearing vector containing a sector indicator variable of value 1 and two indicator variables of value 0. If two similar CID's are detected from the NMR, then we monitor their corresponding channel entries to check for the possibility that the mobile is located at the intersection of the two cells. For example, consider the following scenario:

Assume that the first two channel entries in the NMR correspond to sectors of the same base station. We will refer to the first entry as the serving sector and the area it covers as the serving cell. Similarly, we will refer to the second entry as the neighbour sector and the area it covers as the neighbour cell. Walking away from the trial reference position, we observe the signal strength associated with each of the sectors. The aim is to check whether the serving sector maintains the highest RSS value until we have covered a distance of at least 200 metres. If the serving sector maintains its first position in the NMR, then we can assume that the mobile is located closer to the centre of the serving cell. On the other hand, if the mobile terminal switches to the neighbour sector after we have walked a distance of less than 100 metres, then we can assume that the mobile is located closer to the intersection area between the two cells. As a result, a value of 0.5 is given to both sectors in the measurement vector $Y_\theta(k)$ of (3.26). The input of the bearing measurement will be clarified in Chapter 6.

According to the adopted representation of the bearing observation, the actual measurement is an indication that the true relative BTS-MT bearing is an angle within the 120^o interval corresponding to the BTS sector communicating with the mobile terminal. In fact, the real bearing measurement described in (3.26) can be expressed as:

$$Y_\theta(k) = \begin{pmatrix} I_1(k) \\ I_2(k) \\ I_3(k) \end{pmatrix} = h_\theta\big(\theta(k)\big) + v_\theta(k) \qquad (3.27)$$

$\theta(k)$ represents the true relative bearing between the BTS position and the true state of the mobile terminal. As it is a function of the displacement between the transmitter and the receiver, $\theta(k)$ is referred to here as the displacement bearing and can be described as:

$$\theta(k) = \vartheta(X_m(k), B_i) \qquad (3.28)$$

Where:

- B_i is the known position of the ith observed BTS.
- ϑ is the nonlinear function describing the true BTS-MT displacement bearing.

Substituting $\theta(k)$ in (3.27) with expression (3.28) will allow the observation model h_θ to relate the measurement vector to the state of the mobile terminal. In fact, h_θ becomes a composite function which lends itself to expression (3.26) as it can be rewritten as:

$$Y_\theta(k) = h_\theta\big(\vartheta(X_m(k), B_i)\big) + v_\theta(k) \qquad (3.29)$$

3.4.2 Bearing Measurement Prediction

During the estimation process, the EKF iterates through the list of base stations updating the state of the mobile terminal at each step using the range and bearing measurements. Once, the state is initialised, the position of each observed BTS is retrieved from the database according to its corresponding CID. As stated previously, the latter also identifies which of the three sectors is communicating with the mobile so that the appropriate bearing measurement vector $Y_\theta(k)$ is constructed. In order to take into account the contribution of the bearing observation in the estimation process, the EKF relies on the observation model function h_θ to predict the bearing measurement in its ternary representation as follows.

$$\hat{Y}_\theta(k) = \begin{pmatrix} \hat{I}_1(k) \\ \hat{I}_2(k) \\ \hat{I}_3(k) \end{pmatrix} = h_\theta\left(\hat{\theta}(k)\right) \tag{3.30}$$

It is important to note that the measurement prediction of (3.30) is based on the assumption that the noise $v_\theta(k)$ pervading the bearing measurement in (3.27) is Gaussian distributed with mean zero and variance $R_\theta(k)$. The term $\hat{\theta}(k)$ in expression (3.30) is the predicted BTS-MT displacement bearing which allows the model function h_θ to identify the sector communicating with the mobile terminal and thus produce the corresponding prediction of the measurement vector $\hat{Y}_\theta(k)$. As described in (3.28), the relative BTS-MT bearing is a function of the mobile state and the position of the BTS which is assumed to be a perfect measurement. Therefore, the nonlinear function ϑ in expression (3.28) can be used to predict the BTS-MT displacement bearing using the estimate of the mobile state at time instant k as follows:

$$\hat{\theta}(k) = \vartheta\left(\hat{X}_m^-(k), B_i\right) \tag{3.31}$$

By substituting $\hat{\theta}(k)$ with expression (3.31), the measurement prediction function h_θ of (3.30) lends itself to the observation model described in (3.29) assuming that $v_\theta(k)$ is the zero-mean Gaussian noise:

$$\hat{Y}_\theta(k) = \begin{pmatrix} \hat{I}_1(k) \\ \hat{I}_2(k) \\ \hat{I}_3(k) \end{pmatrix} = h_\theta\left(\vartheta\left(\hat{X}_m^-(k), B_i\right)\right) \tag{3.32}$$

Using the a priori estimate of the mobile state $\hat{X}_m^-(k)$ and the position of the ith base station B^i, the relative BTS-MT bearing is predicted first before it is translated into the bearing measurement vector $\hat{Y}_\theta(k)$. Figure 3.2 illustrates this bearing value predicted by the function ϑ expressed in (3.31).

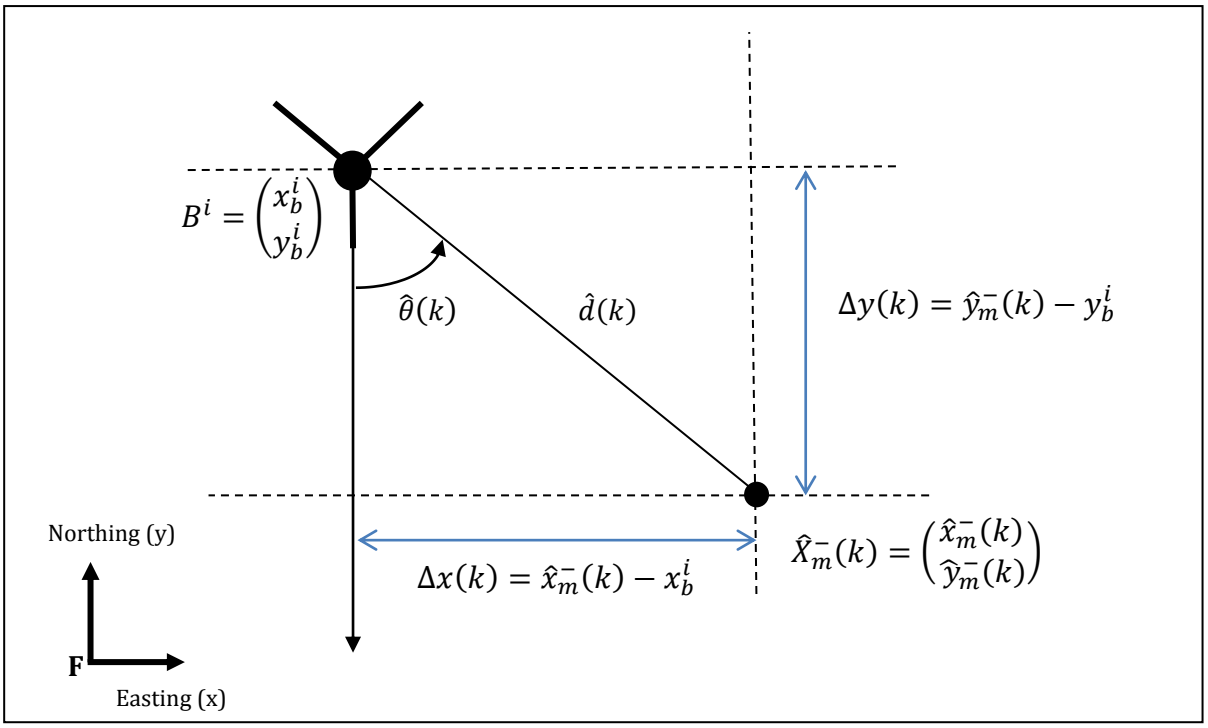

Figure 3.2 The Predicted Bearing Value

As stated previously, the BTS position and the mobile state are parameterised by Cartesian coordinates of some global reference frame F. Recall that this Cartesian space represents a topological chart resulting from the map projection of the earth's surface using the ellipsoid orthographic perspective. As shown in Figure 3.2, the angle $\hat{\theta}(k)$ results from the displacement of the mobile terminal with respect to the BTS position within the global frame F. In fact, the function ϑ described in (3.31) and (3.32) can predict the angle $\hat{\theta}(k)$ using the displacement along the easting axis $\Delta x(k) = \hat{x}_m^-(k) - x_b^i$ and the displacement along the northing axis $\Delta y(k) = \hat{y}_m^-(k) - y_b^i$. Thus, as the easting and northing displacements are functions of the mobile state as well as the BTS position, the bearing prediction function ϑ of (3.31) can also be expressed as:

$$\hat{\theta}(k) = \vartheta(\Delta\hat{x}(k), \Delta\hat{y}(k)) \qquad (3.33)$$

It is important to note that the function ϑ should map the relative BTS-MT displacement defined by $\Delta\hat{x}(k)$ and $\Delta\hat{y}(k)$ to a unique angular value of $\hat{\theta}(k)$. As it is measured in radians, this angle is bounded within the interval $[0, 2\pi[$. Therefore, the function ϑ can be defined in topological terms as a transition function that provides the homeomorphism between the Cartesian space of the global chart F and a local chart $\mathbb{C}$. The latter is defined by a local Cartesian coordinates system whose origin is the BTS position B^i. In order to coincide with the sectorisation setup of figure (3.1), the x-axis of $\mathbb{C}$ is parallel to the northing axis of F with positive values in the south direction. On the other hand, the y-axis is parallel to the easting axis of F with positive values in the east direction. Similarly to the azimuth in a polar coordinate system, the angle $\hat{\theta}(k)$ is measured between the mobile position and the origin with respect to the x-axis in the anticlockwise direction. As a result, the chart $\mathbb{C}$ can be defined as the set of points forming a disk with the BTS position B^i as origin and the Euclidean distance $\hat{d}(k)$ as radius. In order to compute the BTS-MT bearing $\hat{\theta}(k)$, the function ϑ links the global and local charts as illustrated in Figure 3.3.

Let the mobile position be defined by the Cartesian coordinates (x_s, y_s) in the local chart $\mathbb{C}$. The function ϑ transforms the global northing displacement $\Delta y(k)$ into x_s and the easting displacement $\Delta x(k)$ into y_s. The subscript s is added to differentiate between the local coordinates of the mobile and its global coordinates expressed in the state vector (3.1). As B^i is the origin of the local coordinate system, thus $x_s = \Delta y(k)$ and $y_s = \Delta x(k)$. With the radius being $r_s = \sqrt{{x_s}^2 + {y_s}^2} = d(k)$, then $x_s = d(k)\cos\left(\hat{\theta}(k)\right)$ and $y_s = d(k)\sin\left(\hat{\theta}(k)\right)$.

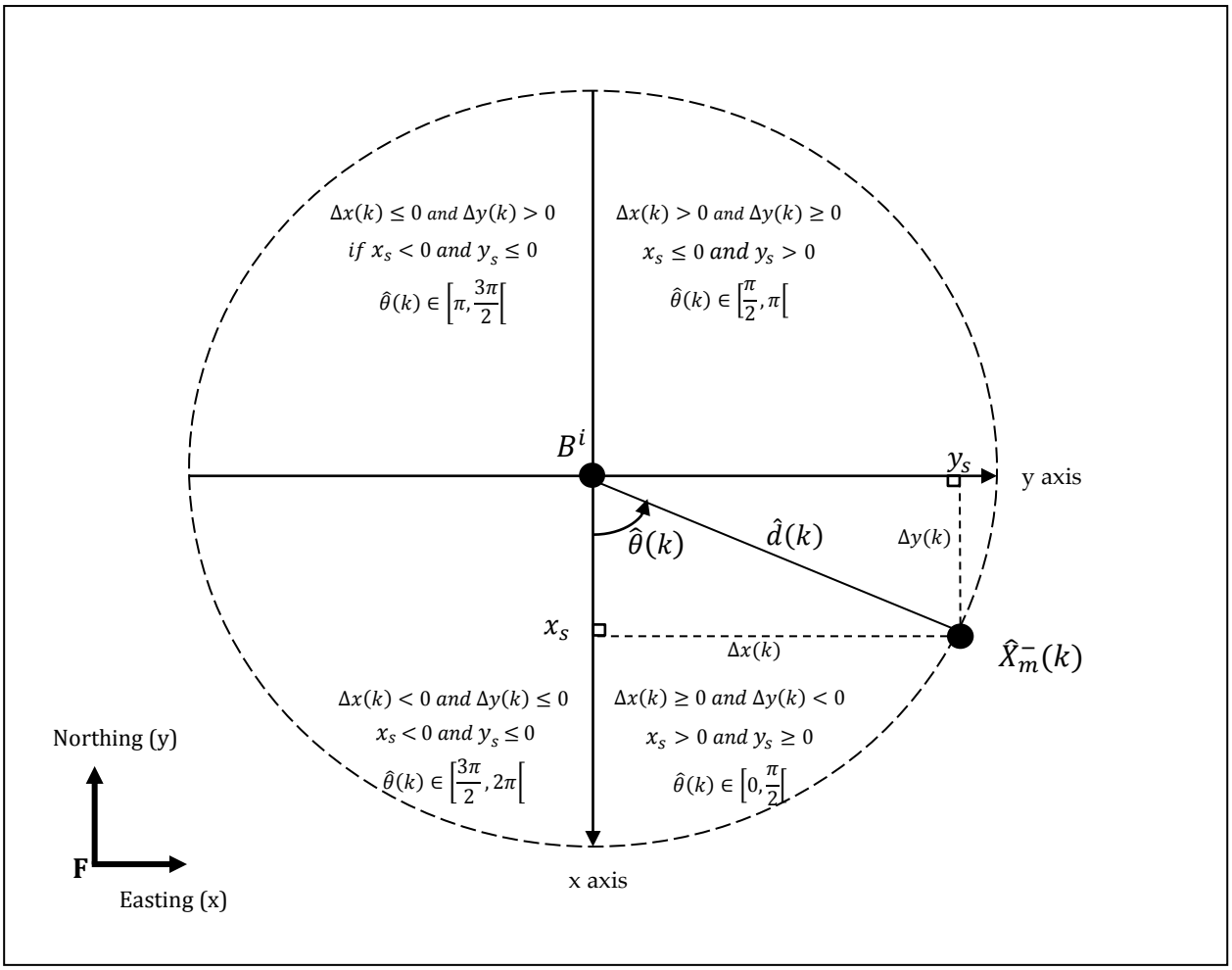

Figure 3.3 The Bearing Transition Function

The transition function ϑ applies the coordinate transformation and computes the angle $\hat{\theta}(k)$ by taking into account the quadrant of the local Cartesian system as follows.

$$\vartheta(x_s, y_s) = \begin{cases} sin^{-1}\left(\frac{y_s}{r_s}\right) & if\ x_s > 0\ and\ y_s \geq 0 \\ \pi - \sin^{-1}\left(\frac{y_s}{r_s}\right) & if\ x_s \leq 0\ and\ y_s > 0 \\ \pi + \sin^{-1}\left(\frac{y_s}{r_s}\right) & if\ x_s < 0\ and\ y_s \leq 0 \\ 2\pi - \sin^{-1}\left(\frac{y_s}{r_s}\right) & if\ x_s \geq 0\ and\ y_s < 0 \end{cases} \tag{3.34}$$

With the inverse sine function defined within the local chart, the function ϑ describes the predicted bearing $\hat{\theta}(k)$ within the global reference frame F as follows:

$$\hat{\theta}(k) = \vartheta\left(\hat{X}_m^-(k), B_i\right) = \begin{cases} sin^{-1}\left(\frac{\Delta\hat{x}(k)}{\hat{d}(k)}\right) & if\ \Delta\hat{x}(k) \geq 0\ and\ \Delta\hat{y}(k) < 0 \\ \pi - \sin^{-1}\left(\frac{\Delta\hat{x}(k)}{\hat{d}(k)}\right) & if\ \Delta\hat{x}(k) > 0\ and\ \Delta\hat{y}(k) \geq 0 \\ \pi + \sin^{-1}\left(\frac{\Delta\hat{x}(k)}{\hat{d}(k)}\right) & if\ \Delta\hat{x}(k) \leq 0\ and\ \Delta\hat{y}(k) > 0 \\ 2\pi - \sin^{-1}\left(\frac{\Delta\hat{x}(k)}{\hat{d}(k)}\right) & if\ \Delta\hat{x}(k) < 0\ and\ \Delta\hat{y}(k) \leq 0 \end{cases} \quad (3.35)$$

Where:

- $\Delta\hat{x}(k)$ is the predicted displacement along the x-axis:

  $$\Delta\hat{x}(k) = \hat{x}_m^-(k) - x_b^i$$

- $\Delta\hat{y}(k)$is the predicted displacement along the y axis:

  $$\Delta\hat{y}(k) = \hat{y}_m^-(k) - y_b^i$$

- $\hat{d}(k)$ is the predicted distance between the BTS position and the mobile state:

  $$\hat{d}(k) = \sqrt{\left(\hat{x}_m^-(k) - x_b^i\right)^2 + \left(\hat{y}_m^-(k) - y_b^i\right)^2}$$

Note that the function ϑ is not defined if the predicted distance $\hat{d}(k)$ is zero. Recall from Section 3.2 that the state of the mobile terminal is initialised so that it does not coincide with any of the base stations to avoid the zero-distance condition. In fact, the latter violates the definition of the path loss model equation which is a logarithmic function of the BTS-MT distance. With an appropriate state initialisation, this condition is avoided during the prediction of the range and bearing observations.

As it is defined within the interval $[0,2\pi[$, the function ϑ described in (3.35) is a periodic angular function with a jump discontinuity at the x-axis of the local chart $\mathbb{C}$ which translates to $\Delta\hat{x}(k) = 0$ in the global perspective. The bearing prediction function ϑ is therefore not differentiable if the mobile state estimate is located exactly south of the BTS position. Since it is used by the observation model function h_θ which must be infinitely differentiable, the function ϑ must be described as an analytic function. In this respect, the Heaviside unit

function allows us to translate the discontinuous function ϑ into a single analytical expression of the predicted bearing $\hat{\theta}(k)$. It is now clear why the ternary representation of the bearing measurement is designed to coincide with the values of the unit step function. Given a real number λ, let μ be the Heaviside unit function defined as:

$$\mu(\lambda) = \begin{cases} 1 & if\ \lambda > 0 \\ 0.5 & if\ \lambda = 0 \\ 0 & if\ \lambda < 0 \end{cases} \tag{3.36}$$

Note that μ is defined in this work using the conventional half-maximum convention which allows for analytic approximation of the function. In fact, it can be defined in terms of the sign function to exploit the smooth approximation of this latter as follows:

$$\mu(\lambda) = \frac{1}{2}[1 + sgn(\lambda)] \quad \forall \lambda \in \mathbb{R} \tag{3.37}$$

Since $sgn(\mu) \approx \tanh(c\mu)\ \ for\ c \gg 1$, thus expression (3.37) is rewritten as:

$$\mu(\lambda) = \frac{1}{2}[1 + \tanh(c\lambda)] \quad for\ c \gg 1 \tag{3.38}$$

In the following outline, the bearing prediction function ϑ is expressed in terms of the Heaviside function μ defined in (3.36). The resulting expression will then be translated into a differentiable equation using the analytic approximation of μ described in (3.38).

Recall that the bearing prediction function ϑ depends on the easting and northing displacements $\Delta\hat{x}(k)$ and $\Delta\hat{y}(k)$ between the BTS and the MT. As shown in figure 3.2, the function ϑ transforms $\Delta\hat{x}(k)$ and $\Delta\hat{y}(k)$ into local coordinates within the chart $\mathbb{C}$ to compute the bearing $\hat{\theta}(k)$ in each quadrant. Describing ϑ in terms of the unit step function combines the value of the angle $\hat{\theta}(k)$ in each quadrant in a single expression. The signs of the horizontal and vertical displacements specify the quadrant of $\mathbb{C}$ which contains the mobile

position, and hence, the angle value is extracted from definition (3.35). Using the conventional form of μ defined in (3.36), the reformulated expression of the function ϑ reads as:

$$\hat{\theta}(k) = \left[sin^{-1}\left(\frac{\Delta\hat{x}(k)}{d(k)}\right)\right] \mu(\Delta\hat{x}(k)\,)\,\mu\big(-\Delta\hat{y}(k)\big) + \left[\pi - sin^{-1}\left(\frac{\Delta\hat{x}(k)}{d(k)}\right)\right] \mu\big(\Delta\hat{x}(k)\big)\,\mu\big(\Delta\hat{y}(k)\big)$$

$$+ \left[\pi + sin^{-1}\left(\frac{\Delta\hat{x}(k)}{d(k)}\right)\right] \mu\big(-\Delta\hat{x}(k)\big)\,\mu\big(\Delta\hat{y}(k)\big) + \left[2\pi - sin^{-1}\left(\frac{\Delta\hat{x}(k)}{d(k)}\right)\right] \mu\big(-\Delta\hat{x}(k)\big)\,\mu\big(-\Delta\hat{y}(k)\big) \tag{3.39}$$

Finally, expression (3.39) is rewritten as an analytic function using the smooth approximation of the unit step function μ denoted in (3.38), as follows:

$$\begin{aligned}\hat{\theta}(k) = \frac{-1}{4}&\left[sin^{-1}\left(\frac{\Delta\hat{x}(k)}{d(k)}\right)\right]\left[1 + \tanh\big(c.\,\Delta\hat{x}(k)\big)\right]\left[1 + \tanh\big(-c\Delta\hat{y}(k)\big)\right] \\ &+ \frac{1}{4}\left[\pi - sin^{-1}\left(\frac{\Delta\hat{x}(k)}{d(k)}\right)\right]\left[1 + \tanh\big(c.\,\Delta\hat{x}(k)\big)\right]\left[1 + \tanh\big(c\Delta\hat{y}(k)\big)\right] \\ &+ \frac{1}{4}\left[\pi + sin^{-1}\left(\frac{\Delta\hat{x}(k)}{d(k)}\right)\right]\left[1 + \tanh\big(-c.\,\Delta\hat{x}(k)\big)\right]\left[1 + \tanh\big(c\Delta\hat{y}(k)\big)\right] \\ &+ \frac{1}{4}\left[2\pi - sin^{-1}\left(\frac{\Delta\hat{x}(k)}{d(k)}\right)\right]\left[1 + \tanh\big(-c.\,\Delta\hat{x}(k)\big)\right]\left[1 + \tanh\big(-c\Delta\hat{y}(k)\big)\right]\end{aligned} \tag{3.40}$$

As described in (3.32), the observation model h_θ predicts the measurement vector $\hat{Y}_\theta(k)$ using the predicted bearing $\hat{\theta}(k)$. According to the definition of the sector-based bearing measurement presented in section 3.31, the function h_θ should produce a unique ternary combination of the indicator variables that matches the predicted bearing $\hat{\theta}(k)$. This combination constitutes the predicted measurement vector $\hat{Y}_\theta(k)$ as shown in Figure 3.4.

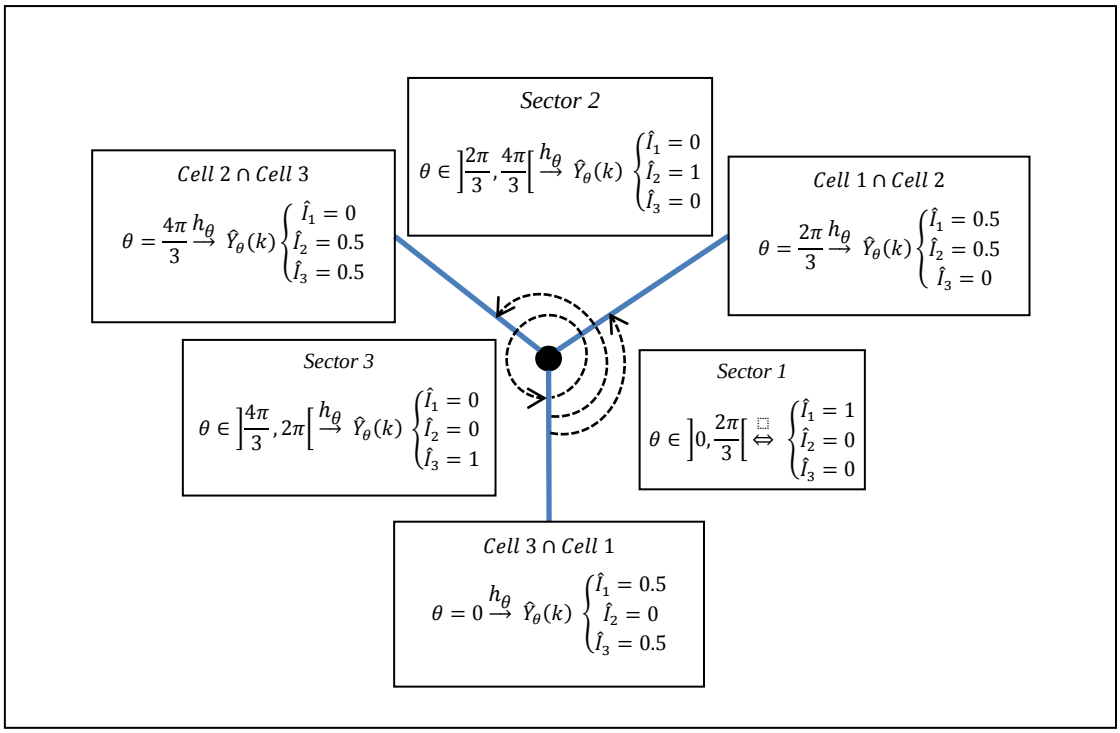

Figure 3.4 Predicted bearing value and its corresponding ternary representation

Note that each sector indicator variable I_i is itself a function of the predicted angle $\hat{\theta}(k)$. As the latter is defined within the interval $[0,2\pi[$, each indicator function I_i is defined as follows:

$$\hat{I}_1 = \begin{cases} 1 & , \ 0 < \hat{\theta}(k) < \dfrac{2\pi}{3} \\ 0.5 & , \ \hat{\theta}(k) = 0 \ \vee \ \hat{\theta}(k) = \dfrac{2\pi}{3} \\ 0 & , \ \dfrac{2\pi}{3} < \hat{\theta}(k) < 2\pi \end{cases} \tag{3.41}$$

$$\hat{I}_2 = \begin{cases} 1 & , \ \dfrac{2\pi}{3} < \hat{\theta}(k) < \dfrac{4\pi}{3} \\ 0.5 & , \ \hat{\theta}(k) = \dfrac{2\pi}{3} \ \vee \ \hat{\theta}(k) = \dfrac{4\pi}{3} \\ 0 & , \ 0 < \hat{\theta}(k) < \dfrac{2\pi}{3} \ \vee \ \dfrac{4\pi}{3} < \hat{\theta}(k) < 2\pi \end{cases} \tag{3.42}$$

$$\hat{I}_3 = \begin{cases} 1 \quad , \ \dfrac{4\pi}{3} < \hat{\theta}(k) < 2\pi \\ 0.5 \ , \ \hat{\theta}(k) = \dfrac{4\pi}{3} \ \vee \ \hat{\theta}(k) = 0 \\ 0 \quad , 0 < \hat{\theta}(k) < \dfrac{2\pi}{3} \end{cases} \tag{3.43}$$

Being a discontinuous function with output values {0, 0.5, 1}, each sector indicator function (3.43), (3.44) and (3.45) is expressed in terms of the Heaviside function as follows:

$$\hat{I}_1\left(\hat{\theta}(k)\right) = \mu\left(\tfrac{2\pi}{3} - \hat{\theta}(k)\right)\left[1 - \mu\left(-\hat{\theta}(k)\right)\right] \tag{3.44}$$

$$\hat{I}_2\left(\hat{\theta}(k)\right) = \mu\left(\tfrac{4\pi}{3} - \hat{\theta}(k)\right)\mu\left(\hat{\theta}(k) - \tfrac{2\pi}{3}\right) \tag{3.45}$$

$$\hat{I}_3\left(\hat{\theta}(k)\right) = \mu\left(\hat{\theta}(k) - \tfrac{4\pi}{3}\right) + \mu\left(-\hat{\theta}(k)\right) \tag{3.46}$$

Using the smooth approximation of the unit function, the indicator variables (3.44), (3.45) and (3.46) are translated into analytic functions of the predicted bearing $\hat{\theta}(k)$ as follows:

$$\hat{I}_1\left(\hat{\theta}(k)\right) = \tfrac{1}{4}\left[1 + \tanh\left(c\left(\tfrac{2\pi}{3} - \hat{\theta}(k)\right)\right)\right]\left[1 - \tanh\left(-c\hat{\theta}(k)\right)\right] \tag{3.47}$$

$$\hat{I}_2\left(\hat{\theta}(k)\right) = \tfrac{1}{4}\left[1 + \tanh\left(c\left(\tfrac{4\pi}{3} - \hat{\theta}(k)\right)\right)\right]\left[1 + \tanh\left(c\left(\hat{\theta}(k) - \tfrac{2\pi}{3}\right)\right)\right] \tag{3.48}$$

$$\hat{I}_3\left(\hat{\theta}(k)\right) = 1 + \tfrac{1}{2}\left[\tanh\left(c\left(\hat{\theta}(k) - \tfrac{4\pi}{3}\right)\right) + \tanh\left(-c\hat{\theta}(k)\right)\right] \tag{3.49}$$

With the predicted bearing $\hat{\theta}(k)$ of the form (3.42), expressions (3.47), (3.48) and (3.49) constitute the bearing observation model h_θ which predicts the bearing measurement vector as described in (3.32). As h_θ is now expressed as an analytic function, the EKF can proceed to

the measurement update cycle starting with the linear approximation of h_θ around the estimate of the mobile terminal state.

3.4.3 The Bearing Observation Jacobian:

The linear approximation of the observation model h_θ described in (3.32) with respect to the mobile state estimate $\hat{X}_m^-(k)$ produces the Jacobian matrix of the form:

$$H_\theta(k) = \frac{\partial h_\theta}{\partial \hat{X}_m^-(k)} = \begin{bmatrix} \frac{\partial \hat{I}_1}{\partial \hat{X}_m^-(k)} \\ \frac{\partial \hat{I}_2}{\partial \hat{X}_m^-(k)} \\ \frac{\partial \hat{I}_3}{\partial \hat{X}_m^-(k)} \end{bmatrix} = \begin{bmatrix} \frac{\partial \hat{I}_1}{\partial \hat{x}_m^-(k)} & \frac{\partial \hat{I}_1}{\partial \hat{y}_m^-(k)} \\ \frac{\partial \hat{I}_2}{\partial \hat{x}_m^-(k)} & \frac{\partial \hat{I}_2}{\partial \hat{y}_m^-(k)} \\ \frac{\partial \hat{I}_3}{\partial \hat{x}_m^-(k)} & \frac{\partial \hat{I}_3}{\partial \hat{y}_m^-(k)} \end{bmatrix} \tag{3.50}$$

As each sector indicator is linked to the state using the intermediate predicted displacement angle $\hat{\theta}(k)$ defined by the function $\vartheta\left(\hat{X}_m^-(k), B_i\right)$ denoted in (3.39), the Jacobian matrix $H_\theta(k)$ is constructed as follows:

$$H_\theta(k) = \begin{bmatrix} \frac{\partial \hat{I}_1}{\partial \hat{\theta}(k)} \frac{\partial \hat{\theta}(k)}{\partial \hat{X}_m^-(k)} \\ \frac{\partial \hat{I}_2}{\partial \hat{\theta}(k)} \frac{\partial \hat{\theta}(k)}{\partial \hat{X}_m^-(k)} \\ \frac{\partial \hat{I}_3}{\partial \hat{\theta}(k)} \frac{\partial \hat{\theta}(k)}{\partial \hat{X}_m^-(k)} \end{bmatrix} = \begin{bmatrix} \frac{\partial \hat{I}_1}{\partial \hat{\theta}(k)} \frac{\partial \hat{\theta}(k)}{\partial \hat{x}_m^-(k)} & \frac{\partial \hat{I}_1}{\partial \hat{\theta}(k)} \frac{\partial \hat{\theta}(k)}{\partial \hat{y}_m^-(k)} \\ \frac{\partial \hat{I}_2}{\partial \hat{\theta}(k)} \frac{\partial \hat{\theta}(k)}{\partial \hat{x}_m^-(k)} & \frac{\partial \hat{I}_2}{\partial \hat{\theta}(k)} \frac{\partial \hat{\theta}(k)}{\partial \hat{y}_m^-(k)} \\ \frac{\partial \hat{I}_3}{\partial \hat{\theta}(k)} \frac{\partial \hat{\theta}(k)}{\partial \hat{x}_m^-(k)} & \frac{\partial \hat{I}_3}{\partial \hat{\theta}(k)} \frac{\partial \hat{\theta}(k)}{\partial \hat{y}_m^-(k)} \end{bmatrix} \tag{3.51}$$

The derivative of each indicator variable with respect to the predicted bearing $\hat{\theta}(k)$ reads as:

$$\frac{\partial \hat{I}_1}{\partial \hat{\theta}(k)} = \frac{-c}{4}\left[1 + \tanh\left(c\left(\frac{2\pi}{3} - \hat{\theta}(k)\right)\right)\right]\left[1 - \tanh\left(-c\hat{\theta}(k)\right)\right]\left[\tanh\left(c\left(\frac{2\pi}{3} - \hat{\theta}(k)\right) + \tanh\left(-c\hat{\theta}(k)\right)\right)\right] \tag{3.52}$$

$$\frac{\partial \hat{I}_2}{\partial \hat{\theta}(k)} = \frac{c}{4}\left[1+\tanh\left(c\left(\frac{4\pi}{3}-\hat{\theta}(k)\right)\right)\right]\left[1+\tanh\left(c\left(\hat{\theta}(k)-\frac{2\pi}{3}\right)\right)\right]\left[2-\tanh\left(c\left(\hat{\theta}(k)-\frac{2\pi}{3}\right)-\tanh\left(c\left(\frac{4\pi}{3}-\hat{\theta}(k)\right)\right)\right)\right]$$

(3.53)

$$\frac{\partial \hat{I}_3}{\partial \hat{\theta}(k)} = \frac{c}{2}\left[\tanh^2\left(c\left(\hat{\theta}(k)-\frac{4\pi}{3}\right)+\tanh^2\left(-c\hat{\theta}(k)\right)\right)\right] \quad (3.54$$

The partial derivatives of the predicted bearing described in (3.41) with respect to the easting and northing coordinates of the mobile state are computed below:

$$\begin{aligned}\frac{\partial \hat{\theta}(k)}{\partial \hat{x}_m^-(k)} = \frac{-1}{4}&\left[1+\tanh\left(c.\Delta\hat{x}(k)\right)\right]\left[1+\tanh\left(-c\Delta\hat{y}(k)\right)\right]\left[\frac{\Delta\hat{y}(k)}{d^2(k)}+sin^{-1}\left(\frac{\Delta\hat{x}(k)}{d(k)}\right)\left[1-\tanh\left(c.\Delta\hat{x}(k)\right)\right]\right]\\ &+\frac{1}{4}\left[1+\tanh\left(c.\Delta\hat{x}(k)\right)\right]\left[1+\tanh\left(c\Delta\hat{y}(k)\right)\right]\left[\frac{\Delta\hat{y}(k)}{d^2(k)}+\left(\pi-sin^{-1}\left(\frac{\Delta\hat{x}(k)}{d(k)}\right)\right)\left[1-\tanh\left(c.\Delta\hat{x}(k)\right)\right]\right]\\ &+\frac{1}{4}\left[1+\tanh\left(-c.\Delta\hat{x}(k)\right)\right]\left[1+\tanh\left(c\Delta\hat{y}(k)\right)\right]\left[\frac{\Delta\hat{y}(k)}{d^2(k)}+\left(\pi+sin^{-1}\left(\frac{\Delta\hat{x}(k)}{d(k)}\right)\right)\left[1-\tanh\left(-c.\Delta\hat{x}(k)\right)\right]\right]\\ &+\frac{1}{4}\left[1+\tanh\left(-c.\Delta\hat{x}(k)\right)\right]\left[1+\tanh\left(-c\Delta\hat{y}(k)\right)\right]\left[\frac{\Delta\hat{y}(k)}{d^2(k)}+\left(2\pi-sin^{-1}\left(\frac{\Delta\hat{x}(k)}{d(k)}\right)\right)\left[1-\tanh\left(-c.\Delta\hat{x}(k)\right)\right]\right]\end{aligned}$$

(3.55)

$$\begin{aligned}\frac{\partial \hat{\theta}(k)}{\partial \hat{y}_m^-(k)} = \frac{-1}{4}&\left[1+\tanh\left(c.\Delta\hat{x}(k)\right)\right]\left[1+\tanh\left(-c\Delta\hat{y}(k)\right)\right]\left[\frac{\Delta\hat{x}(k)}{d^2(k)}+sin^{-1}\left(\frac{\Delta\hat{x}(k)}{d(k)}\right)\left[1-\tanh\left(-c\Delta\hat{y}(k)\right)\right]\right]\\ &+\frac{1}{4}\left[1+\tanh\left(c.\Delta\hat{x}(k)\right)\right]\left[1+\tanh\left(c\Delta\hat{y}(k)\right)\right]\left[\frac{\Delta\hat{x}(k)}{d^2(k)}+\left(\pi-sin^{-1}\left(\frac{\Delta\hat{x}(k)}{d(k)}\right)\right)\left[1-\tanh\left(c.\Delta\hat{y}(k)\right)\right]\right]\\ &+\frac{1}{4}\left[1+\tanh\left(-c.\Delta\hat{x}(k)\right)\right]\left[1+\tanh\left(c\Delta\hat{y}(k)\right)\right]\left[\frac{\Delta\hat{x}(k)}{d^2(k)}+\left(\pi+sin^{-1}\left(\frac{\Delta\hat{x}(k)}{d(k)}\right)\right)\left[1-\tanh\left(-c.\Delta\hat{y}(k)\right)\right]\right]\\ &+\frac{1}{4}\left[1+\tanh\left(-c.\Delta\hat{x}(k)\right)\right]\left[1+\tanh\left(-c\Delta\hat{y}(k)\right)\right]\left[\frac{\Delta\hat{x}(k)}{d^2(k)}+\left(2\pi-sin^{-1}\left(\frac{\Delta\hat{x}(k)}{d(k)}\right)\right)\left[1-\tanh\left(-c\Delta\hat{y}(k)\right)\right]\right]\end{aligned}$$

(3.56)

3.5 The measurement update:

Recall from Section 3.2 that the state of the mobile terminal is initialised using the weighted mean of all BTS positions communicating with the mobile terminal. The EKF then updates the state and its associated covariance recursively using the adopted path loss and bearing observation models. By observing one base station at time, the measurement update cycle of the EKF proceeds as follows:

- The range-bearing measurement vector $Y_{rb}(k)$ denoted by expression (3.20) is inferred from the CID and path loss measurements retrieved from the network.
    - The path loss measurement $Y_r(k)$ is the difference between the received signal strength and the transmitted power of the BTS antenna.
    - The bearing measurement vector $Y_\theta(k)$ is constructed using the sector indicators I_1 , I_2 and I_3 as described in section 3.3.1.
- Using the a priori state estimate $\hat{X}_m^-(k)$ and the position of the observed BTS, the path loss and bearing measurement are predicted by their corresponding models h_r and h_θ constituting the hybrid measurement model h_{rb} denoted by (3.20).
    - The predicted path loss measurement $\hat{Y}_r(k)$ is computed using equation (3.15)
    - The predicted bearing measurement $\hat{Y}_\theta(k)$ is constructed using the prediction of each sector indicator $\hat{I}_1$ in (3.47), $\hat{I}_2$ in (3.48) and $\hat{I}_3$ in (3.49) after computing the intermediary bearing angle $\hat{\theta}(k)$ using (3.38).
- The measurement innovation of the system denoted in (3.21) is therefore rewritten as:
    - $$v_{rb}(k) = \begin{pmatrix} v_r(k) \\ v_{I_1}(k) \\ v_{I_2}(k) \\ v_{I_3}(k) \end{pmatrix} \qquad (3.57)$$

- The linear approximation of both models results in a Jacobian of the form (3.25) which is now rewritten as

  - $$H_{rb}(k) = \begin{bmatrix} \frac{\partial \hat{Y}_r(k)}{\partial \hat{X}_m^-(k)} \\ \frac{\partial \hat{I}_1}{\partial \hat{X}_m^-(k)} \\ \frac{\partial \hat{I}_2}{\partial \hat{X}_m^-(k)} \\ \frac{\partial \hat{I}_3}{\partial \hat{X}_m^-(k)} \end{bmatrix} \quad (3.58)$$

    Where,

    - $\frac{\partial \hat{Y}_r(k)}{\partial \hat{X}_m^-(k)}$ is the derivative of the predicted path loss with respect to the state denoted by the partial derivatives (3.18) and (3.19).
    - The derivatives of the sector indicators with respect to the state are computed in the previous section.

- The covariance of the measurement innovation $S(k)$ denoted by (3.22) is now rewritten with subscript *rb* as follows:

  - $$S_{rb}(k) = H_{rb}(k)P_m^-(k)H_{rb}(k)^T + R_{rb}(k) \quad (3.59)$$

    Where,

    - $$R_{rb}(k) = \begin{bmatrix} R_r & 0 & 0 & 0 \\ 0 & R_{I_1} & 0 & 0 \\ 0 & 0 & R_{I_2} & 0 \\ 0 & 0 & 0 & R_{I_3} \end{bmatrix} \quad (3.60)$$

- The Kalman Gain weights the contribution of the measurement innovation as described by (3.11)
- Finally, the state and its covariance are updated using (3.12) and (3.13) respectively.

CHAPTER 4 - Constrained Cellular SLAM

4.1 Introduction

This chapter presents a novel approach to cellular positioning which allows the mobile terminal to build a map of base stations and then use this map to deduce its own location. The EKF-SLAM formalism is adopted to create a localisation system which can accommodate the GSM network in which it is deployed. As introduced previously, the received signal strength (RSS) is used in this work to infer range relationships between reference base stations and the mobile terminal. The main advantage of RSS over timing measurements is to overcome the need for additional hardware and network modifications. In fact, the system proposed in this chapter is implemented as a pure software-based solution by exploiting the availability of RSS observations within the GSM network infrastructure. To the best of our knowledge, the SLAM approach is applied in the cellular positioning framework for the first time in this work, CCS represents the main contribution of this thesis.

The proposed cellular SLAM methodology implements a constrained SLAM approach due to the lack of motion sensing capability in this framework. As typical SLAM applications in navigation problems rely on dead reckoning measurements to build a map of the environment, CCS uses an alternative method to track the movement of the mobile terminal

and initialise newly observed landmarks. For this reason, we refer to the methodology as the Constrained Cellular SLAM (CCS). As it is fundamental to solve the SLAM problem, CCS performs the state augmentation process and maintains the correlations between the state of the mobile terminal and all the landmark states. However, an initial map is constructed during a pre-processing stage to compensate for the lack of real-time motion data. This pre-processing stage is referred to here as the Initial Mapping Stage, in which, landmarks are initialised using known mobile locations. This calibration stage enables the system to apply the EKF-SLAM method during the Network Localisation Stage. The latter only relies on network information i.e. CID to identify base stations and RSS to infer relative range observations. In this discussion, we will refer to the estimation process employed during the Initial Mapping Stage as the BTS Initialisation Model (BIM). Similarly, the EKF-SLAM process performed online in the Network Localisation Stage is referred to as the Network Localisation Filter (NLF). Both of these algorithms rely on the same propagation model to link the relative BTS-MT displacement to RSS observations. As stated previously, the path loss model adopted in this work is developed empirically by fitting the propagation parameters using RSS measurements in the trial area in which the experimental evaluation of the system is conducted.

In addition to the constraint mentioned above, the system assumes that the mobile terminal can only measure the signal strength received from the serving base station. This second constraint affects the Network Localisation Stage as it does not allow the mobile terminal to localise itself using range observations relative to different BTS locations. As a result, the EKF-SLAM approach is a sequential algorithm which updates the map augmented state vector using a single observation at a time. Without dead reckoning measurements and

multiple range observations, the CCS exploits the Initial Mapping Stage to associate mobile location fingerprints to each landmark in the map. This process is similar to the location fingerprinting methods applied in RF-based localisation systems which were discussed in Section 2. In this work however, the fingerprints are not used as independent measurements for location estimations but rather used as available information to predict the movement of the mobile terminal.

This chapter begins with an overview of the Constrained Cellular SLAM methodology in Section 4.2. It will then provide the mathematical formulation of the CCS methodology. Detailed structure of each of the adopted observation model, the BTS Initialisation Model and the Network Localisation Filter are presented in Section 4.3, Section 4.4 and Section 4.5 respectively. The smartphone application implementing CCS is described in Chapter 5 while Chapter 6 will present the experimental evaluation of the system.

4.2 System Overview

This section provides a detailed description of the Constrained Cellular SLAM methodology. It will first describe the underlying constraints of the framework in Section 4.2.1. It will then state the main contribution presented by CCS to improve the accuracy of RF-based localisation in Section 4.2.2. The Initial Mapping Stage and the network Localisation stage are described in Section 4.2.3 and 4.2.4 respectively.

4.2.1 Constrained SLAM Approach

As introduced previously, Simultaneous Localisation and Map building (SLAM) has been applied in various localisation frameworks to overcome the need for an a priori map of the environment as well as to adapt to any environmental changes. In a standard EKF-SLAM

system, the EKF predicts the position of the target using dead reckoning measurements retrieved from internal sensors.

- Initially, the EKF maintains the target position within the state vector and its associated uncertainty within the covariance matrix.
- When the external sensors obtain a range and/or bearing measurement relative to a newly encountered landmark, the latter is then initialised using the measurement and the estimated target position.
- The initialised landmark is then registered within the map by augmenting the state vector with the landmark's state.
- Upon receiving subsequent measurements associated with a registered landmark, the EKF updates the estimate of the target's location thus reducing the error accumulated during the prediction cycle.

Due to state augmentation, the EKF does not only update the target state but also the states of all landmarks within the state vector. As a result, the update step correlates the error in the target estimate with the error of each landmark state estimate. The resulting correlations, which grow at each update, are crucial for the consistency and the accuracy of the location estimation. However, the computational effort scales quadratically with the number of landmarks maintained within the state vector [Dis01]. Therefore, in order to implement a successful EKF-SLAM approach for Cellular positioning, CCS adopts the fundamental formalism of state augmentation while keeping the computational effort low for efficient implementation.

The system assumes that the mobile terminal does not have access to motion sensors. As a result, this constraint does not allow the system to track the movement of the mobile

terminal using dead reckoning measurements. However, these measurements are used in typical EKF-SLAM applications to predict the target state and initialise newly observed landmarks. Therefore, CCS must use an alternative SLAM method to track the movement of the mobile location and perform the landmark mapping process. In this framework, GPS is the available solution to obtain reliable location data, which can be used to initialise BTS locations. Since the aim of CCS consists of performing cellular positioning by relying solely on network information, the GPS-dependent task of landmark initialisation must be carried out offline during a pre-processing phase, referred to here as the Initial Mapping Stage. In the Network Localisation Stage however, GPS does not contribute to the estimation and is only used to evaluate the mobile state estimates produced by the EKF-SLAM process.

The alternative SLAM approach treats the initialisation of landmarks as a mapping problem in which ground-truth mobile position data and range-based observations are used for the localisation of BTS landmarks. The map resulting from the Initial Mapping Stage will then be used as reference during the Network Localisation Stage, in which the EKF-SLAM methodology is performed. This includes the state augmentation process as well as the simultaneous update of the mobile and landmark states. The Cell Identity Code is used to identify BTS landmarks in both stages of the system. In the former stage, the CID identifies the initialised base station and plays the role of an identifier within the entry representing the BTS stored in the database. In the latter stage, the CID is used as a data association process which links RSS observations to landmark states that have already been integrated into the state vector.

4.2.2 Improved RF-Based Localisation

As described in Chapter 2, the concept of postponing online location estimation after conducting an offline calibration phase is common within RF-based localisation techniques. In the cellular localisation framework, this concept has been adopted by the database correlation method (DCM) [Lai01]. The latter consists of creating a database of location fingerprints during an initial calibration stage, which is then used as reference during the location estimation stage. A location fingerprint consists of the mapping between a known location of the mobile terminal and the RSS measurement taken from the same location. In the location estimation stage, the measured RSS is processed by a correlation algorithm to extract the best matching fingerprint from the database. The Constrained Cellular SLAM bears an interesting relationship with database correlation methods not only because of the two-phase approach. In fact, the concept of location fingerprinting can also be applied in this work to compensate for the lack of dead reckoning measurements during the Network Localisation Stage. During the Initial Mapping Stage of the system, each GPS-RSS sample used to estimate the position of a BTS is stored as a location fingerprint. At the end of the survey, each base station is represented by a database entry containing the estimated position as well as a list of mobile location fingerprints. During the Network Localisation Stage, the fingerprints will provide the EKF-SLAM algorithm with a priori location information that can be used to predict the position of the mobile terminal. Similarly to DCM, a correlation algorithm scans through the list of fingerprints belonging to the observed BTS to find the best matching fingerprint. Moreover, the integration of fingerprint location information during the prediction step of the EKF allows the system to update the a priori estimate using a single RSS observation. As introduced previously, the ability to only observe the serving base station is

the system's second constraint which affects the range-only localisation task rather than the SLAM procedure.

As described in Chapter 2, DCM performs well in dense urban areas given that a high resolution radio map is constructed during the calibration phase. The main disadvantage of DCM is the laborious task of building and maintaining large databases. The Kalman Filter has been used in the literature to improve the performance of DCM. For instance, Hellebrandt and Mathar [Hel99] and Takenga et Al [Tak07] proposed the use of Kalman Filtering to track the movements of the mobile terminal by smoothing the location estimates produced using DCM. In this work however, the EKF-SLAM algorithm employed by CCS does not take the fingerprints as independent measurements. It rather exploits the fingerprint location as the available information related to the state dynamics of the system. Once the a priori state estimate is produced, the EKF integrates the RSS measurements taken by the MT relative to the observed BTS. Compared to other cellular techniques adopting DCM, CCS performs the mapping of BTS locations which will improve the accuracy of the MT localisation without requiring a high resolution fingerprint map. It will be shown in Chapter 6 that adopting the SLAM formalism of state augmentation improves the estimation of the mobile position and achieves better accuracy than using a standard database correlation method.

4.2.3 The Initial Mapping Stage

CCS begins with the Initial Mapping Stage (IMS) to collect the information needed to perform the EKF-SLAM process during the Network Localisation Stage. During a survey of the trial area, the Initial Mapping Stage performs an iterative process which initialises the base stations encountered by the mobile terminal. The BTS Initialisation Model (BIM) estimates the position of each BTS landmark using samples comprising of:

- A GPS position fix given in latitude and longitude coordinates measured by the built-in GPS module of the mobile terminal.
- The Cell Identity Code (CID) identifying the base station antenna in communication with the mobile terminal.
- The received signal strength (RSS) measured at the mobile terminal from the sample GPS position with respect to the observed BTS.

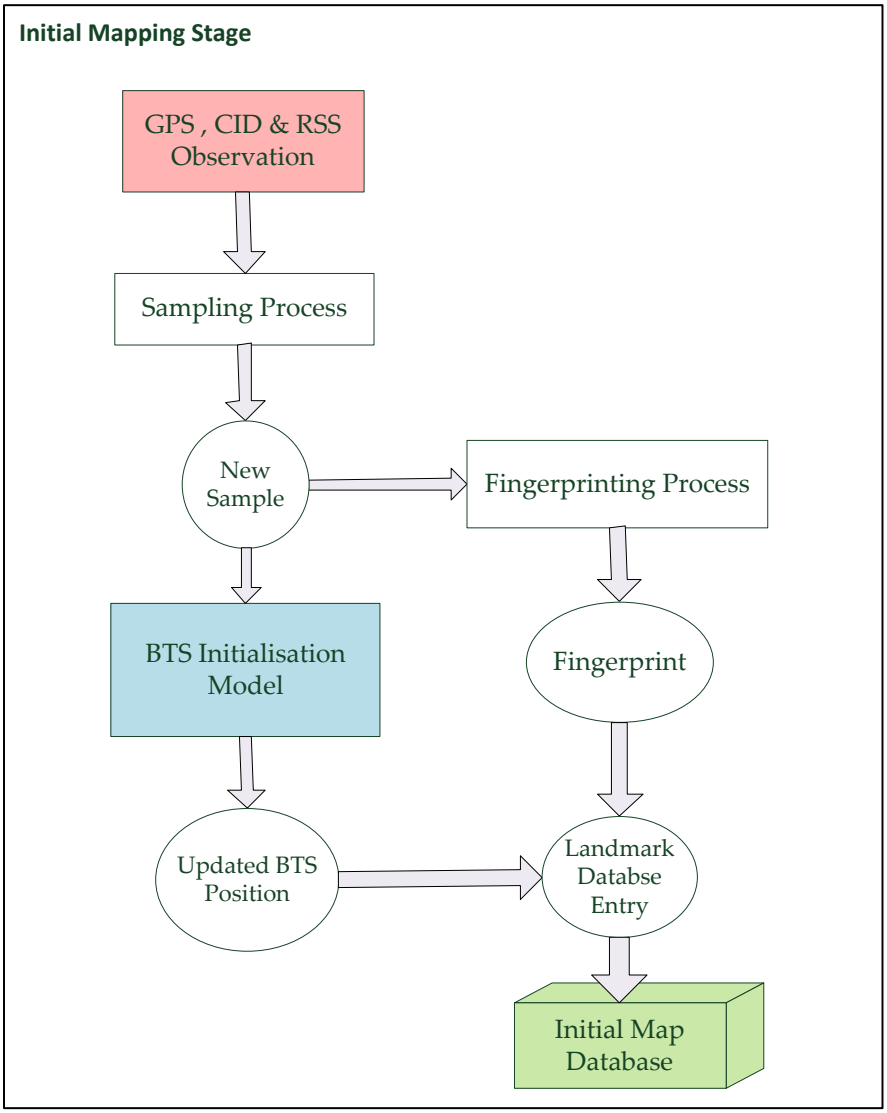

Figure 4.1 Initial Mapping Stage

The BTS Initialisation Model is a recursive EKF algorithm which estimates the position of the serving BTS each time a new sample is collected. As a global Cartesian frame is used to parameterise the state of the BTS landmark, the geodetic coordinates of the GPS sample are transformed into Cartesian coordinates within the global frame F. The observation model linking the BTS state to RSS measurements is the adopted path loss model described in Section 4.3. The observation model consists of the path loss equation that has been calibrated using RSS measurements in the same trial area as that of the mapping survey. As stated previously, empirical fitting of the propagation model parameters improves the accuracy of the measurement prediction and the positioning result. Since the landmark to be localised is stationary, BIM is a static model of the EKF with a stationary motion model. In fact, it is similar to the static cellular positioning system presented in Chapter 3 with the target being the BTS rather than the mobile terminal. The accuracy of the landmark position estimation depends on the survey itself, namely the path of the mobile terminal relative to the true position of the base station. As a range-based algorithm, BIM produces more accurate estimates if the reference GPS samples are taken in a circular manner around the target base station. The factors effecting the accuracy of landmark estimation are discussed in further detail in Chapter 6.

As introduced previously, a fingerprinting process is deemed necessary during the Initial Mapping Stage to enable the system to model the dynamics of the mobile terminal in the Network Localisation Stage. Each time a new sample is used to estimate the BTS landmark position, it is taken as a mobile location fingerprint which is then associated with the landmark entry in the database. As illustrated in figure 4.1, the Landmark Database Entry (LDE) consists of:

- The CID identifying the BTS antenna
- The estimated BTS location converted into local Cartesian Coordinates
- The list of fingerprints associated with the base stations.

The fingerprinting process reiterates while the mobile terminal is connected to the same BTS. When a handover to a different BTS is detected, the LDE is stored in the database that will be used as reference for positioning in the Network Localisation Stage. The size of the database depends on the area covered by the survey as well as the resolution of the fingerprinting process. As stated in the previous section, the CCS system does not require a high resolution fingerprint map to achieve good accuracy. In fact, adopting a SLAM-based approach overcomes the need for the laborious task of building a high resolution database.

4.2.4 The Network Localisation Stage

In the Absolute Map Filter (AMF) approach to EKF-SLAM, the state vector is augmented with the entire map of landmarks [New99]. The state of each observed landmark is initialised and registered as part of the map that is maintained within the state vector. The error in the vehicle pose estimate during the prediction stage of the EKF propagates to the landmark being observed during the initialisation and subsequent updates of the landmark. Due to the common error in the vehicle estimate, all the error estimates of the landmarks maintained in the state vector become correlated during the update step of the covariance matrix [Cso97]. The complexity of the AMF covariance update is $O(n^3)$ where n is the number of landmark states integrated into the state vector [Gui02]. Several alternatives to the AMF approach have been proposed to reduce the computational cost of large-scale SLAM systems for efficient implementations [Dis01].

In the cellular positioning framework however, the structure of the environment is significantly less complex than that of outdoor navigation problems in which the map may contain hundreds of landmarks. Similarly to other range-only SLAM frameworks in which the environment is made up of beacons or transponders, the number of BTS landmarks in the cellular network is limited within the experimental setup. Compared to large-scale SLAM, the implementation of AMF approach in this framework does not suffer as much from the computational burden associated with the full-SLAM covariance update. However, the Constrained Cellular SLAM system is implemented as a mobile application with limited computational resources and thus requires some complexity reduction approach. In fact, CCS employs the Network Localisation Filter (NLF) which implements a simple local map approach to EKF-SLAM. The NLF maintains the state of the mobile terminal augmented with a local map of BTS landmarks in the vicinity of the MT. In this discussion, the term 'local map' refers to the list of landmark states integrated into the state vector, whereas the term 'global map' refers to the database resulting from the Initial Mapping Stage. Moreover, the state vector of the system containing the mobile state augmented with the local map will be referred to here as the 'SLAM State'.

Due to the limited number of BTS landmarks in this cellular SLAM framework, the global frame of reference F used in the Initial Mapping Stage is again used to parameterise the SLAM State in this Network Localisation Stage. In order to reduce the computational burden of the application, a limited number of BTS landmarks are kept in the SLAM state vector. As it is already stored by the application in an auxiliary database, the global map is not transferred entirely from the database to the state vector. Therefore, the Constrained Cellular SLAM system must adopt a landmark management technique to maintain both the local and

global maps. Figure 4.3 shows a block diagram illustrating the procedure followed by the CCS system during the Network Localisation Stage.

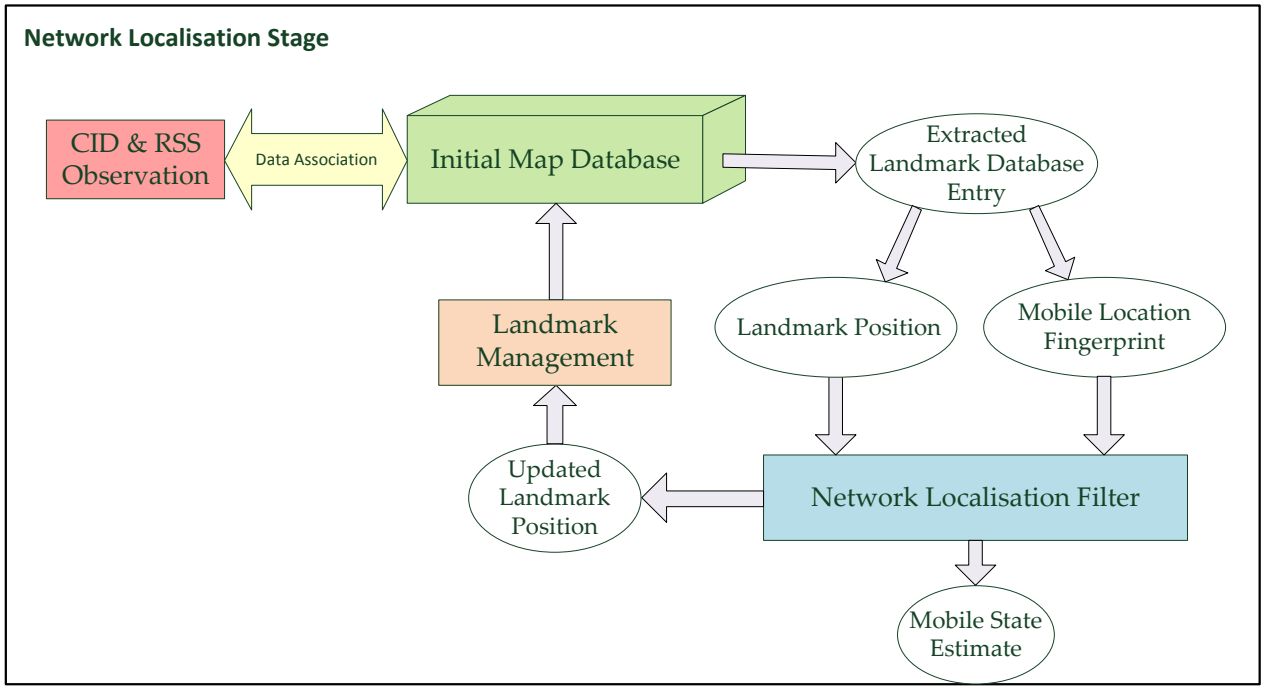

Figure 4.2 The Network Localisation Stage

When the network localisation phase begins, the NLF retrieves the CID and RSS measurements from the network monitoring process. It then initialises the SLAM state using the adopted database correlation method. A search algorithm is firstly employed to scan through the list of landmark database entries in order to find an entry matching the observed CID. Once identified, the position stored within the landmark entry is extracted and then integrated into the SLAM state vector. Secondly, the observed signal strength is compared against each fingerprint associated with the extracted landmark. The fingerprint yielding the smallest Euclidean distance in signal space is used to initialise the mobile state. This database correlation algorithm is employed each time a new CID or signal strength observation is received from the network monitoring process of the system. Once the mobile state is

initialised and the state of the first serving BTS is registered, the NLF starts a recursive prediction-update cycle.

The location fingerprinting process is not only used to initialise the state of the mobile terminal but also to model its dynamics. Upon receiving a new CID and/or RSS measurement, the NLF retrieves the matching fingerprint from the map and produces the a priori state estimate. The EKF prediction step uses the relative displacement between the previous and current matching fingerprints to estimate the new position of the mobile terminal. In fact, this inter-fingerprint range and bearing are applied as the system's control inputs which drive the mobile state during the prediction step. The process model of the NLF is described in detail in Section 4.5.3. The a priori estimate of the mobile terminal state and the state of the observed BTS are then used to predict the RSS measurement according to the adopted observation model described in Section 4.3. By applying the linear approximation about the MT and the serving BTS state estimates, the EKF algorithm updates the entire SLAM state. The measurement update step is described in more detail in Section 4.5.4.

4.3 The Observation Model

The CCS system uses a range-only observation model based on signal strength measurements taken at the mobile terminal with respect to the serving base station. The relationship between the observed RSS and the range separating the mobile receiver and the BTS transmitter is defined by an empirical propagation model which has been calibrated in the same trial area as that of the positioning experiments. Both the BTS Initialisation Model and the Network Localisation Filter employ this model to predict the path loss incurred by the BTS-MT downlink signal.

The path loss is modeled with a simple power law model of the form:

$$L = \beta + 10\,\alpha log(d) \qquad (4.1)$$

Where,

- L is the path loss incurred by the downlink signal.
- d is the Euclidean distance between the BTS and the MT measured in kilometres.
- β is the absolute loss value which represent the contribution of effects related to multipath propagation to the total path loss. Being the intercept of the power law model, β corresponds to the loss value at the reference distance of 1 km.
- α represents the path loss exponent which mainly depends on the environmental system parameters.

The path loss value can be measured in decibels (dB) by subtracting the measured RSS value p_r at the mobile terminal from the transmitted power p_t of the BTS antenna, that is:

$$L = p_t - p_r \qquad (4.2)$$

The linear regression process used for the model fitting has been presented in Section 2.4. As the transmitted power is assumed unknown in this framework, it is also fitted along with the model parameters α and β. Since the measurement available to the system is the received signal strength $p_r$denoted in expression (4.2), the log-distance model expressed in (4.1) is rewritten to describe the RSS measurement as follows:

$$p_r = p_t - \beta - 10\alpha\, log(d) \qquad (4.3)$$

Given the positions of the mobile terminal and the serving BTS with respect to a global Cartesian frame F, expression (4.3) can be rewritten as:

$$p_r = p_t - \beta - \ 10\alpha \, log\left(\sqrt{(x_b - x_m)^2 + (y_b - y_m)^2}\right) \qquad (4.4)$$

Where:

- x_b and y_b represent the Cartesian coordinates of the BTS.
- x_m and y_m represent the Cartesian coordinates of the MT.

As the Path Loss Model expressed in (4.4) links the displacement between the MT and the BTS to the RSS measurement, it can be used as an observation model in both stages of the Constrained Cellular SLAM system. Given the true MT state $X_m(k)$ and the true BTS state $X_b(k)$ at time k, the observation model (4.4) describes the true RSS observation $Y(k)$ in state space notation as follows:

$$Y(k) = h\big(X_m(k), X_b(k)\big) + w(k) \qquad (4.5)$$

Where:

- *h* is the nonlinear function which represents the propagation model of (4.4)
- $w(k)$ represents the zero-mean Gaussian noise which accounts for the measurement noise and also the prediction error in the observation model h.

4.4 The BTS Initialisation Model:

During the calibration stage of the system, the BTS Initialisation Model operates concurrently with the network monitoring subsystem and the GPS sampling process. The network monitor runs continuously to detect RSS variations and cell handovers, whereas the sampling process is controlled by the user to request GPS position data at discrete time intervals. When the position fix is returned by the GPS module, it is combined with the CID and RSS measurements to create a position sample. While the mobile terminal is moving, samples are collected relative to the serving BTS and stored in the list of samples. Using the observation model described in the previous section, the BIM estimates the position of BTS landmark recursively each time a new sample is obtained. When a handover is detected, the list of samples is handled by a fingerprinting process to produce a list of location fingerprints. The latter is then associated with the state of the landmark in order to create a landmark database entry that will be stored in the map.

As stated previously, the BTS Initialisation Model is a static model of the extended Kalman Filter maintaining the state of the serving BTS. The state vector at time instant k is parameterised by the Cartesian coordinates and has the form:

$$X_B(k) = \begin{bmatrix} x_B(k) \\ y_B(k) \end{bmatrix} \tag{4.6}$$

x_B and y_B are the easting and northing coordinates of the target base station within ellipsoidal orthographic coordinate system. Subscript b denotes that the state only contains the coordinates of the base station. As the latter is a fixed point in the Cartesian plane, the BIM employs a stationary motion model in which the priori estimate at the current time step (k) is

the same as the posteriori estimate from the previous step (k-1). The state model is shown below.

$$\hat{X}_B^-(k) = X_B^+(k-1) \tag{4.7}$$

Similarly, the time update of the state covariance is:

$$P_B^-(k) = P_B^+(k-1) \tag{4.8}$$

In this state model, the posterior state is estimated using the current measurement obtained at time k. The measurement consists of the sample collected from the current position of the mobile terminal during the survey of the base station transmitter. The sample at time k has the following form:

$$\mathrm{Z}_k = \left(CID_k,\ G_k \begin{pmatrix} L_G \\ l_G \end{pmatrix}, p_{r_k} \right) \tag{4.9}$$

Where

- $CID_k$is the cell identity code identifying the serving BTS communicating with the mobile terminal at time k.
- G_k is the GPS position fix measured at time k in latitude L_G and longitude l_G coordinates. It is important to note that these geodetic coordinates are converted to Cartesian easting and northing coordinates x_{G_k} and y_{G_k} respectively in the global east north frame F.
- p_{r_k} is the received signal power measured at the MT from the GPS ground-truth.

Initially, there is no prior knowledge about the location of the target BTS until the first GPS sample is taken by the mobile terminal. The state estimate is therefore initialised using the GPS position G_0 of the first sample Z_0. At time 0, the state vector is initialised as follows:

$$\hat{X}_B^-(0) = G_0 + \omega \qquad (4.10)$$

ω is a vector used to initialise the BTS state to coincide with a position within a certain distance from the GPS sample. The state is not initialised to coincide with the first GPS samples as it would lead to a zero distance between the mobile and the BTS, which violates the definition of the log-distance observation model expressed in (4.4).

The covariance matrix associated with the landmark state estimate is the following diagonal matrix:

$$P_B^-(0) = \begin{bmatrix} \sigma_{x_0}^2 & 0 \\ 0 & \sigma_{y_0}^2 \end{bmatrix} \qquad (4.11)$$

The error in the initial state estimate is assumed to coincide with the typical error of the Cell Id proximity sensing method. This error is relative to the size of the cell covered by the BTS transmitter. As far as the BIM is concerned, the BTS position is the state to be estimated and the observation model expressed in 4.4 is rewritten as:

$$Y(k) = h\big(X_B(k)\big) + w(k) \qquad (4.12)$$

Note from the observation model expressions (4.4) and (4.12) that the state of the mobile terminal is omitted from the model function h. Indeed, in this case, the MT position is not the state to be estimated as it is measured by the GPS module as part of the sample Z_k denoted in (4.9). It is considered by the system as a perfect measurement as the GPS uncertainty is negligible compared to the error in the BTS state estimate.

The BTS initialisation model is a sequential Kalman Filter which updates the state of the BTS landmark using a single RSS measurement. Thus, the measurement $Y(k)$ of (4.12) is a scalar which is assumed uncorrelated with previous measurements. The noise $w(k)$ is

assumed to be Gaussian distributed with mean zero and variance R. As a result, the observation model function h denoted in 4.12 lends itself to the propagation model equation of (4.4) to predict the RSS measurement $\hat{Y}(k)$ as follows:

$$\hat{Y}(k) = p_t - \beta - \ 10\alpha \ log\left(\sqrt{\left(\hat{x}_B(k) - x_{G_k}\right)^2 + \left(\hat{y}_B(k) - y_{G_k}\right)^2}\right) \quad (4.13)$$

When a new measurement sample Z_k is collected at time k, the BTS initialisation model uses the coordinates of the a priori state estimate $\hat{x}_B(k)$ and $\hat{x}_B(k)$ equation (4.13) to predict the path loss measurement $\hat{Y}(k)$ in order to proceed to the EKF measurement update stage. Subtracting the predicted measurement from the real measurement yields the measurement innovation $v(k)$, which represents the contribution of the measurement to update the state estimate.

$$v(k) = \hat{Y}(k) - Y(k) \quad (4.14)$$

Following the EKF approach, the BTS initialisation model relies on the linear approximation of the observation model around the a priori state estimate $X_b^-(k)$. As only one RSS measurement is processed at a time, the Jacobian of the predicted measurement function is the following row matrix:

$$H(k) = \left[\frac{\partial \hat{Y}(k)}{\partial \hat{x}_B(k)} \quad \frac{\partial \hat{Y}(k)}{\partial \hat{y}_B(k)}\right] \quad (4.15)$$

The partial derivatives of the predicted observation with respect to the landmark's eating and northing coordinates are shown below:

$$\frac{\partial \hat{Y}(k)}{\partial \hat{x}_B(k)} = \frac{\gamma\left(\hat{x}_B(k) - x_{G_k}\right)}{\left(\hat{x}_B(k) - x_{G_k}\right)^2 + \left(\hat{y}_B(k) - y_{G_k}\right)^2} \tag{4.16}$$

$$\frac{\partial \hat{Y}(k)}{\partial \hat{y}_B(k)} = \frac{\gamma\left(\hat{y}_B(k) - y_{G_k}\right)}{\left(\hat{x}_B(k) - x_{G_k}\right)^2 + \left(\hat{y}_B(k) - y_{G_k}\right)^2} \tag{4.17}$$

The constant γ in expressions (4.16) and (4.17) is denoted below:

$$\gamma = \frac{10\alpha}{\ln(10)} \tag{4.18}$$

The constructed Jacobian matrix is then used to compute the innovation variance $S(k)$ and the filter gain $K(k)$ as shown below:

$$S(k) = H(k)P_B^-(k)H(k)^T + R(k) \tag{4.19}$$

$$K(k) = P_B^-(k)H(k)^T S(k)^{-1} \tag{4.20}$$

Finally, the measurement innovation and the Kalman Filter gain are used to produce the a posteriori estimate of the state and its associated covariance as follows:

$$X_B^+(k) = X_B^-(k) + K(k)v(k) \tag{4.21}$$

$$P_B^+(k) = (I - K(k)H(k))P_B^-(\mathrm{k}) \tag{4.22}$$

When the network monitoring subsystem detects a handover to a new BTS, the state estimate produced by the BIM is used to initialise the BTS landmark within the map. As explained in Section 4.2.3, the initialisation consists of creating a Landmark Database Entry within the database representing the initial map of landmarks. The CCS system starts a new iteration of the BTS initialisation model to estimate the position of the new serving BTS after the handover event is detected. The EKF iteration starts by initialising the state using the first

GPS sample as shown in (4.10). The state is then updated using the EKF equations as more samples are received until the next handover and so on. If the CID of the newly observed BTS matches that of a landmark already stored in the database, the state of the matching landmark entry is extracted from the database. It is then integrated into the state vector so that the EKF resumes the estimation using new measurements.

As stated previously, the initialisation of a BTS does not only consist of estimating the position of the landmark. The database entry representing the initialised landmark associates mobile location fingerprints to the position of the BTS. These location fingerprints are the very same samples that were used during the BIM calibration phase to initialise the BTS landmark. This fingerprint association process is performed by the BTS initialisation model to prepare the system for the Network Localisation Stage.

4.5 The Network Localisation Filter

This section presents the mathematical formulation of the Network Localisation Filter (NLF), which represents the state space solution performing the proposed EKF-SLAM approach. According to the framework constrains mentioned previously, the constrained Cellular SLAM system builds an initial map of BTS landmarks before tracking the movement of the mobile terminal in real-time. The result of the Initial Mapping Stage is a database of identifiable BTS positions each linked to a list of mobile location fingerprints. Each landmark database entry stores the following information:

- The CID identifying the BTS transmitter.
- The coordinates of the BTS landmark with respect to the global frame F .
- The list of fingerprints collected during the initialisation of the landmark.

Recall from Section 4.2.4 that this initial map is referred to here as the global map which is stored by the application in an auxiliary database. The term auxiliary is used to denote that this list of BTS landmarks is maintained outside the state vector of the EKF-SLAM system. Firstly, this section describes how the state vector is maintained by the NLF in section 4.5.1. It will then describe the fingerprint-based motion model in Section 4.5.2 and the measurement update step in Section 4.5.3.

4.5.1 The State Vector

As introduced previously, the NLF model adopts a local map approach which consists of integrating the states of the landmarks in the vicinity of the mobile terminal. As it is stored in an auxiliary database, the global map resulting from the Initial Mapping Stage is not transferred directly to the SLAM state. By maintaining a limited number of landmark states within the state vector, the computation effort required during the covariance update is significantly reduced. The size of the local map can be chosen to coincide with the number of base stations that are communicating with the mobile terminal. In addition to the serving BTS, up to six neighbour base stations are transmitting signals to the MT. By following the strong trend that the mobile terminal is likely to connect to one of these neighbour base stations, the size of the local map should be greater than 6.

At time k, let $X_{slam}(k)$ be the true state of the SLAM system which contains the mobile terminal state $X_m(k)$ augmented with the local map of n BTS landmark states, each denoted by $X_{b_i}(k)$ for $i = 1, \dots, n$. The true SLAM State has the form:

$$X_{slam}(k) = \begin{bmatrix} X_m(k) \\ X_{b_1}(k) \\ \vdots \\ X_{b_n}(k) \end{bmatrix} \tag{4.23}$$

Thus, the Network Localisation Filter maintains the SLAM State estimates as follows:

$$\hat{X}_{slam}(k) = \begin{bmatrix} \hat{X}_m(k) \\ \hat{X}_{b_1}(k) \\ \vdots \\ \hat{X}_{b_n}(k) \end{bmatrix} \tag{4.24}$$

Let the covariance matrix associated with the SLAM state be defined as:

$$P_{slam}(k) = \begin{bmatrix} P_{mm}(k) & P_{m1}(k) & \cdots & P_{mn}(k) \\ P_{1m}(k) & P_{11}(k) & \cdots & P_{1n}(k) \\ \vdots & \vdots & \ddots & \vdots \\ P_{nm}(k) & P_{n1}(k) & \cdots & P_{nn}(k) \end{bmatrix} \tag{4.25}$$

Where:

- $P_{mm}(k)$ is the covariance matrix of the mobile state estimate $\hat{X}_m(k)$
- $P_{ii}(k)$ is the covariance matrix associated with the i^{th} BTS state estimate $\hat{X}_{b_i}(k)$
- The terms $P_{mi}(k) = P_{im}^T(k)$ consist of the cross-covariance matrices measuring the correlation between the error in the MT and the BTS state estimate

As the mobile terminal can only observe at a given time one single landmark, namely the serving BTS, landmarks are extracted individually from the global map and registered as part of the local map. As introduced in Section 4.2.4, the SLAM state is initialised at the start of the Network Localisation Stage with an initial MT state estimate $\hat{X}_m(0)$ augmented with the first BTS landmark $\hat{X}_{b_1}(k)$, which has been extracted from the database. The Cell ID is used to identify and extract the Landmark Database Entry corresponding to the first serving base

station. Recall that each LDE in the database contains a list of fingerprints each defined in expression (4.9). One of the fingerprints associated with the serving BTS landmark will be used to initialise the state of the mobile terminal $\hat{X}_m(k)$. The fingerprint yielding the smallest Euclidean distance in signal space is considered the best matching fingerprint. The location of the latter is taken as an initial estimate of the mobile state $\hat{X}_m(0)$.

Recall that the position of the ith registered landmark $\hat{X}_{b_i}(k)$ has been estimated by the BTS initialisation model during the Initial Mapping Stage. The BIM reduced the uncertainty of the landmark estimate, which was initialised to coincide with the typical CID proximity sensing error. In this Network Localisation Stage, after the integration of an extracted landmark into the SLAM State, we can assume that the uncertainty of the landmark is less than the typical rms error of the Cell Identification technique described in Section 2.2.1. As a result, the covariance matrix $P_{ii}(k)$ of the extracted BTS landmark is initialised accordingly. The covariance matrix of the mobile state estimate $P_{mm}(k)$ is initialised at time zero taking into consideration the displacement between the initial MT state estimate $\hat{X}_m(0)$ and the first landmark state estimate $\hat{X}_{b_1}(k)$.

The 'nearest neighbour' data association process is executed each time a change in the observed signal strength or CID is detected leading to the extraction of a new fingerprint from the database. The motion model described in the next section uses the new fingerprint to produce the a priori state estimate. If a new CID is observed meaning that the MT is connected to a new serving BTS, the LDE associated with the CID is extracted from the database and integrated into the state vector. Each time a handover occurs, the three-step procedure consisting of CID look-up, LDE extraction and state registration is repeated. The following outline shows how the fingerprint correlation is performed.

Suppose that the LDE corresponding to the observed BTS has M fingerprints. Recall that each fingerprint coincides with a GPS sample that was used during the Initial Mapping Stage to initialise this BTS landmark. As a result, we will denote each fingerprint using the same notation as the GPS sample defined in (4.9). Let Z_i be the ith fingerprint ($i = 1, \dots, M$) consisting of the ground-truth position $G_i \begin{pmatrix} x_{G_i} \\ y_{G_i} \end{pmatrix}$ and the RSS measurement p_{r_i}taken by the MT from the ground-truth. As stated previously, the coordinates of the fingerprint have been converted from the GPS geodetic to Cartesian coordinates defined by the global frame F. Given the signal strength measurement taken by the mobile terminal $Y(k)$, the Euclidean distance function d_{ki} is defined as:

$$d_{ki}(Z_i) = \sqrt{\left(Y(k) - p_{r_i}\right)^2} \qquad (4.26)$$

The database correlation algorithm iterates through the M fingerprints to produce M distance measures. The fingerprint Z_i yielding the smallest distance is considered the nearest neighbour fingerprint matching the current RSS observation. As a result, the system extracts the position G_i from the fingerprint. If the correlation algorithm finds N fingerprints with equal distances, it extracts the corresponding N ground-truth locations G_j for j=1,…,N and computes their mean convex combination as follows:

$$G_{mean} = \begin{pmatrix} \frac{1}{N}\sum_{j=1}^{N} x_{G_j} \\ \frac{1}{N}\sum_{j=1}^{N} y_{G_j} \end{pmatrix} \qquad (4.27)$$

The SLAM state is extended until the limit size of n landmarks is reached. At this stage, the adopted map management process starts monitoring the covariance of each landmark state in the local map. Using the determinant of the covariance matrix as a measure of uncertainty, the landmark state estimate with the lowest uncertainty is removed from the state vector and

reinserted into the database representing the global map. As a result, the Landmark Database Entry corresponding to this landmark is updated with the new state estimate. This LDE is also extended to include the covariance matrix of the updated landmark state. The aim of this extension is to save the error of this landmark state estimate for future observation, extraction and registration of this landmark. Upon re-observing the landmark, the saved covariance matrix is used to refine the SLAM state covariance $P_{slam}(k)$ by integrating it into its corresponding submatrix within $P_{slam}(k)$. It is important to note that there is some information loss associated with the deletion of a landmark state and covariance from the SLAM state and covariance matrix respectively. In fact, the error of this landmark estimate is decorrelated from the rest of the map once the landmark is deleted form the system.

4.5.2 The Process Model

Let the state dynamics of the mobile terminal be described by the following discrete time process model:

$$X_m(k) = f(X_m(k-1), u(k)) + w_p(k) \qquad (4.28)$$

Where:

- f is the non-linear function which models the kinematics of the mobile terminal by linking the past state $X_m(k-1)$to the current one $X_m(k)$ given the control input $u(k)$.
- $w_p(k)$ represents the process noise describing the uncertainties in the control input measurements and the motion model itself.

The Kalman Filter assumes the process noise to be Gaussian distributed with mean zero and covariance matrix $Q(k)$. As a result, the state estimate of the mobile terminal can be predicted as follows:

$$\hat{X}_m^-(k) = f\left(\hat{X}_m^+(k-1), u(k)\right) \tag{4.29}$$

In order to model the dynamics of the mobile user, the Network Localisation Filter exploits the history of the fingerprints extracted using the adopted database correlation algorithm. In fact, the control inputs of the system are inferred from the location fingerprints and consist of the transition distance $d_t(k)$ and the transition bearing $\theta_t(k)$, that is:

$$u(k) = \begin{pmatrix} d_t(k) \\ \theta_t(k) \end{pmatrix} \tag{4.30}$$

The state estimate expressed in (4.29) can thus be rewritten as:

$$\hat{X}_m^-(k) = f\left(\hat{X}_m^+(k-1), d_t(k), \theta_t(k)\right) \tag{4.31}$$

As shown in the previous section, each measurement received by the mobile terminal is processed by the database correlation algorithm to extract a fingerprint location. The state of the mobile terminal is initialised to coincide with the fingerprint location matching the first CID and RSS measurements. When a second fingerprint is extracted from a second RSS/CID measurement, the relative distance and bearing between the two fingerprint locations are computed. Taking the relative displacement between two consecutive fingerprints as the control input, a new a priori state estimate is produced. As illustrated in Figure 4.3, the transition distance $d_t(k)$ consists of the displacement between the previous state at time k-1 and the current state at time k. The transition bearing is the forward azimuth with respect to northing axis of the reference frame F.

Therefore, the a priori estimate of the mobile terminal state $X_m^-(k)$ in the global reference frame F is calculated as follows:

$$\hat{x}_m^-(k) = \hat{x}_m^+(k-1) + d_t(k)\sin\big(\theta_t(k)\big)$$

$$\hat{y}_m^-(k) = \hat{y}_m^+(k-1) + d_t(k)\cos(\theta_t(k)) \qquad (4.32)$$

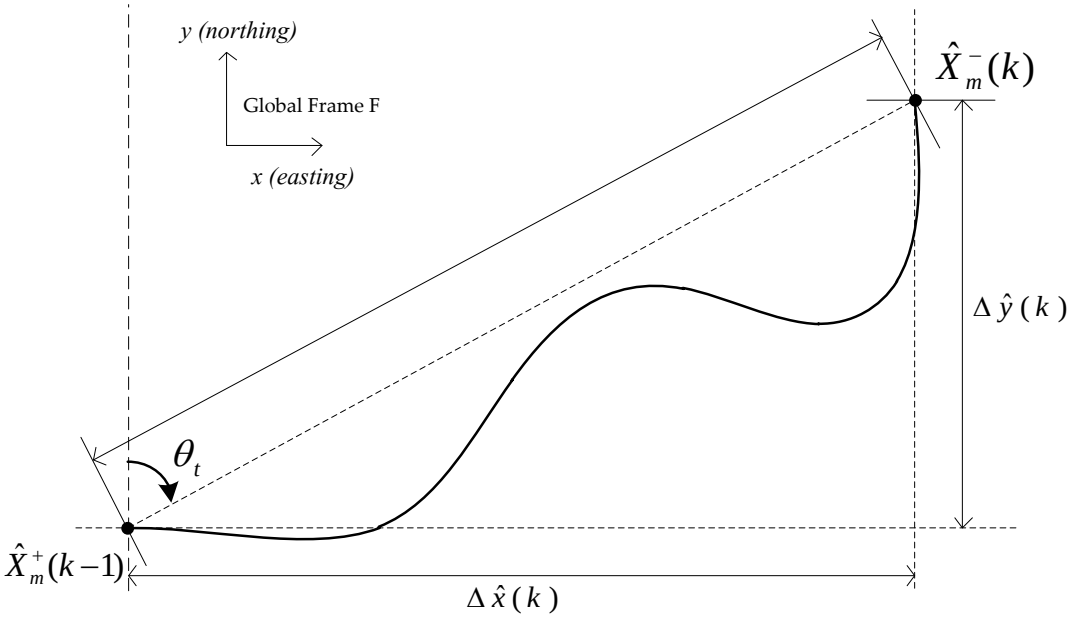

Figure 4.3 The motion model

In order to extend the motion model to predict the whole SLAM state defined in (4.23), the state of the ith landmark within the local map is modeled as:

$$\hat{X}_{b_i}^-(k) = \hat{X}_{b_i}^+(k-1) \qquad (4.33)$$

As the landmark state is also parameterised in easting and northing coordinates, the landmark model is rewritten as:

$$\hat{x}_{b_i}^-(k) = \hat{x}_{b_i}^+(k-1)$$

$$\hat{y}_{b_i}^{-}(k) = \hat{y}_{b_i}^{+}(k-1) \tag{4.34}$$

Thus, the prediction step of the Network Localisation Filter for the whole SLAM system proceeds as follows:

$$\begin{aligned}
\hat{X}_{slam}^{-}(k) &= f\left(\hat{X}_{slam}^{+}(k-1), d_t(k), \theta_t(k)\right) \\
&= \begin{bmatrix} f\left(\hat{X}_{m}^{+}(k-1), d_t(k), \theta_t(k)\right) \\ \hat{X}_{b_1}(k) \\ \vdots \\ \hat{X}_{b_n}(k) \end{bmatrix} \\
&= \begin{bmatrix} \hat{x}_{m}^{+}(k-1) + d_t(k)\sin\left(\theta_t(k)\right) \\ \hat{y}_{m}^{+}(k-1) + d_t(k)\cos(\theta_t(k)) \\ \hat{x}_{b_1}^{+}(k-1) \\ \hat{y}_{b_1}^{+}(k-1) \\ \vdots \\ \hat{x}_{b_i}^{+}(k-1) \\ \hat{y}_{b_i}^{+}(k-1) \end{bmatrix}
\end{aligned} \tag{4.35}$$

As each landmark state is constant in the prediction step, the covariance prediction only affects the mobile state. The propagation of the SLAM state covariance through the process model takes into account the uncertainty of the current mobile state estimate, as well as the error in the transition distance and bearing measurements. The covariance prediction equation reads as:

$$P_{slam}^{-}(k) = F_X(k)P_{slam}^{+}(k-1){F_X}^{T}(k) + F_u(k)U(k){F_u}^{T}(k) + Q(k) \tag{4.36}$$

Where:

- $F_X(k)$ is the Jacobian of the function *f* approximating the uncertainty propagation about the a posteriori state estimate of the previous step $\hat{X}^+_{slam}(k-1)$.
- $F_u(k)$ is the Jacobian of *f* which approximating the uncertainty propagation about the control input vector u(k) containing the transition distance $d_t(k)$ and the transition bearing $\theta_t(k)$.
- U(k) is the covariance of the vector u(k) defined by the matrix $\begin{bmatrix}\sigma_d^2 & 0\\ 0 & \sigma_\theta^2\end{bmatrix}$, in which σ_d^2 is the variance associated with the distance measurement and σ_θ^2 is the variance associated with the bearing measurement.
- Q(k) is the covariance matrix of the process noise $w_p(k)$ described in (4.28).

The Jacobian matrix $F_X(k)$ holds the partial derivatives of the predicted SLAM state $\hat{X}^-_{slam}(k)$ with respect to the mobile state and each landmark state as follows:

$$F_X(k) = \begin{bmatrix}\frac{\partial \hat{X}^-_{slam}(k)}{\partial \hat{X}^+_m(k-1)} & \frac{\partial \hat{X}^-_{slam}(k)}{\partial \hat{X}^+_{b_1}(k-1)} \cdots & \frac{\partial \hat{X}^-_{slam}(k)}{\partial \hat{X}^+_{b_n}(k-1)}\end{bmatrix}$$

$$= \begin{bmatrix}\frac{\partial \hat{X}^-_m(k)}{\partial \hat{X}^+_m(k-1)} & \frac{\partial \hat{X}^-_m(k)}{\partial \hat{X}^+_{b_1}(k-1)} & & \frac{\partial \hat{X}^-_m(k)}{\partial \hat{X}^+_{b_n}(k-1)}\\ \frac{\partial \hat{X}^-_{b_1}(k)}{\partial \hat{X}^+_m(k-1)} & \frac{\partial \hat{X}^-_{b_1}(k)}{\partial X^+_{b_1}(k-1)} & \cdots & \frac{\partial \hat{X}^-_{b_1}(k)}{\partial \hat{X}^+_{b_n}(k-1)}\\ \vdots & \vdots & \ddots & \vdots\\ \frac{\partial \hat{X}^-_{b_n}(k)}{\partial \hat{X}^+_m(k-1)} & \frac{\partial \hat{X}^-_{b_n}(k)}{\partial \hat{X}^+_{b_1}(k-1)} & & \frac{\partial \hat{X}^-_{b_n}(k)}{\partial \hat{X}^+_{b_n}(k-1)}\end{bmatrix}$$

$$= \begin{bmatrix} I_2 & 0_{2,2} & \cdots & 0_{2,2}\\ 0_{2,2} & I_2 & \cdots & 0_{2,2}\\ \vdots & \vdots & \ddots & \vdots\\ 0_{2,2} & 0_{2,2} & \cdots & I_2\end{bmatrix} \qquad (4.37)$$

As shown in expression (4.37), the Jacobian matrix $F_X(k)$ of the entire slam state is equal to the identity matrix. Thus, the covariance propagation equation (4.36) can be simplified in (4.38).

$$P^-_{slam}(k) = P^+_{slam}(k-1) + F_u(k)U(k)F_u(k)^T(k) \qquad (4.38)$$

Similarly, the Jacobian matrix of the control inputs $F_u(k)$ is constructed as follows:

$$F_u(k) = \begin{bmatrix} \frac{\partial \widehat{X}^-_{slam}(k)}{\partial d(k)} & \frac{\partial \widehat{X}^-_{slam}(k)}{\partial \theta(k)} \end{bmatrix}$$

$$= \begin{bmatrix} \frac{\partial \widehat{X}^-_{m}(k)}{\partial d(k)} & \frac{\partial \widehat{X}^-_{m}(k)}{\partial \theta(k)} \\ \frac{\partial \widehat{X}^-_{b_1}(k)}{\partial d(k)} & \frac{\partial \widehat{X}^-_{b_1}(k)}{\partial \theta(k)} \\ \vdots & \vdots \\ \frac{\partial \widehat{X}^-_{b_n}(k)}{\partial d(k)} & \frac{\partial \widehat{X}^-_{b_n}(k)}{\partial \theta(k)} \end{bmatrix}$$

$$= \begin{bmatrix} \sin(\theta(k)) & d\cos(\theta(k)) \\ \cos(\theta(k)) & -d\sin(\theta(k)) \\ 0_{2,1} & 0_{2,1} \\ \vdots & \vdots \\ \vdots & \vdots \end{bmatrix} \qquad (4.39)$$

4.5.3 The Measurement Update Step

In the proposed CCS approach, the initialisation of new landmarks is performed offline during the Initial Mapping Stage. Therefore, all the measurements received by the Network Localisation Filter are associated with an existing landmark within the global map and integrated into the SLAM State vector. The CID is used for data association. Similarly to the BTS initialisation model, the Network Localisation Filter adopts the path loss model described in Section 4.3 to map the state to a signal strength observation. The NLF uses the observation model to correct the predicted state of the MT and update the local map of BTS landmarks simultaneously. By adopting the typical EKF-SLAM measurement update, the RSS

observation is taken by the mobile terminal relative to one of the landmarks registered as part of the SLAM state vector. If it has not been observed previously and is not part of the local map, the landmark is extracted from the database.

Let the nonlinear function h be the observation model representing the propagation model equation (4.4), which maps the true SLAM state denoted in (4.24) to the true RSS measurement $Y(k)$ as follows:

$$Y(k) = h\big(X_{slam}(k)\big) + w_m(k) \tag{4.40}$$

In expression (4.40), $w_m(k)$ denotes the measurement noise pervading the signal strength measurement. It accounts for both the multipath distortion in the RSS measurement as well as the error in the observation model h predicting the measurement. $w_m(k)$ is assumed Gaussian distributed with mean zero and covariance R and uncorrelated with the process noise $w_p(k)$ described in (4.28). As a result, the RSS observation can be predicted using the adopted observation model h as follows:

$$\hat{Y}(k) = h\big(X^-_{slam}(k)\big) \tag{4.41}$$

Let$\hat{X}_{b_i}(k) = \begin{bmatrix} x^-_{b_i}(k) & y^-_{b_i}(k) \end{bmatrix}^T$ be the state estimate of the ith registered BTS being observed by the MT whose a priori estimate is $\hat{X}^-_m(k) = [x^-_m(k) \quad y^-_m(k)]^T$.

Given the displacement $\hat{D}_{im}(k)$ between the estimated mobile and landmark states, the propagation model expressed in (4.4) predicts the RSS observation relative to the ith BTS as follows:

$$\hat{Y}_i(k) = p_t - \beta - \ 10\alpha\, log\big(\hat{D}_{im}(k)\big) \tag{4.42}$$

With,

$$\widehat{D}_{im}(k) = \sqrt{\left(x_{b_i}^{-}(k) - x_m^{-}(k)\right)^2 + \left(x_{b_i}^{-}(k) - x_m^{-}(k)\right)^2} \tag{4.43}$$

Note that subscript i is used to denote the observed BTS landmark. As it is a function of the mobile and landmark states, the RSS prediction equation (4.42) lends itself to the observation model function h in (4.41). As a result, the NLF can use expression (4.42) to predict the observation and update the SLAM State by applying the linear approximation of the model with respect to SLAM state estimates. As a single RSS measurement is processed by the EKF at a time, the underlying Jacobian matrix $H(k)$ has the form:

$$H(k) = \left[\frac{\partial \widehat{Y}_i(k)}{\partial \hat{X}_m^{-}(k)} \quad \frac{\partial \widehat{Y}_i(k)}{\partial \hat{X}_{b_1}^{-}(k)} \quad \cdots \quad \frac{\partial \widehat{Y}_i(k)}{\partial \hat{X}_{b_n}^{-}(k)}\right] \tag{4.44}$$

Since the RSS observation is related to a single landmark, namely the serving BTS, the Jacobian matrix $H(k)$ contains a large number of zeros which correspond to the state derivatives of the remaining (n-1) unobserved landmarks. The Jacobian is computed below:

$$H(k) = \left[\frac{\partial \widehat{Y}_i(k)}{\partial \hat{X}_m^{-}(k)} \quad 0 \quad \cdots \quad 0 \quad \frac{\partial \widehat{Y}_i(k)}{\partial \hat{X}_{b_i}^{-}(k)} \quad 0 \quad \cdots\right] \tag{4.45}$$

The derivative of the observation model with respect to the mobile state estimate $\hat{X}_m^{-}(k)$ reads as:

$$\begin{aligned}\frac{\partial h}{\partial X_m^{-}(k)} &= \left[\frac{\partial \hat{Y}(k)}{\partial x_m^{-}(k)} \quad \frac{\partial \hat{Y}(k)}{\partial y_m^{-}(k)}\right] \\ &= \left[\frac{\gamma\left(\hat{x}_{b_i}^{-}(k) - \hat{x}_m^{-}(k)\right)}{(\widehat{D}_{im}(k))^2} \quad \frac{\gamma\left(\hat{y}_{b_i}^{-}(k) - \hat{y}_m^{-}(k)\right)}{(\widehat{D}_{im}(k))^2}\right]\end{aligned} \tag{4.46}$$

Similarly, the derivative of the observation model with respect to the serving BTS state estimate $\hat{X}_{b_i}^{-}(k)$ reads as:

$$\frac{\partial h}{\partial X_{b_i}^{-}(k)} = \left[\frac{\partial \hat{Y}(k)}{\partial x_{b_i}^{-}(k)} \quad \frac{\partial \hat{Y}(k)}{\partial y_{b_i}^{-}(k)}\right]$$

$$= \left[\frac{\gamma\left(\hat{x}_m^{-}(k) - \hat{x}_{b_i}^{-}(k)\right)}{(\widehat{D}_{im}(k))^2} \quad \frac{\gamma\left(\hat{y}_m^{-}(k) - \hat{y}_{b_i}^{-}(k)\right)}{(\widehat{D}_{im}(k))^2}\right] \tag{4.47}$$

The constant γ in expressions (4.46) and (4.47) is denoted below:

$$\gamma = \frac{10\alpha}{\ln(10)} \tag{4.48}$$

The EKF equations which update the SLAM state proceed as follows:

$$S(k) = H(k)P^{-}(k)H(k)^T + R(k) \tag{4.49}$$

$$K(k) = P^{-}(k)H(k)^T S(k)^{-1} \tag{4.50}$$

$$X_{slam}^{+}(k) = X_{slam}^{-}(k) + K(k)\left(Y_i(k) - \widehat{Y}_i(k)\right) \tag{4.51}$$

$$P_{slam}^{+}(k) = \left(I - K(k)H(k)\right)P_{slam}^{-}(k) \tag{4.52}$$

CHAPTER 5 - Software Design

5.1 Introduction

The emergence of smartphones with the multi-touch interface[23] and the ability to download and install applications directly into the device without connecting to a PC changed the definition of the term "smartphone". Indeed, handsets which were considered smartphones few years ago due to their PC-like operating system are now considered feature phones as they lack this user-friendly interface and increased mobility of downloading applications on the go. As a result, Location-Based Services quickly became popular due to the wide variety of location-aware applications which are not restricted to turn-by-turn navigation but include other services such as transport information, mobile banking, mobile gaming …etc.

This chapter is concerned with the high-level software design of the positioning solutions presented in this thesis, namely, the static positioning system described in Chapter 3 and the Constrained Cellular SLAM (CCS) system described in Chapter 4. As presented in Chapter 6, these software solutions are mobile applications that have been used to perform positioning experiments and evaluate the proposed positioning systems. The static EKF system is implemented by the "GSM Mobile Locator" LBS application whereas the CCS

[23] Beginning with Apple's iPhone in 2007.

system is implemented by the Constrained Cellular SLAM application. "GSM Mobile Locator" and the CCS application are described in Section 5.2 and Section 5.3 respectively. This chapter presents the high-level UML design of the proposed positioning systems and considers the UML use case model only. The design and implementation models of the UML design are not considered in this thesis. As a result, all the UML diagrams depicted in this chapter are initial diagrams from the use case model.

5.2 GSM Mobile Locator Application

Recall from Chapter 3 that the static positioning system employs an Extended Kalman Filter algorithm which was developed in two stages. The first stage of this EKF-based positioning system was developed as part of the Author's MEng project [Ham05]. It used a range-only observation model and relied on translating signal strength measurements to distance measurements via generic propagation models prior the application of the EKF positioning process. During the Author's research presented in this thesis, the second stage of the EKF positioning system was implemented with two major improvements:

- The first consists of the use of a calibrated propagation model to predict the RSS measurements as accurately as possible within the environment of the positioning trials. With a simplified path loss equation, the range-based observation model no longer requires the intermediate step of translating RSS measurements to distance measurements. This range-only EKF system is described in Section 3.3.
- The second consists of extending the EKF observation model to handle bearing measurements in order to improve the positioning outcome in terms of accuracy.

As outlined in Section 3.4, bearing observations are derived from the sector configuration setup of reference base stations.

The software application implementing the static positioning system presented in Chapter 3 is referred to in this thesis as "GSM Mobile Locator". This application implemented the first stage of the positioning system during the Author's MEng project [Ham05]. The system's second stage, which is developed as part of the work presented in this thesis, consists of updating the "GSM Mobile Locator" application to implement the functionality of the two static EKF models described in Chapter 3. As stated previously, theses positioning systems require an initial BTS identification survey to associate each BTS location with its relevant CID code(s). The locations of the surveyed base stations are retrieved from Ofcom's Sitefinder website, which also provides us with some details regarding the transmitter mounted on each site. These details include the height, transmitted power and frequency, but not the associated CID code(s). As detailed in Section 6.4, this survey is conducted using a separate engineering network monitoring tool called Netmonitor, which displays the CID code of the serving base station, measures the received signal strength and shows the Network Measurement Report. The BTS identification process generates a database of BTS entries which is linked to the GSM Mobile Locator application in order to conduct positioning experiments. This database stores all the BTS information required for the positioning process, namely the latitude and longitude coordinates, the CID code(s), the height and transmitter power.

5.2.1 LBS Functionality

The "GSM Mobile Locator" application was implemented in C# and deployed on a PDA using Microsoft Visual Studio.NET 2003. It was designed as a location-based service (LBS) application to provide the user with practical information based on the location determined

using the static EKF positioning method. GSM Mobile Locator is a .NET application that accesses the Microsoft MapPoint Web Service (MWS) in order to add location-based functionality to the positioning system. MWS an XML service with a SOAP API comprised of four constituent services: finding locations, rendering maps, calculating routes, and a set of common utility function objects and methods. As illustrated in figure 5.1, MWS allows our GSM Mobile Locator application to:

- Display on a map the position of the mobile terminal and each base station used as reference points for positioning.
- Find nearby points-of-interest (POI) and display them on the map.
- Compute and visualise routes selected by the user.

The platform on which GSM Mobile Locator is deployed (Windows Mobile 2003) does not allow us to implement the process of observing CID codes and measuring the received signal strength. For this reason, a network monitoring tool called Netmonitor is used to obtain the measurements required to conduct our positioning trials. Therefore, GSM Mobile Locator and Netmonitor will be used simultaneously to test the performance of the range-only and range-bearing EKF models described in Chapter 3.

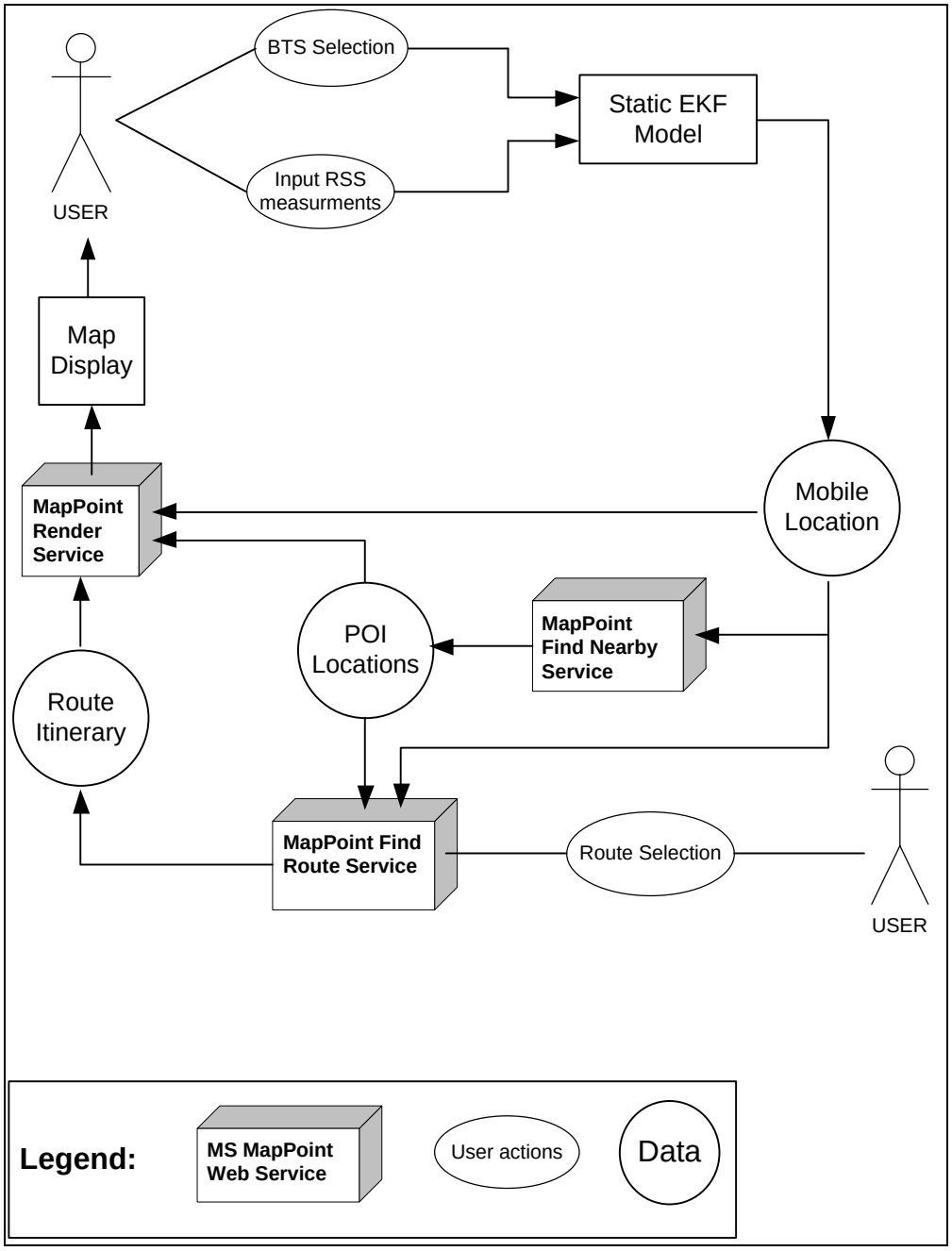

Figure 5.1 GSM Mobile Locator interation with Mappoint Web Service

5.2.2 Use Case Scenario

When the application is started to conduct a positioning experiment, the user should select which of the range-only or range-bearing EKF models will be used as the positioning process. The user should also choose which propagation model will be used as an observation model for the EKF positioning process.

During the experimental evaluation of the system in Section 6.4, positioning outcomes will be compared according to which propagation model was used to define the distance relationship between the mobile terminal and reference base stations. During the length of the experiment, the network monitoring tool is used to observe the Network Measurement Report which displays the downlink signals transmitted by hearable base stations. Using to the observed CID codes, the base stations which can be identified from the survey database will be selected for the positioning trial. In fact, the application's graphical user interface (GUI) provides the user with a list view of the surveyed base stations.

The user proceeds by selecting a single BTS at a time and entering its associated RSS measurement as displayed in Netmonitor's measurement report [Ham06]. In case a generic propagation model is chosen as the EKF's observation model, the user should use the propagation model view of the application to convert the measured RSS to a distance observation. The path loss equation of generic models also requires the user to specify the type of area as well as the values other parameters such as the BTS height, MT height and frequency. In case a calibrated propagation model is selected, the user should enter the calibrated parameters, namely, the path loss exponent and absolute loss value, so that the application sets the observation model of the EKF algorithm. Moreover, the user should directly link the RSS observation to the selected BTS from the list view. For evaluation purposes, the user should also specify the exact location of the experiment with the help of a GPS device.

Once measurements have been allocated to at least two distinct base stations, the user can activate the EKF positioning process to initialise the mobile position estimate. The latter should be displayed on a map rendered using the web service, which the user can navigate through by zooming and panning. The system should then locate the nearest points-of-

interest (POI) from the computed mobile position and displays them on the downloaded map. Moreover, the user can request a route calculation by selecting the route's starting and ending points among the list of POI. When signal strength measurements vary or additional base stations appear in the NMR, the user can enter new measurements to update the MT position estimate. The use case scenario described in this section is illustrated in figure 5.2.

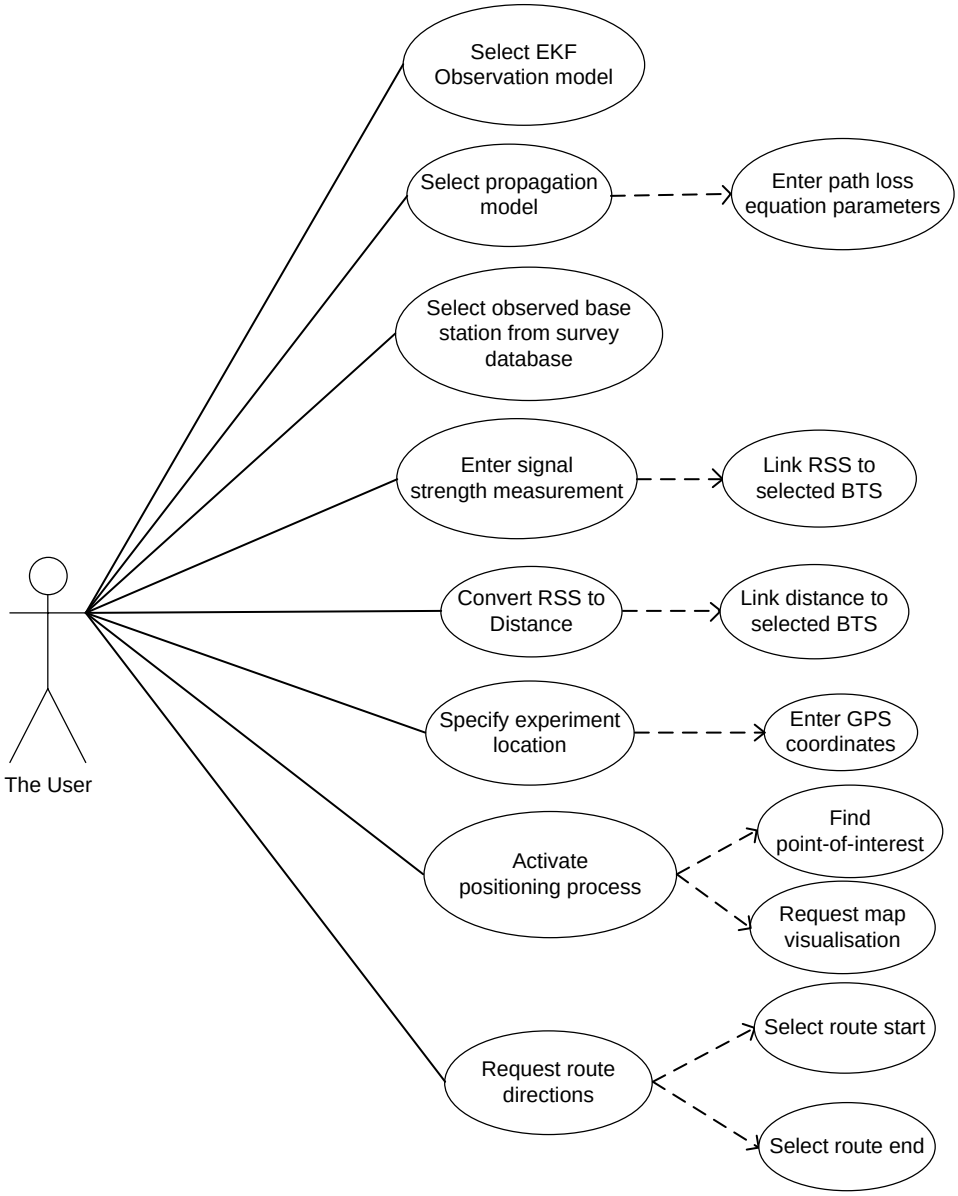

Figure 5.2 GSM Mobile Locator Use Case Diagram

5.2.3 Identification of Classes

The noun identification technique is used in this section to identify key domain classes from the use case scenario described in the previous section. The nouns and phrases that are potential class identifiers are: base stations, database, system, graphical user interface, propagation model, EKF algorithm and points-of-interest. Because of the visual nature of this application and the extensive use of its graphical user interface, the class "MobileLocatorInterface" is designed to implement the GUI functionality as well as the system's control tasks instead of having a separate controller class. The control tasks consist of the following:

- accessing the database of base stations and retrieving the details of selected BTS,
- setting propagation model parameters according to the user selection
- communicating with the EKF positioning process to integrate measurements, initialise/update the mobile terminal position and retrieve the positioning result.
- accessing the MapPoint Web Service to download maps, find POI and calculate routes.

The identified classes are briefly described below:

- **BTS class:** represents a single base-transceiver station and holds the details in its instance fields i.e. latitude, longitude, height, transmitter power, street name (used to discriminate between base stations). An instance of this class is created by **MobileLocatorInterface class** for each base station used during the positioning experiments.

- **PropagationModels Class:** responsible for MT-BTS distance calculation using a selected generic propagation model among Hata, Extended Hata and CCIR. If the calibrated propagation model has been selected for the experiment, the parameters of the path loss equation are set by the user via the MobileLocatorInterface class.
- **KalmanFilter Class:** responsible for implementing the EKF static positioning system described in Chapter 3. It includes the EKF recursive algorithm which iterates through the list of base stations and updates the estimate at each time the user enters a new RSS measurement.

The interaction between these classes is illustrated by the initial UML class diagram depicted in figure 5.3.

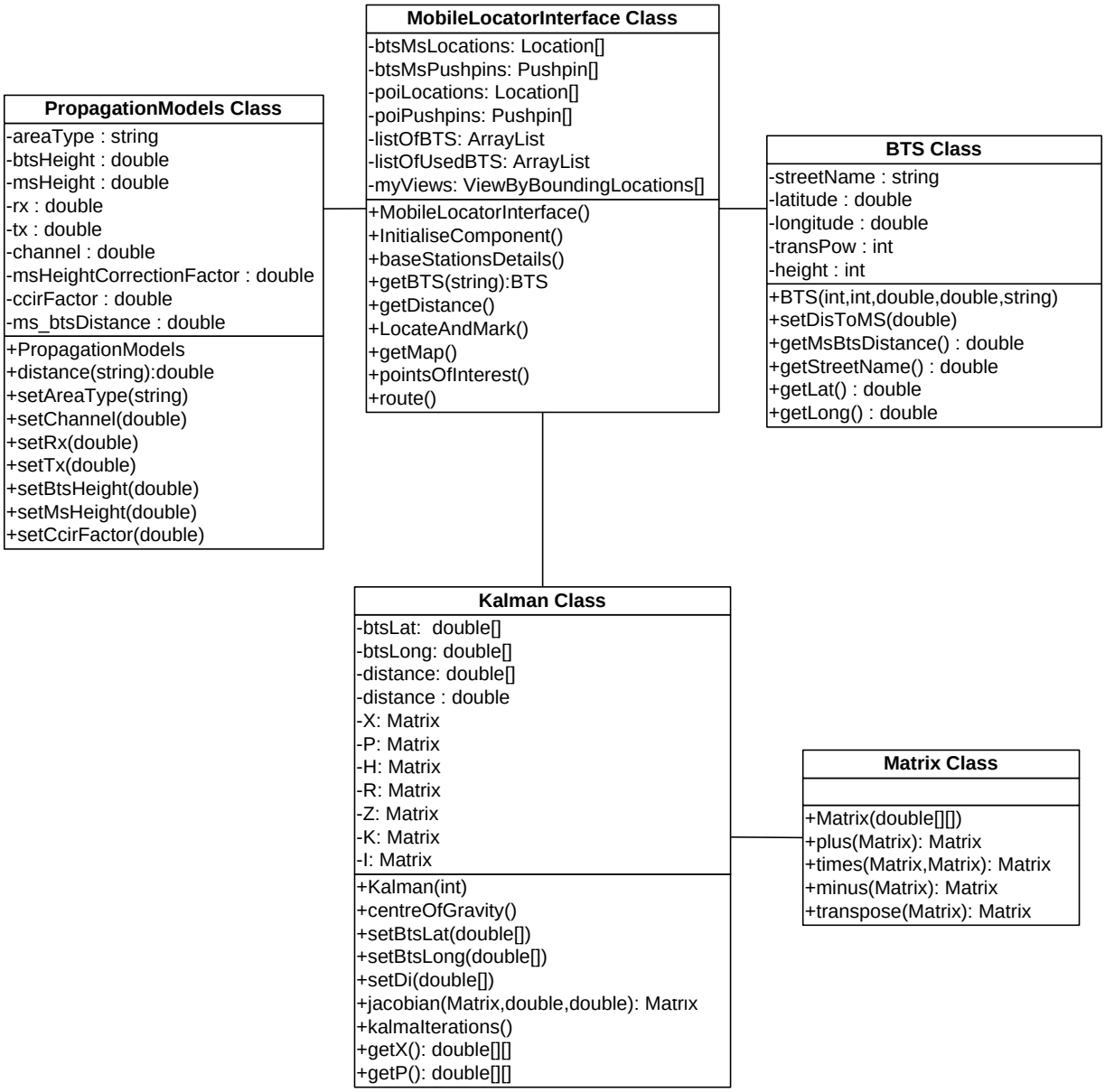

Figure 5.3 GSM Mobile Locator Initial Class Diagram

5.3 Constrained Cellular SLAM Application

As introduced previously, the Constrained Cellular SLAM system aims to overcome the need to rely on commercial or third-party databases of BTS location and CID information required to implement mobile Location–Based Services. By adopting a Simultaneous Localisation And Mapping approach, CCS allows third-party developers to build their own map of base stations for use as reference location information required in LBS application development. Moreover, the CSS methodology has been developed to run on low-cost smartphones or feature phones as they are still sold in higher number than state-of-the-art smartphones.

The CCS system has been deployed on a Symbian OS powered Nokia smartphone with built-in GPS. It has been implemented in Symbian C++ which is an object-oriented language derived from C++. This section presents the design of the software implementing Cellular SLAM using UML. In terms of software development, the CCS application represents an extension of the BTS Locator program which was developed during the early stages of this research in order to map base station locations. The BTS Locator application implements the monitoring of GSM signals as well as GPS position retrieval as perquisite tasks to apply the SLAM methodology. In fact, the functionality of the BTS Locator application coincides with the map building stage of the Constrained Cellular Slam system.

Apart from the Symbian OS smartphone itself, the only required hardware is a GPS receiver. Only the Cell Identity code (CID) identifying the serving base station and its associated received signal strength (RSS) can be retrieved from the device. In fact, the capability of the Symbian OS platform restricts the application to access the Network Measurement Report and retrieve CID and RSS measurements from neighbour base stations.

Another implementation related restriction affecting the adoption of a SLAM-based approach consists of the lack of mobility information such as the orientation, velocity and acceleration of the smartphone user. In order to build a map of the cellular network and use it to estimate the position of the mobile terminal, a constrained SLAM methodology is proposed in this thesis which interleaves the map building and localisation tasks. A two-stage approach is therefore adopted so that a Constrained Cellular SLAM system can be implemented without relying on the integration of external measurements, in other words, without using separate network monitoring tools or dead reckoning devices. As current smartphones are equipped with motion sensors such as accelerometers and gyroscopes, the proposed cellular SLAM methodology can be extended to exploit motion sensing capability in the future, as discussed in Chapter 7.

5.3.1 Requirement Analysis

From the structure of Cellular SLAM, the domain model of the system consists of the following functional requirements:

5.3.1.1 Network monitoring

- The application needs to access the phone's modem to retrieve the CID of the serving base station as well as the received signal strength (RSS).
- It must detect cell handovers and signal strength variations as soon as they occur.
- All this data should be displayed to the user on the smartphone's screen.

5.3.1.2 GPS Measurement

- GPS position data must be retrieved from the built-in GPS device.

- The application should allow the user to request this data when needed or at fixed time intervals using the application's menu commands.

5.3.1.3 Sampling Process

- The exploration stage of cellular slam requires a sampling process which uses GPS and GSM network observations to estimate the position of BTS landmarks.
- Each GPS position fix should be linked to the observed CID and RSS and form a position sample.
- A sample should be created when a GPS position fix is obtained while network monitoring is active. This implies that the application should retrieve GPS and network measurements simultaneously.
- Each position sample is then taken a location fingerprint associated with the initialised base station which communicates with the smartphone.
- The sampling process should stop taking measurements while the smartphone is stationary in order to avoid redundant fingerprints of the same location.

5.3.1.4 BTS Landmark Initialisation

- Each time a new sample is retrieved, it is used by an Extended Kalman Filter model to estimate the position of the serving BTS landmark.
- During the Initial Mapping Stage, the system should synchronize the operation of the EKF with the location fingerprinting task required to prepare the system for its network localisation stage.
- When the mobile switches to a different BTS, the system should detect the change in the observed Cell Id as soon as it occurs.

- As a result of the handover, the system should stop the sampling process.
- The Initial Mapping Stage for each trial area where the system will be evaluated should be conducted in several surveys in order to progressively build the map of the GSM network. As a result, the user should be able to save the map of initialized base stations at any time and access the database at the start of future surveys.

5.3.1.5 EKF-SLAM

- The application should implement the extended Kalman Filter (EKF) responsible for maintaining the state of the SLAM system (the SLAM state).
- The EKF uses the adopted observation model to update the mean and covariance of the augmented SLAM state which combines the mobile state and the registered landmark states.
- Using the map built during the exploration stage, the system should be able to estimate the position of the smartphone by identifying the base station through CID observation and by measuring the received signal strength.
- The observed BTS has one or more mobile position fingerprints collected during the exploration stage. The system should implement the nearest neighbour association method described in Section 4.5 to retrieve the fingerprint position which best matches the measurement
- The mobile position fingerprint is used by the EKF process model to predict the state of the mobile terminal.
- The signal strength measurement is then used to update the entire SLAM state.

5.3.2 The Use Case Model

The following user scenario description is derived from the above requirement analysis and illustrated by the use case diagram of Figure 5.4.

Using the phone's keypad, the user starts the application and activates the network monitoring process, which consists of observing the changes in the Cell ID and RSS. Before initiating the sampling process at the start of an Initial Mapping Stage survey, the user decides whether to create a new map of base stations to start a new survey or to retrieve an existing map from the smartphone's memory to continue an existing survey. While walking or driving a vehicle, the user can request GPS position measurements in order to collect the position samples. The user can also activate the period timer which generates successive GPS updates at fixed time intervals. Whilst waiting for a position fix, the user can cancel the request or disable the update process if already enabled. The system automatically executes the EKF localisation algorithm to estimate the landmark position each time a new GPS sample is collected. This is illustrated by the <<extends>> arrow in the use case diagram of Figure 5.4.

In the uses case diagram of Figure 5.4, note the system's boundary which separates the user's actions from the processes performed by the system. Finally, the network positioning stage can be started by the user to estimate the position of the mobile using the map of landmarks resulted from the exploration stage.

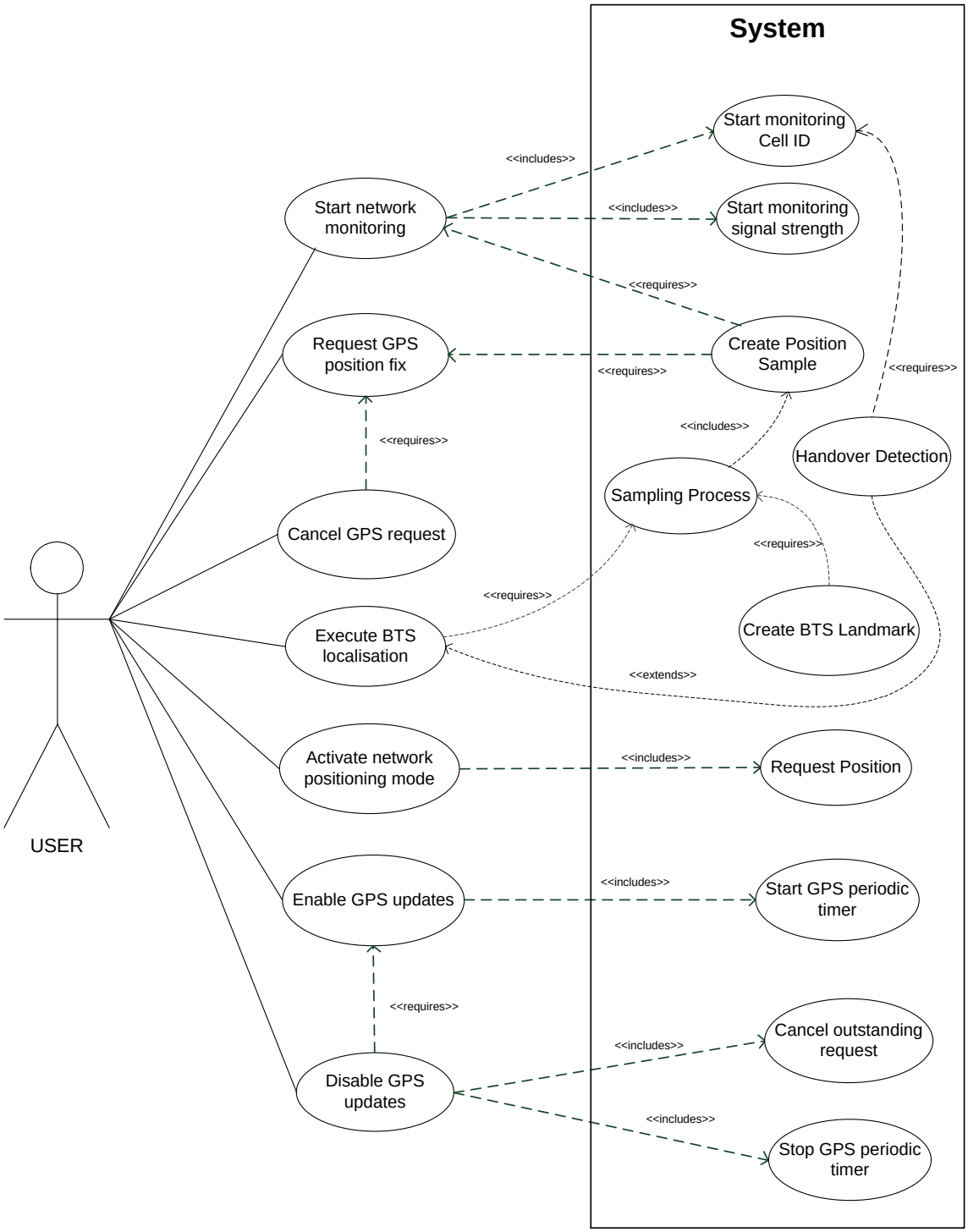

Figure 5.4 CCS Application Use Case Diagram

5.3.2.1 Identification of classes

In order to facilitate the process of identifying key domain classes, we named each task of the above requirement analysis and then use the noun identification technique. Table 1 shows the list of all the nouns and phrases in each requirement in the order of their occurrences. Only the potential class identifiers are listed after removing the candidates which are clearly inappropriate.

Table 5.1 List of candidate class identifiers

Task	**Potential Class identifiers**
Network monitoring	Application, modem, base station, screen
GPS Measurement	GPS position, GPS device, time intervals, menu commands
Sampling Process	GPS position, propagation model, sample, system, list of samples, base station
BTS Localisation	BTS, system, sampling process, Landmark, menu commands
Map Management	Application, map management, landmark
Extended Kalman Filter	Application, extended Kalman Filter, mobile state, landmark state, fingerprinting process, position fingerprint, landmark
Mobile Position Estimation	Map, system, position, base station, position fingerprint, proximity sensing

In the above requirement analysis, the terms application and system can either refer to the model of the system responsible for performing the required tasks, or the interface of the system which allows the user to interact with the system. The system's model should be implemented by the control class responsible for managing the operations of other classes. Since the name of our system is 'Cellular SLAM', we should call the control class 'CellularSLAMControl'.

The term control is one of the three stereotypes used in UML. The other stereotypical classes consist of the boundary and entity classes. The boundary classes represent the

interface to the user as well as the systems external to our system. In table 1, 'screen' and 'menu command' are the identifiers referring to the user interface classes but they are not themselves suitable class names. For example, 'UserInterfaceView' is a more adequate name for the class responsible for displaying information and 'UserInterfaceControl' can be the class receiving user commands. The structure of the graphical user interface (GUI) is outside the scope of use case modeling. Therefore, the GUI should be represented with one class 'UserInterface' at this stage.

The systems external to the application itself consist of the GPS device and the phone's modem. Boundary classes should be implemented to allow the control class to access these systems. The class responsible for retrieving CID and RSS from the modem can be called NetworkMonitor. The propagation model responsible for deriving range measurements from signal strength measurements should be implemented as an entity class. We chose the name 'GPS positioner' to represent the class responsible for accessing GPS information and the name 'GpsTimer' to represent the entity class responsible for the generation of GPS updates. The entity classes are responsible for implementing the important operations of the system. Cellular SLAM has two EKF algorithms which can be included in the entity class 'KalmanFilterSLAM. Entity classes are also used to instantiate objects encapsulating a large collection of data. In our system, samples are such objects as they hold the position measured by the GPS device, the cell ID of the BTS, RSS and its associated MS-BTS range. The class 'PositionSample' will be used to create sample objects as part of the sampling process. Similarly, the base station or landmark should be represented by the class 'Landmark' to create objects encapsulating the position of the BTS and its associated data. .i.e. the CID, the covariance matrix of the estimate and the number of samples used to produce the estimate.

As described in task 6, the created landmark should also be linked to the mobile position updated by the Kalman Filter. The updated MS position becomes a position fingerprint associated with the landmark object. 'PositionFingerprint' is therefore an appropriate class identifier. During the network localisation stage of the system, a proximity sensing algorithm is performed to estimate the mobile position. Since the fingerprint objects are owned and maintained by the landmark object, this proximity sensing algorithm should be implemented in the Landmark class, rather than in a separate class. Table 5.1 shows the initial identified classes listed according to their stereotypes.

Table 5.2 CCS Class Names

Stereotype	**Classes**
Boundary	*UserInterface, NetworkMonitor, GpsPositioner*
Control	*CellularSLAMControl*
Entity	*PositionSample, GpsTimer, KalmanFilterSLAM, Landmark, PropagationModel, PositionFingerprint*

5.3.2.2 CRC cards

Once classes have been identified, CRC cards can be used to show the responsibilities and collaborators of each class. The responsibilities describe the role and operations carried out by the class at a high level, while the collaborators represent the other classes interacting with the class. Although CRC cards are not part of the UML design, they are useful when identifying the responsibilities of classes and their associations. They also provide insights on the quality of the design as they help avoid low cohesion and high coupling.

UserInterface	
Responsibilities	**Collaborators**
This class creates the graphical user interface (GUI) of the application. It allows the user to issue commands to the systems which will be handled by the control class CellularSLAMControl. The latter handles the operations and sends information to be displayed by the GUI.	CellularSLAMControl

NetworkMonitor	
Responsibilities	**Collaborators**
This class provides the system access to the GSM network in order to retrieve the cell id of the serving base station and the received signal strength. Once network monitoring is enabled by the user, this class is used by the CellularSLAMControl class to send messages to the telephony subsystem requesting the network information. After receiving the data from the telephony server, the NetworkMonitor class forwards the data to the control class.	CellularSLAMControl

GpsPositioner	
Responsibilities	**Collaborators**
This class is responsible for obtaining GPS position data from the built-in GPS module upon receiving requests from the user interface via the control class. On startup, CellularSLAMControl instantiates a GpsPositioner object which enables the GPS module and connects to it. The object can then request a GPS measurement from the module and wait while the GPS device connects to the satellites and compute the position fix. Once produced, the position data is sent back to the control class.	CellularSLAMControl

PositionSample	
Responsibilities	**Collaborators**
This class represents a sample collected as part of the exploration stage of the system. A position sample is created by combining the measured GPS latitude and longitude coordinates with network information including the CID, RSS and MS-BTS distance. The PositionSample class therefore groups all the data together as attributes and is instantiated by the control class when a GPS position fix is produced. The PositionSample object is constructed by combining the GPS position with the network data observed at the time of the position fix.	CellularSLAMControl

PropagationModel	
Responsibilities	**Collaborators**
This class implements our propagation model described in Chapter Section 2.4. The class uses the model's path loss equation to compute the distance between the mobile phone and the serving bases station using the signal strength as measurement and the transmitted power the value of which has been calibrated as part of the model's development. This class is used by the control class to translate RSS measurements to MS-BTS range observations each time the signal strength changes.	CellularSLAMControl

MobileFingerprint	
Responsibilities	**Collaborators**
This class represents a mobile position fingerprint which consists of the mobile state position updated by the KalmanFilterSLAM class following each landmark localisation. The state pose or mobile position fingerprint is constituted of the following attributes: - The position of the mobile position updated by the Kalman Filter. - The average of the signal strength measurements associated with the landmark position estimate. - The determinant of the innovation covariance matrix used in the measurement update stage of the EKF to update the SLAM state vector. KalmanFilterSLAM instantiates this class and adds the created object to the list of MobileFingerprint objects. This list is associated with the landmark that has been recently initialised.	KalmanFilterSLAM Landmark

Landmark	
Responsibilities	**Collaborators**
This class represents a base station landmark that has been initialised as part of the mapping process. It includes the following attributes: the landmark's CID identifier; the estimated latitude and longitude coordinates of the landmark; the covariance matrix associated with the landmark position estimate; the list of mobile fingerprints. The landmark position and its covariance have been estimated by the localisation algorithm implemented by the KalmanFilterSLAM class. The latter creates a landmark object for each identified BTS and associates a mobile position to the landmark. In order to implement the fingerprinting process, the landmark should maintain a list of MobileFingerprints objects that will be used in the network localisation stage of the system.	KalmanFilterSLAM CellularSLAMControl

CellularSLAMControl	
Responsibilities	**Collaborators**
This is the control class of the application responsible for managing the actions of all other classes. It provides the link between the user interface with the rest of the system. It creates the NetworkMonitor and GpsPositioner objects and uses them to retrieve network and GPS data. It is responsible for performing the sampling process of creating sample objects needed for landmark localisation. These objects are instances of the PositionSample class encapsulating CID, RSS, GPS coordinates and the MS-BTS range measurement produced using the PropagationModel class. While the phone is connected to the same BTS, the sampling process continues until a handover occurs. The latter is detected by the class by sensing the change in the observed CID at the moment of obtaining a GPS position fix from the GpsPositioner. PositionSample objects are constructed for each observed base station and are stored in a list which will be used by the KalmanFilterSLAM class to estimate the position of the BTS landmark. The CellularSLAMControl also executes the landmark localisation process after receiving a request from the user interface. When the user activates the network positioning mode, the control class accesses the list of landmarks from the KalmanFilterSLAM class and searches for the landmark matching the observed CID to retrieve the target mobile phone position associated with the landmark.	NetworkMonitor GpsPositioner GpsTimer PositionSample PropagationModel KalmanFilterSLAM

KalmanFilterSLAM	
Responsibilities	**Collaborators**
This class implements the landmark localisation algorithm, the map management process, the extended Kalman Filter maintaining the SLAM state. Upon receiving a new position sample from CellularSLAMControl, this class applies the EKF landmark localisation algorithm to estimate the position of the landmark. It then creates an instance of the Landmark calss and stores it in an array representing the global map of landmarks. When the user intitiate the network localisation stage,	*CellularSLAMControl* *Landmark* *MobileFingerprint*
a map management algorithm to check if the BTS can be associated with a previously identified landmark. This class also creates a fingerprint object following each landmark observation. The fingerprint object is initialized using the mobile position retrieved from the state vector and the signal strength measurements that contributed in the localisation of the landmark. It is then added to the list of fingerprints maintained by the landmark object. One of these fingerprints will be considered as the mobile position estimate in the network localisation stage. It is the responsibility of this class to implement the selection process according to the adopted nearest neighbor data association, which is based on signal strength observation.	

The CRC cards help identify the operations and attributes of each class and create the class model of the system. The class diagram depicted in Figure 5.5 shows how classes are associated and includes the main operations and attributes of each class. The arrows with diamond ends represent the aggregation association between the instantiated class and its creator, with the diamond connected to the class creating and using objects. Multiplicities are shown next to each arrow to determine how many objects are created for each instantiated class. In addition, collaboration diagrams are created in order to clarify the design of the system further. The statechart diagram illustrates the different states of the system and the transition between them, while the sequence diagram shows the sequence of messages sent between objects. The class model and the two collaboration diagrams will be refined in the following section, where we proceed to the analysis model which will provide an internal view of the system and describe how its functionality is realized.

5.3.3 Class, State and Sequence Diagrams

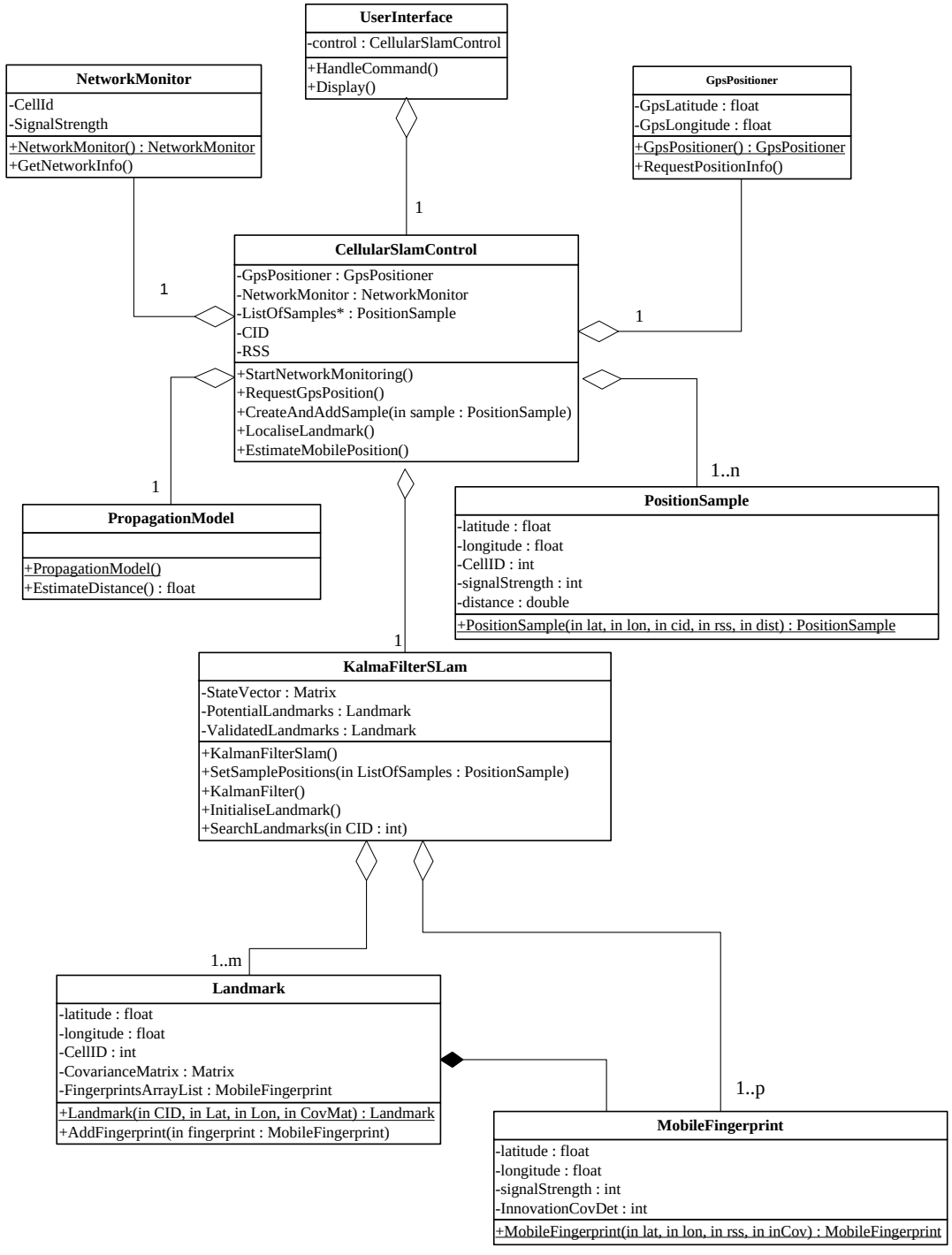

Figure 5.5 CCS Application Initial Class Diagram

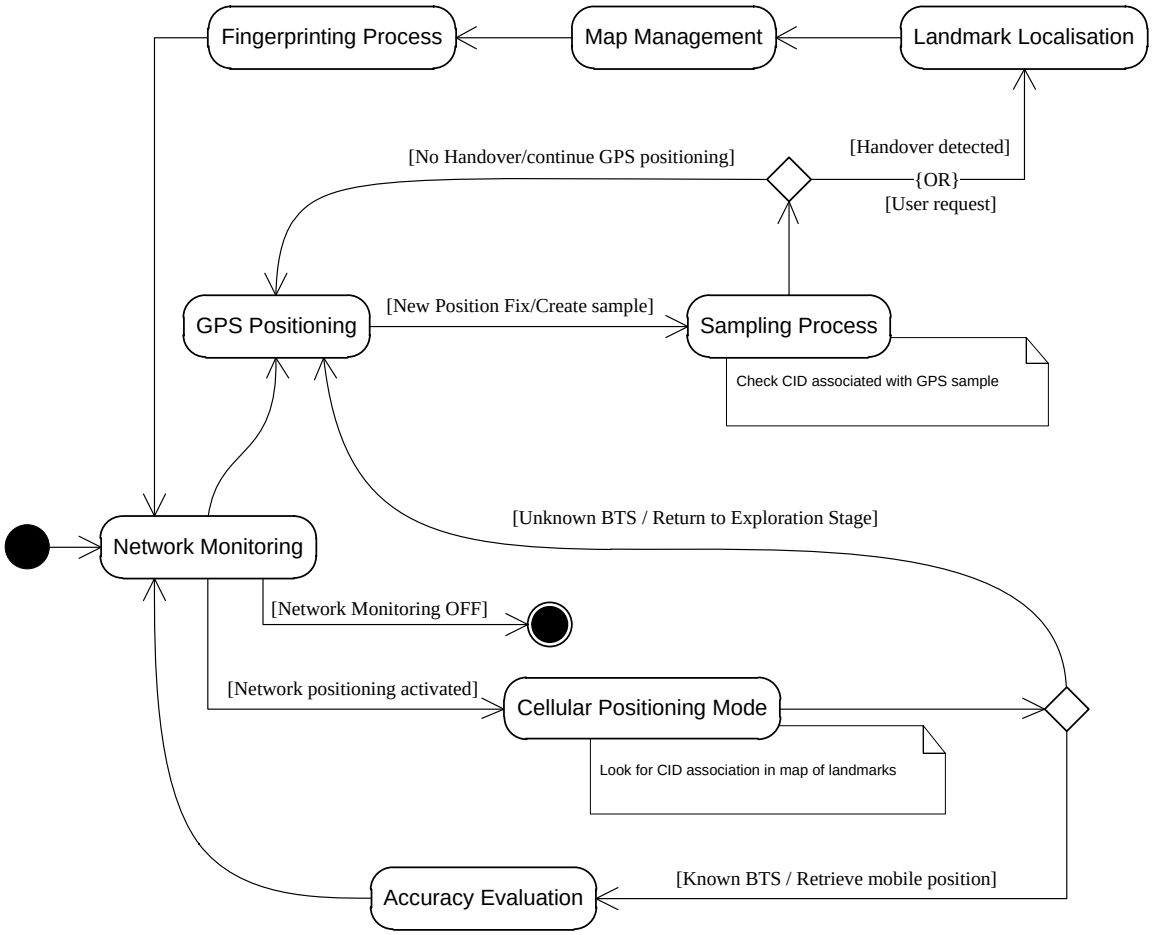

Figure 5.6 CCS Application Initial Statechart Diagram

We can see from the statechart diagram that the network monitoring is the process running throughout the execution time of the application. In fact, it is required in both exploration and cellular positioning stages of the system. As stated in the requirements analysis, the user should activate the network positioning mode after surveying an area using the system in exploration mode. In other words the application starts with the network monitoring and GPS sampling tasks which together form the exploration stage of the system. The latter keeps running until the user activates the network monitoring mode after the system has constructed a map of surrounding landmarks. If the observed CID belongs to a known

landmark, the mobile position can be estimated and the system enters its accuracy evaluation state. The latter will be detailed later in this chapter. If the observed base station is not present in the map of landmarks, the system switches from positioning mode back to the sampling mode. This is illustrated in the diagram by the transition with the condition 'observed BTS with unknown CID'.

The transitions between states provide us with insights on the sequence of message passing between the system's objects. In fact the statechart diagram lends itself to the construction of the initial sequence diagram, depicted in figure 5.7, which shows the communication between objects in the time order that interactions take place. In UML, the sequence diagram is one of the two forms of interaction diagram, the other one being the collaboration diagram. The latter also shows the sequencing of messages but not as clearly as the sequence diagram, especially if the execution of the system involves repetitive tasks. As the exploration stage of Cellular SLAM is an iterative process, the sequence diagram is the preferred choice. The diagram in figure 5.6 shows the execution of two message loops, or loop sequences as described next:

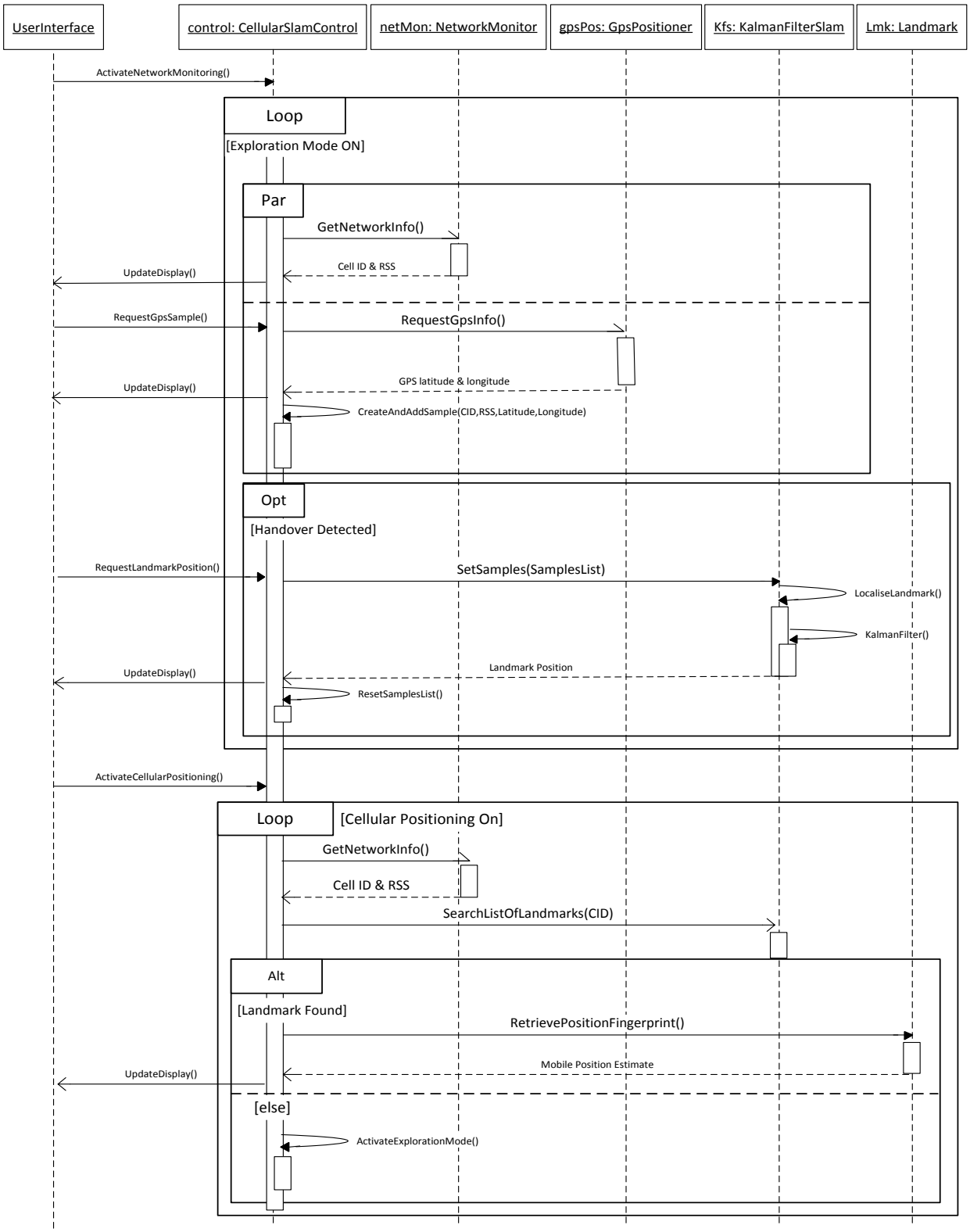

Figure 5.7 CCS Application Initial Sequence Diagram

The first sequence represents the execution of the exploration stage whereas the second represents the execution of the cellular positioning stage. Upon receiving the request of activating the network monitoring mode from the user interface, the control object performs the sampling process which consists of the simultaneously observing network information (CID and RSS) and obtaining GPS position measurements. As described by the CRC cards, GetNetworkInfo() and RequestGpsInfo() are the methods called by objects of the NetwokMonitor and GpsPositioner classes which are owned by the CellularSLAM control object. As the latter should monitor network observation while waiting for a GPS position fix, these methods have to be asynchronous. Asynchronous method invocation (AMI) allows the sending object to stay active while waiting for the reply of asynchronous message calls. In fact, AMI can be implemented by making the NetwokMonitor and GpsPositioner active objects running concurrently. In the sequence diagram, this is represented by the frame with the title 'Par', meaning parallel execution, and a dashed line separating the two observation tasks. When a handover occurs, the landmark localisation sequence is executed within the option frame titled 'Opt' and guarded by the condition 'Handover Detected'. This sequence can also be launched if the user requests an estimate of the observed BTS landmark. In this landmark localisation frame, the control object sends the list of the samples collected during the sampling process to the instance of the KalmanFilterSLAM class responsible for performing the SLAM operations. Only the BTS localisation and Kalman Filter operations are depicted by the diagram as the others will be included in the more detailed sequence diagram in the analysis model.

The second loop frame includes the execution of the cellular positioning stage. As stated previously, this stage performs the localisation of the mobile phone using the data

collected by the fingerprinting process during the exploration stage. Firstly, CID and RSS measurements are taken from the network. A search algorithm then scans through the map of landmarks to check if the observed CID matches a BTS from the map. As shown in the sequence diagram, the search algorithm is implemented by the 'SearchListOfLandmarks' method of the KalmanFilterSLAM class which is invoked by the CellularSLAMControl object passing the observed CID as a parameter. If a match exists, the system can estimate the position of the mobile phone using the proximity sensing method described in section 4.1.2 and implemented by the retrievePositionFingerprint() method of KalmanFilterSLAM. If no matching landmark is found, the system returns to the exploration stage. The alternative frame 'Alt' in the sequence diagram illustrates this if/else logic.

Chapter 6 - Experimental Evaluation

6.1 Introduction

The aim of this chapter is to report the performance of the static positioning system and the Constrained Cellular SLAM system proposed in this thesis as well as to evaluate them in terms of accuracy against other cellular positioning techniques, which have been described in Chapter 2. The cellular positioning systems proposed in this thesis were evaluated by conducting real-world experiments after being implemented as mobile software applications. Section 6.4 presents the static positioning experiments conducted using the 'GSM Mobile Locator' application running on a Windows Mobile PDA. Section 6.5 presents the positioning experiments which test the performance of the Constrained Cellular SLAM system using the Symbian OS smartphone application on which it is deployed. The design of these software applications was outlined in Chapter 5.

In addition to providing a summary of the positioning results, this chapter presents the practical details of an example experiment for each of the static EKF and the CCS positioning systems. It begins by outlining the preparation stages required to conduct the positioning trials, which are twofold:

- The base station identification process of associating BTS locations to CID codes, which is described in Section 6.2.
- The calibration process of the propagation model adopted by the positioning systems presented in this thesis, which is described in Section 6.3.

The base station identification process affects the proposed positioning systems differently. It is required by the static positioning system because it defines the BTS reference points used for positioning. In other words, the absolute knowledge of BTS locations and their identification is crucial for the accuracy of the positioning outcome. On the other hand, the BTS identification process is used by the CCS system for evaluation purposes only. As described in Chapter 4, the BTS locations are estimated in both stages of the adopted SLAM methodology as they are initialised during the Initial Mapping Stage and updated during the Network Localisation Stage. Thus, the true BTS positions are only required to evaluate the accuracy of the estimated BTS landmark positions.

During positioning trials conducted in central Birmingham as part of the Author's previous work [Ham06], various propagation models have been tested and compared to evaluate the accuracy of the distance estimation and the positioning results. The experiments conducted using the Walfish-Ikegami model produced the most accurate range predictions when compared to the Hata model and its extensions .i.e. the COST 231 and ERC report 68. In this work however, an empirical propagation model is calibrated using a linear regression process in the same trial area as the positioning experimental setup. As stated previously, the aim of tuning the propagation model in a positioning trial area is to improve the accuracy of BTS-MS range predictions in that specific area. In fact, it will be demonstrated in this chapter

that more accurate BTS-MT range relationships will allow the proposed positioning systems to achieve more accurate positioning outcomes.

As far as the visual presentation of the trials presented in this chapter, the mapping software Microsoft MapPoint 2010 is used to display the positions of the base stations and the mobile position estimates. The accuracy of the positioning outcome is evaluated by measuring the distance separating the estimated mobile position and the reference or 'true' mobile position, which is obtained using GPS and pinpointed using the MapPoint software. All the latitude and longitude coordinates specified as part of the positioning trials in this chapter are expressed in decimal format[24]. Another engineering software tool called Netmonitor [Ham06] was used during the BTS identification process and the static EKF positioning experiments. As stated previously, Netmonitor can be used to measure the CID and received signal strength for the serving base station as well as to monitor the Network Measurement Report, which displays the details of up to six neighbouring BTS transmitters. As introduced in Chapter 3 and detailed in Section 6.4, monitoring the history of the NMR is required by the range-bearing EKF system to derive bearing measurements. Netmonitor was required to perform these experiments since the 'GSM Mobile Locator' PDA application does not have the capability of monitoring the GSM network. On the other hand, the use of a standalone tool was not required to perform the experimental evaluation of the Constrained Cellular SLAM system because the Symbian OS smartphone application implementing CCS is able to measure the CID of the serving BTS as well as the RSS observed by the mobile terminal.

[24] Latitude north and longitude west.

6.2 Base Station Identification

Extensive surveys have been conducted in order to identify well-known base stations and build the database required for the operation of the 'GSM Mobile Locator' application implementing the static EKF positioning system. The location of the base stations are obtained from Ofcom's Sitefinder website, which includes maps displaying the locations of base stations as well as other information such as antenna height and transmitted power. Sitefinder is a reliable source to obtain BTS information as the latter is provided by network operators themselves. However, Sitefinder does not provide the Cell Identity Codes associated with each base station, nor does it state how many sector antennas are present on each site.

Figure 6.1 Ofcom Sitefinder database

Figure 6.1 is an example screenshot from the Sitefinder website showing a map of base stations in one of the CCS positioning experiments reported in Section 6.5. Notice in the right side of the map a table showing the details of one of the base stations.

There are other third party databases available online for the LBS community which list BTS locations by their CID identifiers but they are not as reliable as Sitefinder. As introduced previously, third party databases are built using the data collected by smartphone users and then sent via the Internet to a server which processes the information to estimate the position of each BTS. The accuracy of the estimated BTS positions is poor as it strongly depends on the number of users collaborating to collect the data as well as the path they take during the survey relative to the base stations.

Therefore, the aim of the BTS identification process is to link known base station locations with their relevant CID codes. As far as the software implementation of the static positioning system is concerned, the GSM Mobile Locator application requires the BTS identification process to translate CID inputs received from the user to their corresponding BTS location coordinates, which represent the reference points for positioning. While the performance of the static positioning systems depend on the exact knowledge of base station locations and their corresponding CID's, the Constrained Cellular SLAM system only needs the exact BTS locations for evaluation purposes only. Being a cellular positioning system based on Simultaneous Localisation And Mapping, the CCS software application carries out the mapping of base stations including the CID-BTS location association.

Once the base stations to be used as reference for positioning experiments have been identified and located using Sitefinder, site surveys have been conducted to identify individual sectors of base stations and associate them with their corresponding CID codes.

Firstly, the BTS locations published in Sitefinder are mapped using a GIS mapping software like Microsoft Mappoint or Google Earth. The mapping software is also used to record the latitude and longitude coordinates of each base station.

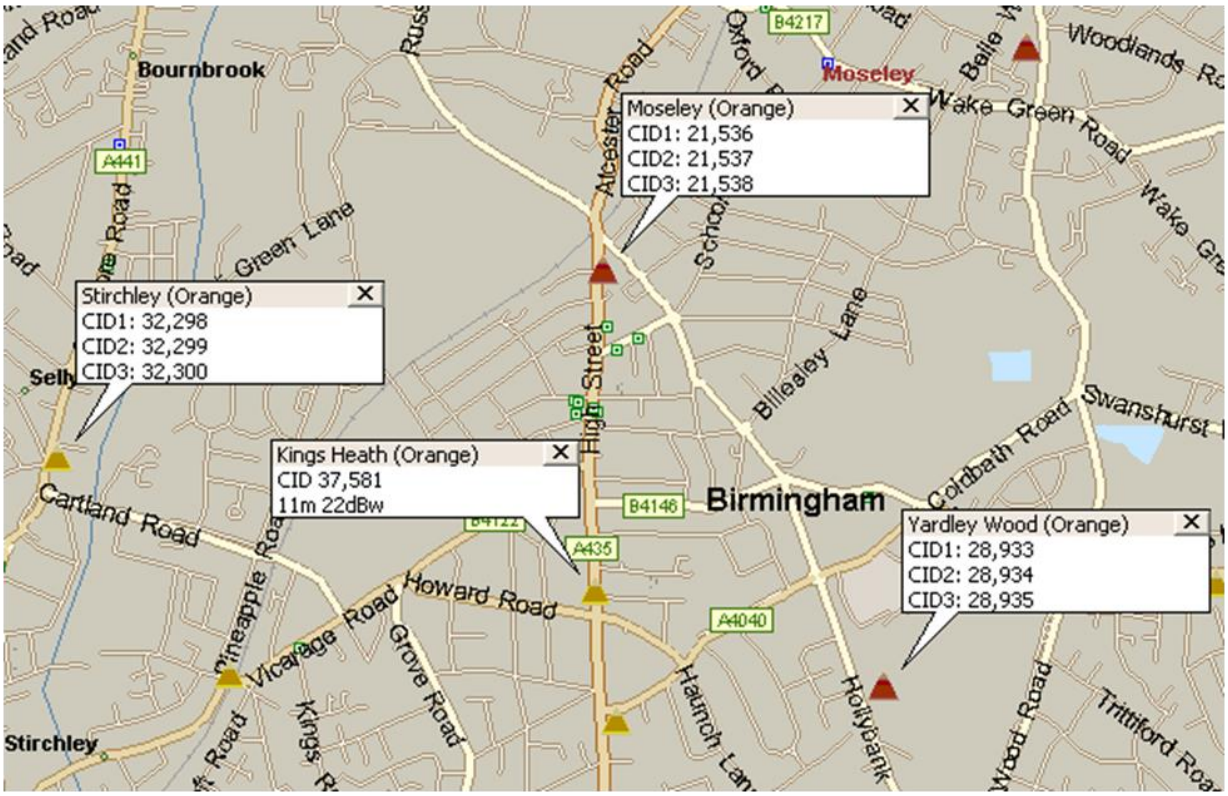

Figure 6.2 Mappoint map displaying identified base stations

Using a GSM network monitoring tool like Netmonitor capable of displaying the Network Measurement Report, each BTS is surveyed by taking CID and RSS measurements in several direction around the BTS. Figure 6.2 shows a Mappoint map displaying the base station identified as a result of the CID matching procedure. Finally, the BTS data is compiled into a database format ready for the software implementation of the proposed positioning applications.

6.3 Propagation Model Fitting

As stated previously, the signal strength-based positioning systems proposed in this work rely on an initial propagation model tuning process which is performed in the same areas as where the experimental evaluation of the positioning outcome is carried out. The parameters of the path loss equation have been fitted using real signal strength measurements in the area of each positioning trial. Each trial area is surveyed in advance in order to identify the base stations according to their corresponding Cell ID's.

As described in Section 2.4, the calibrated propagation model is expressed in the power law form of (2.9), that is:

$$P_r = \beta - 10\alpha log(d) \qquad (6.1)$$

The least square fitting process outlined in Section 2.4 calibrates the path loss exponent α and absolute loss β parameters given the measurement dataset consisting of i data sample pairs (d_i, P_{ri}) where d_i represents the distance as the independent variable and P_{ri} represents the measured signal power as the dependent variable. The experimental procedure to collect the sample dataset for the calibration process is as follows.

- Firstly, a base station of well-known coordinates, sectors and CID codes is chosen.
- For each base station, RSS measurements are taken at regular intervals while travelling along the streets covered by each sector of the BTS.
- From each position of the mobile terminal, a GPS reading is taken and used to measure the true distance between the mobile and the BTS.

In order to provide an example of the measurement dataset resulting from the above the data collection process, few dataset samples are taken from the model calibration experiment in the Stirchley area and shown in Table 6.1.

Table 6.1 Propagation model fitting example dataset.

BTS Position		GPS Position		True Distance	Rx
Latitude (North)	Longitude (West)	Latitude (North)	Longitude (West)	(Metres)	(dBm)
52.432188	-1.918774	52.43053	-1.920525	113.057159	-78
		52.430488	-1.920637	121.628281	-79
		52.430439	-1.920732	130.05162	-80
		52.430413	-1.920805	135.615875	-81
		52.430421	-1.920881	138.751297	-80
		52.430076	-1.920504	152.605942	-83
		52.430291	-1.921341	171.868744	-85
		52.43023	-1.921454	182.100311	-84
		52.430159	-1.921538	191.51857	-86
		52.429977	-1.922028	230.043655	-88
		52.429756	-1.922445	267.485809	-91
		52.429366	-1.922693	308.613861	-93
		52.429185	-1.922682	322.165375	-94
		52.429058	-1.922788	337.35202	-95

The measurement datasets collected for the propagation model tuning process can also visualised using Mappoint as illustrated by Figure 6.3, which consists of a map showing part of the calibration experiment conducted in the Yardley Wood area. In this map, the BTS position is highlighted by the green pushpin while the colour shaded circles represent the mobile position-RSS data pairs. High, medium and low RSS values are represented by the red

white and blue colours respectively[25]. Moreover, few samples are labeled to show the RSS measurement as well as the latitude and longitude coordinates of the sample position.

Tables 6.2 present the results of the data fitting experiments, namely the calibrated parameters α and β as well as the signal strength error standard deviation σ_{P_r}. The calibrated parameters are used to produce the path loss equations which become the range-based observation models for each of the static EKF positioning system and the Constrained Cellular SLAM system. Note that some of the calibration trial areas in Table 6.2 have been used to conduct the positioning test for both systems.

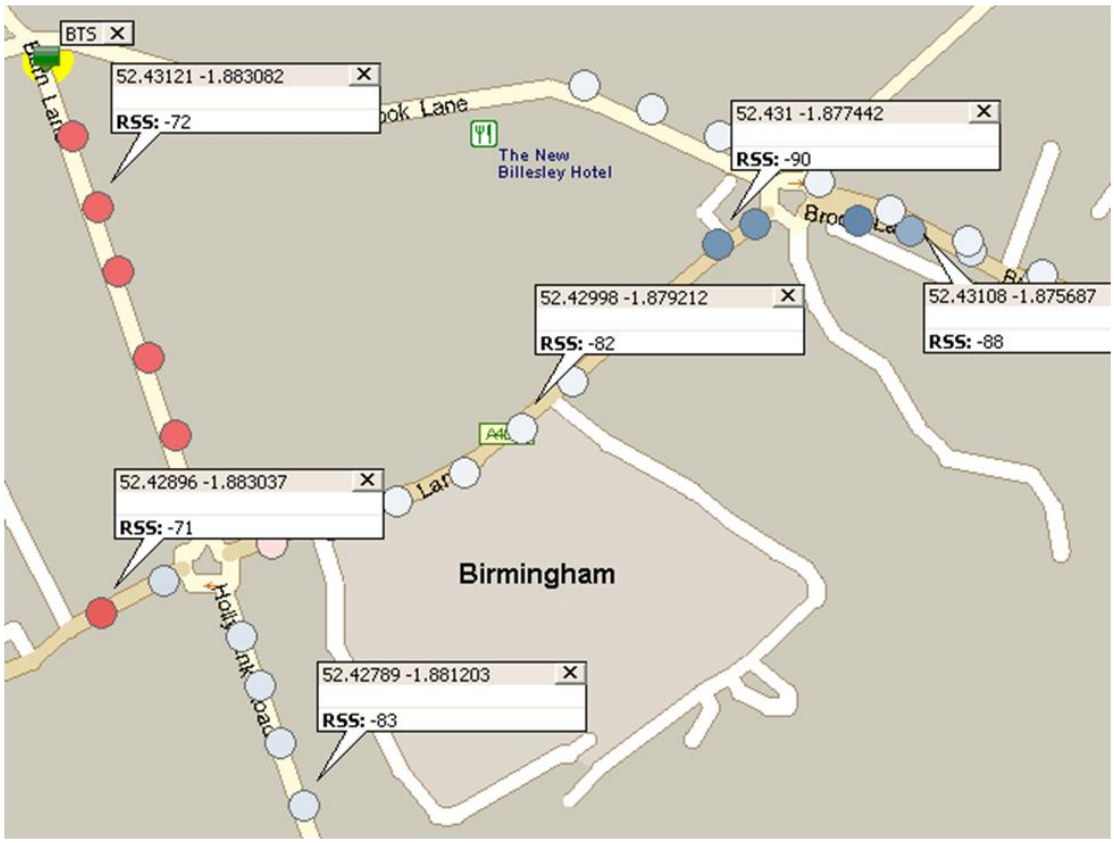

Figure 6.3 Propagation model calibration samples

[25] Note that this gradient colour shading will be used in other maps within this chapter.

Table 6.2 Propagation model calibration in preparation for positioning experiments

Area Name	Area Type	Reference BTS	Area (km²)	Number of Samples	Calibrated Parameters		σ_{P_r} (dB)
					α	β	
Five ways	Urban	3	6	225	4	97	6.2
Edgbaston	Mixed (Urban/Suburban)	5	7.5	250	3.9	93	7.7
New Street	Dense Urban	4	1.5	140	4.2	109	8.6
Colmore Row	Dense Urban	3	1.2	127	4.3	100	7.3
Kings Heath	Urban	3	3	190	4	92	4.5
Moseley	Suburban	2	2.5	125	3.7	93	9.5
Yardley Wood	Suburban	3	4	230	3.5	82	3.8
Stirchley	Suburban	2	1.8	132	3.8	92	4.2
Hall Green	Suburban	2	2	160	3.7	88	7.4
Shirley	Suburban	2	2.2	208	3.8	84	5.9

As stated in Section 2.4, a well-fitted path loss model has an error standard deviation of between 3 and 8 decibels [Sau07]. Note from Table 6.2 that the standard deviation between the RSS measurements and their predicted counterparts varies from 3.8 to 9.5 decibels. As shown in Table 6.2, only two out of ten model tuning experiments produced an error standard deviation of more than 8 dB, namely the urban experiment in the New Street area and the suburban experiment in the Moseley area. Sections 6.4 and 6.5 will present the positioning experiments in each of the areas listed in Table 6.2 and analyses the impact of the goodness of the model fitting process on the positioning outcome. Moreover, it will be shown that using a calibrated propagation model improves the accuracy of the positioning result as opposed to using generic propagation models in the same experimental setup.

The following outline provides an example of the calibration process outcome using the experiment conducted in the suburban area of Stirchley, from which the dataset of Table 6.1 was taken. As shown in Table 6.2, this particular model fitting experiment consisted of surveying two base stations within an area of about 1.8 km²n in which 132 data samples have

been collected. Figure 6.4 and Figure 6.5 show the graphs for the measured and predicted RSS values corresponding to one and two base stations respectively. In both figures, the graph drawn in red illustrates the relationship between the measured RSS values and the true distance separating the mobile position and the reference base station(s). On the other hand, the blue graph shows the predicted RSS values produced by the model function calibrated using the least squares fitting process described in Section 2.4 and which reads as:

$$P_r = -92 - 38\,log(d) \qquad (6.2)$$

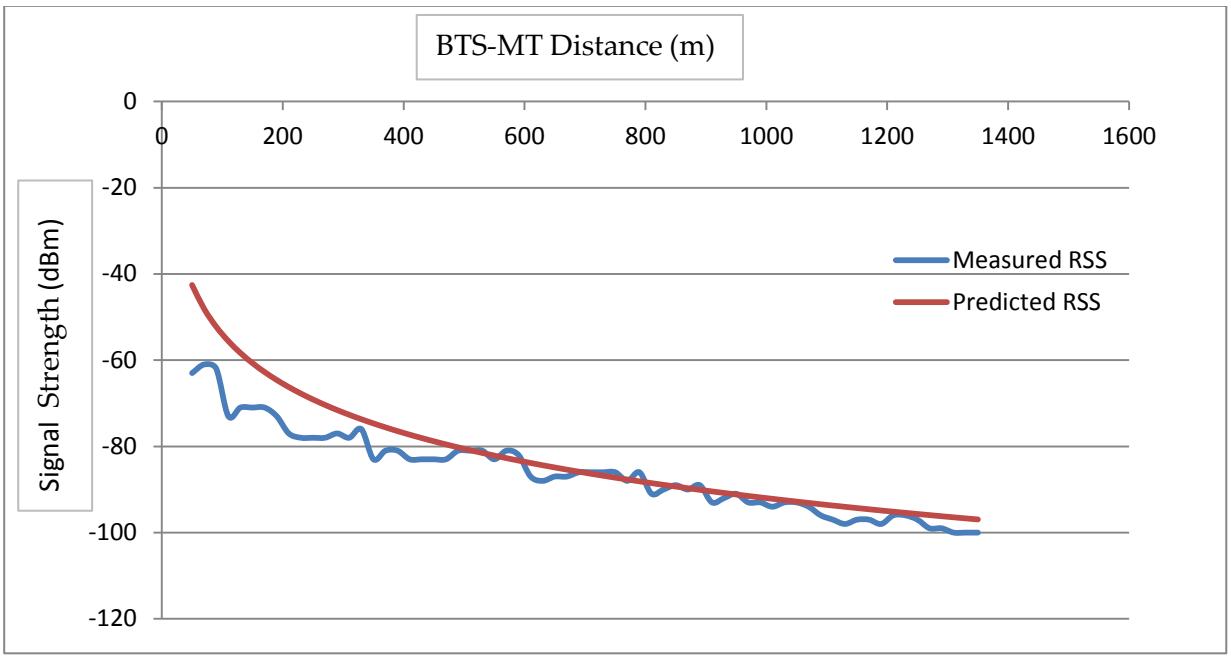

Figure 6.4 Signal strength model calibration: measured and predicted RSS for 1 BTS

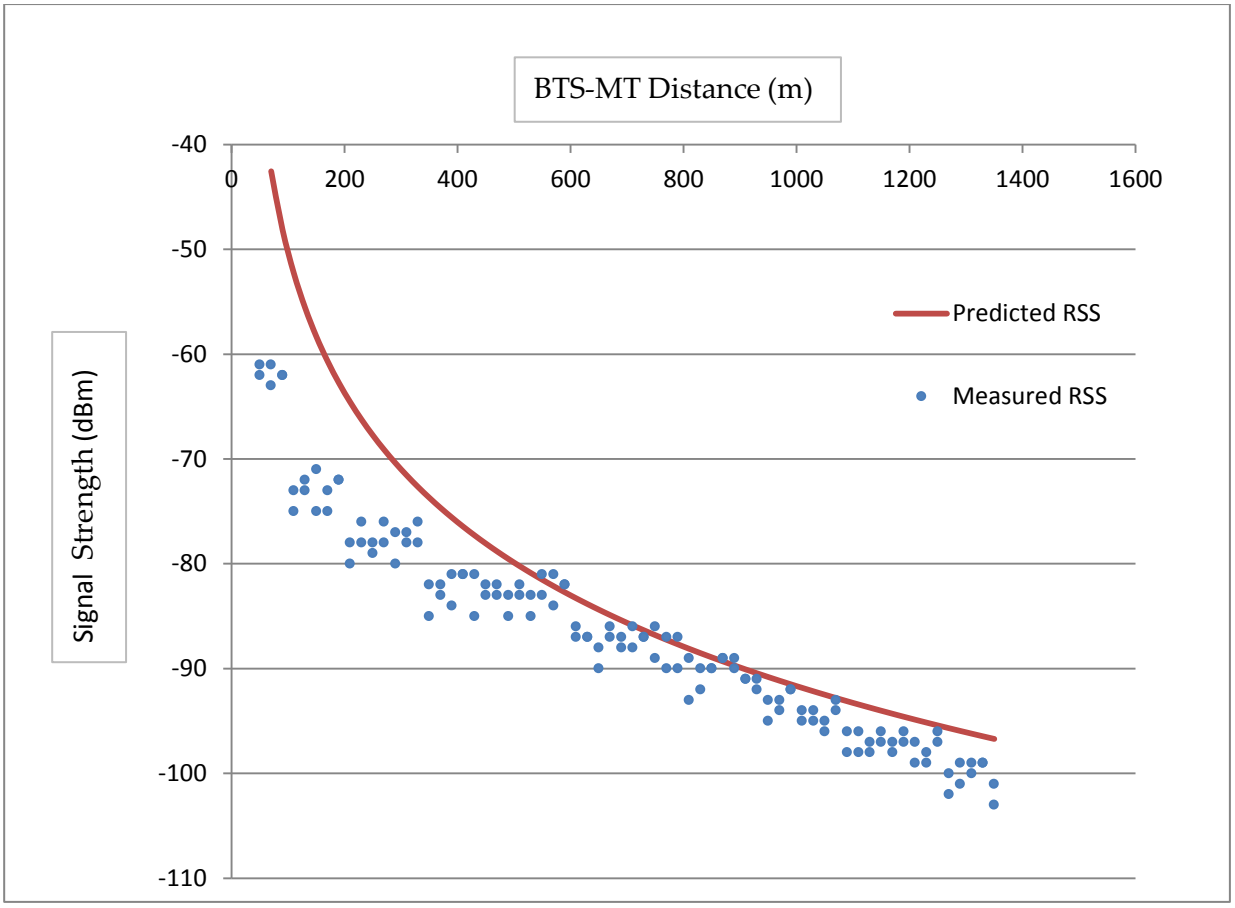

Figure 6.5 Signal strength model calibration: measured and predicted RSS for 2 BTS

Note that there are two RSS measurements associated with each distance value in Figure 6.5, as opposed to a single RSS measurement in Figure 6.4. Knowing that both reference base stations in this trial have a transmitted power of 57 dBm, the calibrated model equation (6.2) can be rewritten to describe the path loss as follows:

$$L = 149 + 38\,log(d) \qquad (6.3)$$

The graph representing the calibrated path loss model in its conventional power law form can thus be produced as shown in Figure 6.6 and Figure 6.7, which consider samples corresponding to one and two base stations respectively

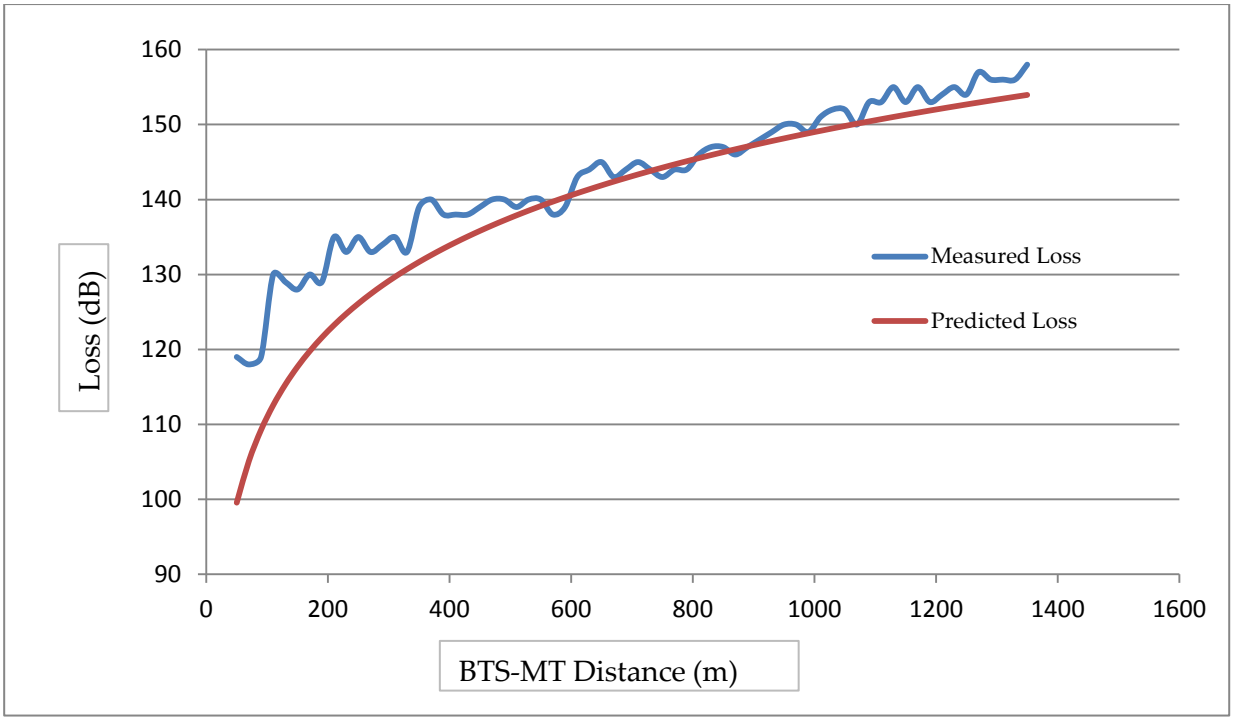

Figure 6.6 Path loss model calibration: measured and predicted path loss for 1 BTS

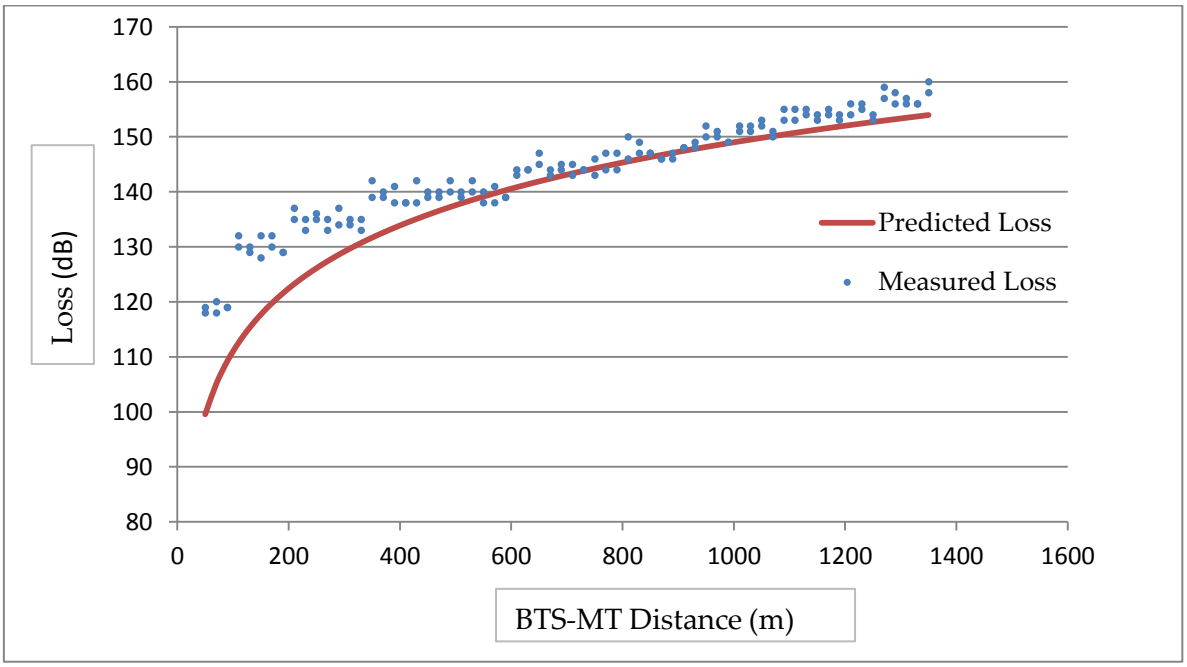

Figure 6.7 Path loss model calibration: measured and predicted path loss for 2 BTS

6.4 Static Positioning

In order to test the performance of the static positioning system presented in Chapter 3, several trials have been conducted using the 'GSM Mobile Locator' PDA application which has been described in Section 5.2. As the E-911 was the main driving force behind the cellular positioning research, the proposed static positioning system will be evaluated against the cellular positioning methods that have been standardised as a result of the E-911 mandate. The static positioning trials reported in this section have been conducted in both urban and suburban areas using the base stations of two different GSM network operators (T-Mobile and Orange).

This section begins by describing the experimental setup of the static positioning trials that have been conducted within the scope of the research. It will then report and discuss the results of the positioning trials before evaluating the accuracy of the proposed method against standardised cellular positioning methods which were used in real-world E-911 trials.

6.4.1 Experimental Setup

In order to be used as reference points for the static positioning trials, a number of known base stations are selected from the database resulting from the identification process described in Section 6.2. As stated in Chapter 3, the known geodetic coordinates of the base stations are transformed to their corresponding ellipsoid orthographic coordinates with respect to a chosen reference location within the trial area. As the 'GSM Mobile Locator' does not have the capability of measuring CID and RSS values from the PDA device, a standalone GSM network monitoring tool such as Netmonitor is used for this purpose.

Using Netmonitor, we observe the Network Measurement Report which lists the BTS transmitters according to their associated CID codes signal strength measurements. As this is the static case, the measurements are taken form a single position which is determined using GPS for accuracy evaluation purposes. The NMR may include unknown CID's since not all the base stations have been identified. As a result the unknown CID's are not taken into account in the positioning process. Using our 'GSM Mobile Locator' application, we operate the EKF positioning process sequentially by inputting each RSS measurement individually. The high variability of RSS due to fast fading is averaged out before inputting RSS measurements into the input view illustrated by the application's screenshot of Figure 6.8. This screenshot is taken from one of the 27 static positioning experiments reported in Table 6.3 and is presented here to illustrate the data input process.

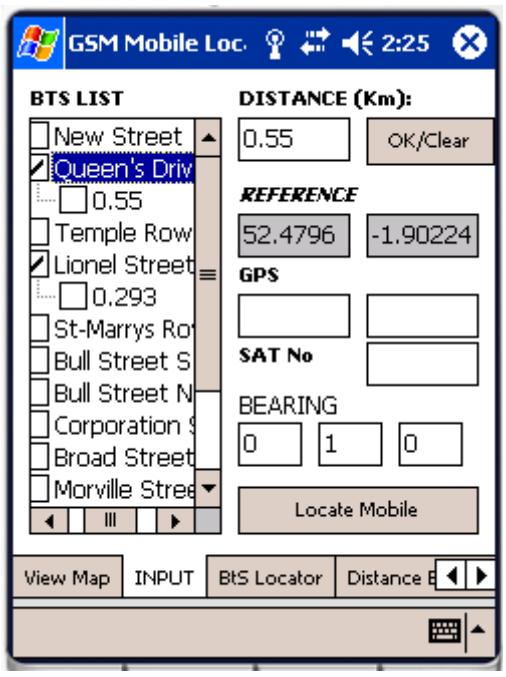

Figure 6.8 GSM Mobile Locator application BTS-RSS input tab.

As shown in Figure 6.8, we select the base stations from the database displayed as a list view in the left side of the application's input tab. Recall that each BTS is identified using the

observed CID following the CID matching process described in section 6.2. As stated in the use case scenario of Section 5.2.2, the propagation model used for the positioning experiment should be specified before applying the positioning process i.e. by pressing the Locate Mobile button in the input tab screenshot of Figure 6.8. If a generic propagation model like the Walfish-Ikegami model is selected, we should first calculate the propagation distance using the model's path loss equation. As shown in Figure 6.9, the GSM Mobile Locator application provides a 'distance estimation' tab in which the user can specify the parameters required by generic propagation models to estimate the BTS-MT distance corresponding to the measured signal strength. The estimated distance is then linked to the relevant BTS specified in the Input Tab using the distance text field and the confirmation button depicted in the right side of the Input Tab screenshot shown in Figure 6.8. If the calibrated path loss model was to be adopted for the experiment, the measured signal strength should be entered directly in the Input Tab. In this case, the calibrated propagation parameters are integrated in the application's code before the deployment of the application onto the PDA device.

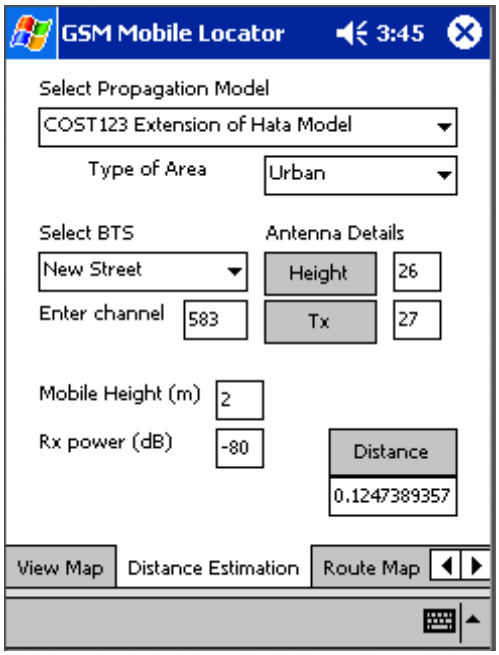

Figure 6.9 GSM Mobile Locator application Distance Estimation tab.

The bearing inputs from figure 6.8 represent the adopted ternary representation of the bearing measurement vector described in Section 3.4. If the bearing inputs are specified, the application will apply the range-bearing EKF model as the positioning process. If bearing inputs are not specified, the range-only observation model will be used. As mentioned in Section 3.4, the bearing measurement is denoted by the BTS sector CID given that the BTS has 3 directional antennae each identified with a CID. For instance, given the knowledge that a certain CID refers to the 120 degrees 'East Sector' I_1 of the BTS according to Figure 3.1, the bearing ternary vector is 1 0 0. In Figure 6.8, the bearing vector is 0 1 0 which indicates that the observed CID belongs to the 'North Sector' I_2 of the BTS. As mention in Section 3.4.1, we monitor the Network Measurement Report using a GSM signal monitoring tool like Netmonitor to determine the ternary code used as bearing measurement. The following outline explains how the bearing ternary representation is deduced from monitoring the history of the NMR.

From the trial reference position, we record the CID and RSS of the serving BTS which is the first entry in the NMR. We also need to identify the other sectors belonging to the serving BTS and record their positions within the NMR. We then start walking away from the reference position in an initially chosen direction while observing the signal strength associated with each of the sectors. The aim is to check whether the serving sector maintains its top position within the NMR with the highest RSS value until we have covered a distance of at least 200 metres. In order to set the bearing vector values, the following four cases are identified while monitoring the evolution of the NMR:

- ***Case1:*** If the serving sector maintains its first position in the NMR, then we can assume that the mobile is located closer to the centre of the serving cell. This will result in a bearing vector comprising of the value of 1 for the sector in question and two 0's for the other two sectors.
- ***Case 2:*** if the mobile terminal switches to one of the neighbour sector after we have walked a distance of less than 100 metres, then we can assume that the mobile is located closer to the intersection area between the two cells belonging to the serving BTS. This implies that the bearing vector will have two 0.5 values for the two sectors in question while the third sector has a value of 0.
- ***Case 3:*** if a handover to a neighbour sector occurs after walking between 100 and 150 metres, we can assume that the mobile is located between the centre of the serving cell and its edge. The bearing vector will be set in the same way as in case 1.
- ***Case 4:*** if a handover to a different base station occurs, we return to the reference position and walk in a different direction as we are interested in the mobile displacement relative to sectors of the same BTS.

Once the bearing vector has been defined, we return to the experiment reference position to continue the static positioning process. Once all the inputs are set for an observed base station, the EKF positioning algorithm updates the mobile terminal position estimate using the measurements relative to this base station. As stated previously, the algorithm proceeds iteratively by updating the mobile state estimate using a single measurement at time, whether the measurement consists of a new RSS relative to the same BTS or relative to another BTS following a handover event.

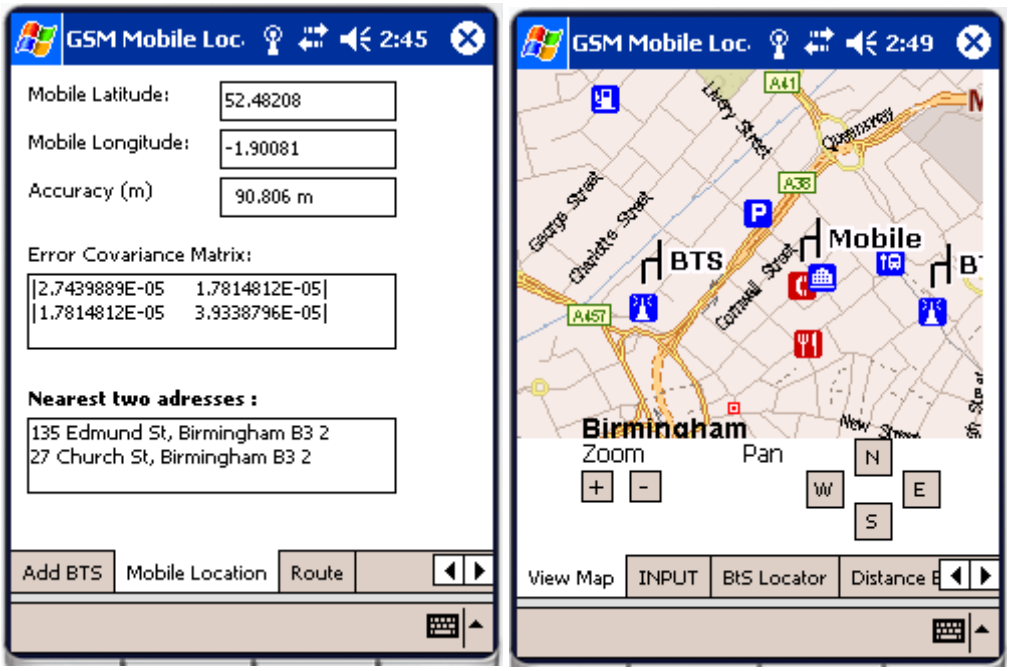

Figure 6.10 The estimated mobile position (GSM Mobile Locator)

An example of the positioning outcome of a static positioning experiment is depicted in Figure 6.10. The latter combines the 'View Map' tab and the 'Mobile Location' tab screenshots of the Mobile Locator application to display the estimated position on a map and show the accuracy of the positioning result and the error covariance matrix associated with the mobile state estimate.

6.4.2 Static Positioning Results

For each of the range-only EKF system and the range-bearing EKF system, Table 6.3 reports the average accuracy from all 27 trials, which is expressed in terms of the Root Mean Square error in the estimated position relative to the 'true' experiment reference position. As the number of trials in different areas varies between 2 to 5 trials, the accuracy reported in Table 6.3 for one area is the mean of the rms values of all the trials conducted in that area. In order to evaluate the performance of the proposed static positioning system against other cellular

positioning methods, Table 6.3 shows the mean accuracy for each of the urban and suburban trials.

Table 6.3 also compares the positioning results obtained using the calibrated propagation model with those obtained using the Walfish-Ikegami model (WI). Only the latter is used in this comparative discussion because it was deemed the most accurate generic propagation model in terms of distance predictions, as presented in the Authors previous work [Ham06].

Table 6.3 Static positioning accuracy

Trial Area Name	Area Type	Trials	BTS	Using Calibrated Model			Using WI Model	
				σ_{P_r} (dB)	Range-Only Accuracy (m)	Range-Bearing Accuracy (m)	Range-Only Accuracy (m)	Range-Bearing Accuracy (m)
Five Ways	Urban	5	6	6.2	107	85	116	98
New Street	Urban	3	5	8.6	152	122	162	148
Colmore Row	Urban	4	3	7.3	168	139	171	155
Urban Environment Mean Accuracy					**142**	**115**	**155**	**142**
Moseley	Suburban	2	4	9.5	188	169	239	225
Yardley Wood	Suburban	5	4	3.8	161	120	195	183
Strichley	Suburban	5	2	4.2	208	185	261	227
Hall Green	Suburban	3	4	7.4	143	118	197	150
Suburban Environment Mean Accuracy					**175**	**148**	**223**	**175**

At first sight, the results reported in Table 6.3 confirm that adopting a calibrated propagation model produce more accurate positioning outcome than using the Walfish Ikegami propagation model in urban or suburban environments. As expected, extending the observation model of the static EKF algorithm to process bearing measurements also improves the positioning outcome. Moreover, it appears that the accuracy improvement of the range-bearing system over the range-only system is more important when using the calibrated model as opposed to using the WI model.

Figure 6.11 illustrates the effect of the number of distinct reference base stations and the RSS model calibration error standard deviation on the positioning accuracy. Note that Figure 6.11 only considers the results of the range-bearing EKF positioning process which used the calibrated propagation model.

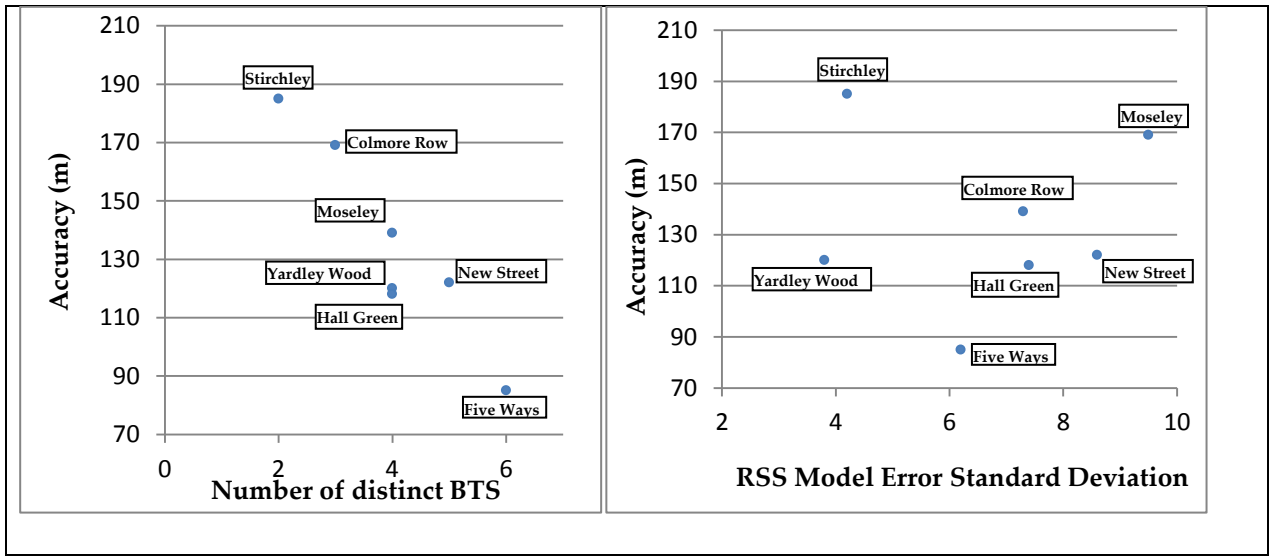

Figure 6.11 Static positioning accuracy analysis

Similarly to lateration and angulation positioning methods, the performance of the proposed static EKF algorithm improves as the number of distinct reference BTS increases. As stated previously, distinct BTS refer to transmitters mounted on different sites of different locations. It is clear from Figure 6.11 that the accuracy increases with the number of base stations. On the other hand, the effect of the calibration error standard deviation σ_{P_r} on the accuracy is less apparent. In fact, the number of distinct base stations has a more important impact on the accuracy. However, one can use σ_{P_r} to compare the accuracies of positioning trials in which the same number of base stations have been used, which is the case for the Moseley, Yardley Wood and Hall Green suburban experiments. In fact, we can notice from Figure 6.11 that the values of σ_{P_r} which resulted from the propagation model calibration stages of the Yardley Wood and Moseley experiments affected the positioning outcome since the former experiment

resulted in a more accurate outcome than the latter. The Hall Green experiment however seems not to be affected by the calibration error standard deviation σ_{P_r}. One can argue that this is the case because the trial area of the Hall Green experiment is smaller than that of Yardley Wood, as shown in Table 6.2, while both positioning trials used the same number of base stations. In addition to the number of distinct reference base stations, another important factor affecting the accuracy consists of the displacements of the BTS reference points relative to the true position of the mobile terminal, that is, the reference experiment position from which the measurements are taken. This factor is defined by the relative geometry between the reference points and the target position and is known in lateration techniques as the geometric dilution of precision (GDOP) [Fig10].

6.4.2.1 Static Positioning Trial

Figures 6.12 is a map showing the positioning results of one of the five experiments conducted in the Five Ways area. This experiment produced the highest positioning accuracy out of all the other static positioning trials conducted in this work. This is mainly due to the use of three distinct base stations, a high GDOP factor and a well fitted propagation model. As shown in the map of Figure 6.12, the displacement of true mobile position relative to each reference BTS allows for a good initialisation of the mobile state estimate. As a result, an accurate positioning outcome is achieved following EKF state updates, which 77m in this particular trial. This is a typical example on the effect of geometric dilution of precision on the positioning outcome. Moreover, Figure 6.12 illustrates the difference in terms of positioning accuracy between the range-only EKF and the range-bearing EKF, which both used the calibrated path loss model. These results are compared to the outcome resulting from the range-bearing EKF process which used the Walfish-Ikegami model as the observation model.

The static positioning system has also been evaluated against a commercial online tracking service called 'Trace A Mobile'. The result of this service is illustrated in the bottom right hand corner of Figure 6.12 with an accuracy of 363 m.

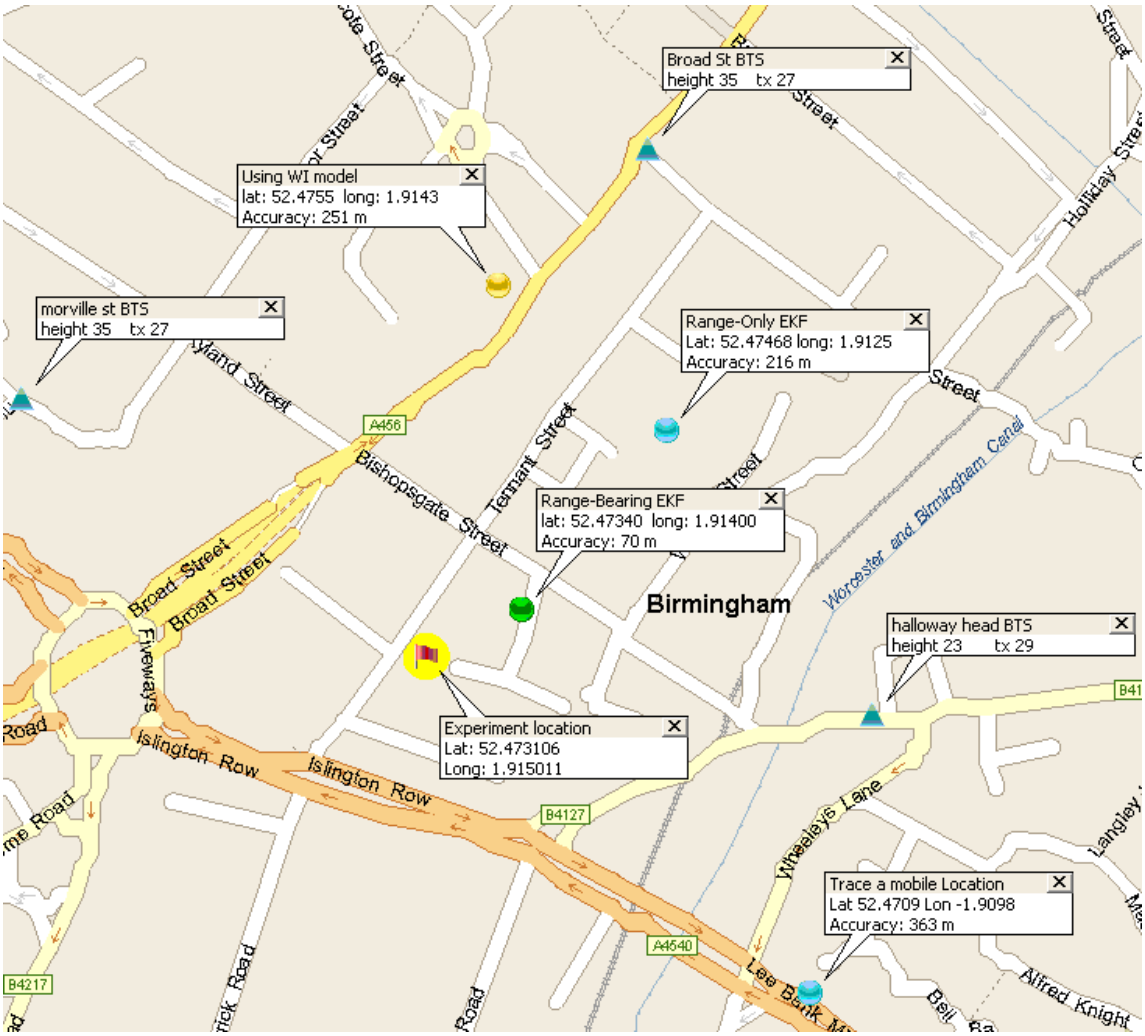

Figure 6.12 Static positioning urban experiment

6.4.2.2 Evaluation against other cellular positioning methods

Table 6.4 reports a real-life evaluation of standardised cellular positioning methods conducted by TruePosition and published by ABI research in [ABI11]. Recall from Section 2.2.3 that TruePosition is the LBS vendor who developed the U-TDOA method which made obsolete E-OTD and was standardised as a result for the E-911 project. According to ABI Research in

[ABI11], U-TDOA, Advanced-Forward Link Trilateration and A-GPS were evaluated using more than 3500 real-life E-911 calls which were received by Public Safety Answering Points in Texas in the second half of 2010, as shown in Table 6.4. Note that the second column reports the results obtained from calls made within Verison's CDMA network, in which A-GPS is used as the primary positioning method and A-FLT as the fallback method that is used in case A-GPS fails to return a position fix.

Table 6.4 U-TDOA, A-FLT and A-GPS evaluation using E-911 calls

	Accuracy (metre)		
Percentile	**U-TDOA**	**A-GPS/AFLT (CDMA)**	**A-GPS (UMTS)**
67th	78.3	22.5	35.6
90th	129.2	50.7	176.3
95th	168.6	74.4	390.3

Our positioning results obtained using range-bearing EKF and the calibrated propagation model were more accurate than U-TDOA and A-GPS results of the Texas E-911 trials in the 95th percentile. Because of the synchronisation of CDMA networks, the A-GPS/AFLT combination performs better than any other network-based method and outperforms the proposed method.

Since it is handset-based[26], the proposed positioning method should be evaluated against another self-positioning RSS-based method such as the Database Correlation Method (DCM), which was described in Section 2.3. Recall that DCM has been applied in the GSM network by Laitinen et Al [Lai01] using a concept known as fingerprinting, which is typically

[26] As stated previously, handset-based or self-positioning methods refer to the methods in which all the measurements and the position estimation process are performed at the level of the mobile terminal.

used for indoor wireless positioning. The accuracy of DCM achieved in [Lai01] was reported in Table 2.2. Compared to the proposed static EKF method, DCM is 25 metres more accurate in urban environments and 42 metres less accurate in suburban environments. However, it is important to note that DCM relies on an extensive fingerprint database collection phase and that the positioning accuracy achieved in the online estimation stage strongly depends on the size and resolution of the fingerprinting database.

The advantage of using DCM as a cellular positioning method is the fact that it does not rely on a priori knowledge of base station locations as the fingerprinting process produces all the required data for position estimation. The proposed SLAM methodology extends this advantage by estimating the locations of base stations during the offline fingerprinting phase which will improve the position estimate during the online positioning phase. The performance of the Constrained Cellular SLAM system will be evaluated against DCM in the next section.

6.5 Constrained Cellular SLAM

This section evaluates the performance of the Constrained Cellular SLAM system by reporting the positioning accuracies achieved during real-world positioning trials. In order to test the proposed cellular SLAM methodology, the CCS trials have been conducted using the smartphone software application which has been developed within the scope of the research. The design of the CSS application was presented in Section 5.3. Similarly to the static EFK positioning system, the EKF-SLAM methodology adopted by CSS relies on the calibrated propagation model as a range-based observation model linking RSS observations to the state estimates. As stated previously, the positioning experiments conducted to evaluate the CCS

system have also been conducted in the areas where the propagation model has been calibrated.

This section begins by explaining the experimental setup and practicalities undertaken to perform the Initial Mapping Stage of the CSS system. It will then discuss the results of the Network Localisation Stage and defines the factors affecting the accuracy of the mobile and landmark estimates. Moreover, it will be demonstrated in this section that the RSS model calibration process affects the accuracy of the landmark initialisation during the Initial Mapping Stage as well as the update of landmark state estimates during the Network Localisation Stage. The importance of the path taken during the IMS survey will also be stressed by providing a map visualisation example of the landmark estimation process. Finally, this section will consider one of the CCS positioning trials in detail in order to show the convergence properties of the adopted EKF-SLAM algorithm.

6.5.1 Initial Mapping Stage Experimental Setup and Evaluation

Recall from Section 4.4 that the IMS employs the EKF-based BTS Initialisation Model (BIM) to estimate the positions of observed BTS landmarks. The mobile terminal positions are measured using the phone's built-in GPS device and the calibrated RSS model is adopted by the BIM as the observation model linking RSS measurements to the BTS landmark state. The outcome of the IMS is a database of BTS entries which represents the initial map of the cellular network. Each BTS entry consists of the BTS position and the list of mobile fingerprints which were used to estimate the entry's position. During the Network Localisation Stage, the BTS map resulting from the IMS will be used by the EKF-SLAM algorithm to estimate the mobile position and update the landmarks that are observed after extracting them from the BTS map database.

The experimental setup of the IMS and the accuracy of the landmark initialisation process are presented in Table 6.5. This table considers the RSS calibration process in order to investigate the impact of the number of calibration samples and the RSS error standard deviation σ_{P_r} on the accuracy of landmark initial estimates.

Table 6.5. CCS experiments Initial Mapping Stage

Trial Area	RSS Model Calibration		Initial Mapping Stage					
	Number of Samples	σ_{P_r} *(dB)*	Area (km²)	Mobililty	Number of Mapped BTS	Number of Fingerprints	RSS Resolution (dB)	Landmark Accuracy (m)
New Street ***(urban)***	124	8.6	3	Walking	8	124	23	193
Kings Heath ***(suburban)***	172	4.5	2.5	Walking	6	172	27	155
Hall Green ***(suburban)***	208	7.4	2	Walking	4	208	21	132
Shirley ***(suburban)***	183	5.9	5.5	Driving	4	183	28	275
Yardley wood ***(suburban)***	220	3.8	9	Driving	10	220	34	244
Edgbaston ***(mixed)***	305	7.7	10	Driving	12	305	36	169

For each of the six CCS experiments listed in Table 6.5, the details of the experimental setup associated with the Initial Mapping Stage are as follows:

- *The area of the IMS survey in km²*. The area comprised all the observed base stations as well as all the fingerprints that were collected to initialise each base station.
- *The number of mapped base stations* is the number of individual BTS antennas that have been observed and estimated during the survey. This is not the number of distinct base stations as it takes into account individual sectors within sectored base stations.

- *The total number of mobile fingerprints* collected during the initialisation of all the observed base stations. For example, if 2 base stations were initialised using 10 fingerprints, the total number of fingerprints collected is 20.
- *The received signal strength measurement resolution*. By considering the RSS measurements encapsulated inside the mobile fingerprints, the RSS resolution consists of the difference between the maximum and minimum RSS values in decibels. For examples, given a list of 10 fingerprints each with a RSS measurement, the maximum RSS value among all 10 fingerprints is -70 dBm and the minimum RSS value is -90 dBm, the resolution is 20 dB.
- *The mobility* is related to the average speed[27] of the mobile terminal during the IMS survey. Two types of mobility scenarios are considered: walking and driving.
- *The landmark accuracy* consists of the mean rms error of all the landmark estimates, produced in the IMS survey of each trial area, relative to the true BTS positions identified from Sitefinder. Since BTS landmarks are defined by individual BTS antennas including sectors of the same BTS site location, the mean accuracy is calculated using individual rms errors for each BTS sector.

In order to provide a map visualisation of the fingerprinting process conducted as part of the Initial Mapping Stage, Figure 6.14 illustrates the fingerprints collected in all the suburban area trials listed in Table 6.5. In total, 913 fingerprints are shown in the map of Figure 6.14 encompassing the Kings Heath, Yardley Wood, Shirley and Hall green areas with a total area of 14.4 km^2. These suburban trial areas are shown in Figure 6.13 which also pinpoints the

[27] The average speed of the mobile terminal could be measured by the application by retrieving it directly from the integrated GPS module.

locations of the base stations identified using Sitefinder. As stated previously, the true locations of base stations are specified in order to evaluate the accuracy of the landmark initialisation process of the CCS Initial Mapping Stage. The position of each BTS is represented by a triangle. Note that some base stations have 3 sector directional antennas while others have a single omnidirectional antenna.

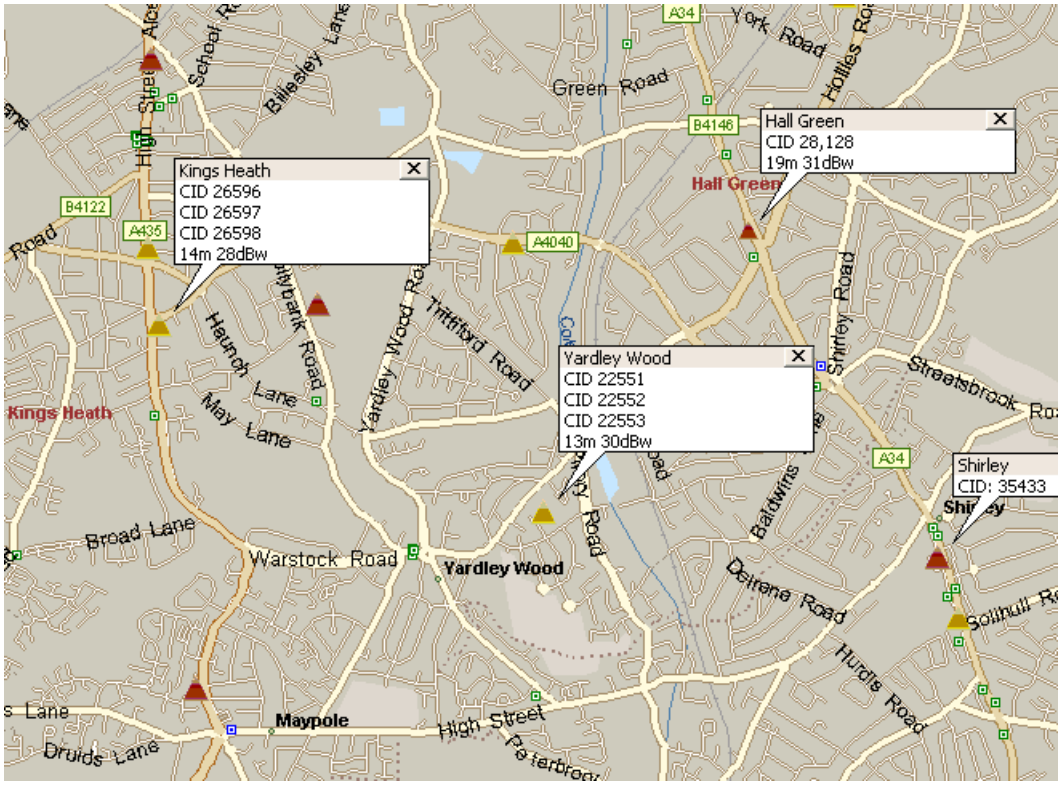

Figure 6.13 True positions of identified base stations for suburban CCS experiments

Note from Figure 6.14 that each fingerprint is represented by a colour coded circle. The position of the circle is determined by the GPS sample where the fingerprint is taken while the colour gradient shading provides an indication on the RSS measurement of the fingerprint. Moreover, the maximum, median and minimum RSS values are represented respectively by the dark red, white and dark blue colours. Their respective values are -65, -85 and -105 dBm and thus the RSS resolution in all the suburban experiments is 40 dB. The colour shades

between the minimum and the median RSS values are represented by the light blue colour whereas the colour shades between the median and maximum RSS values are represented by the light red colour.

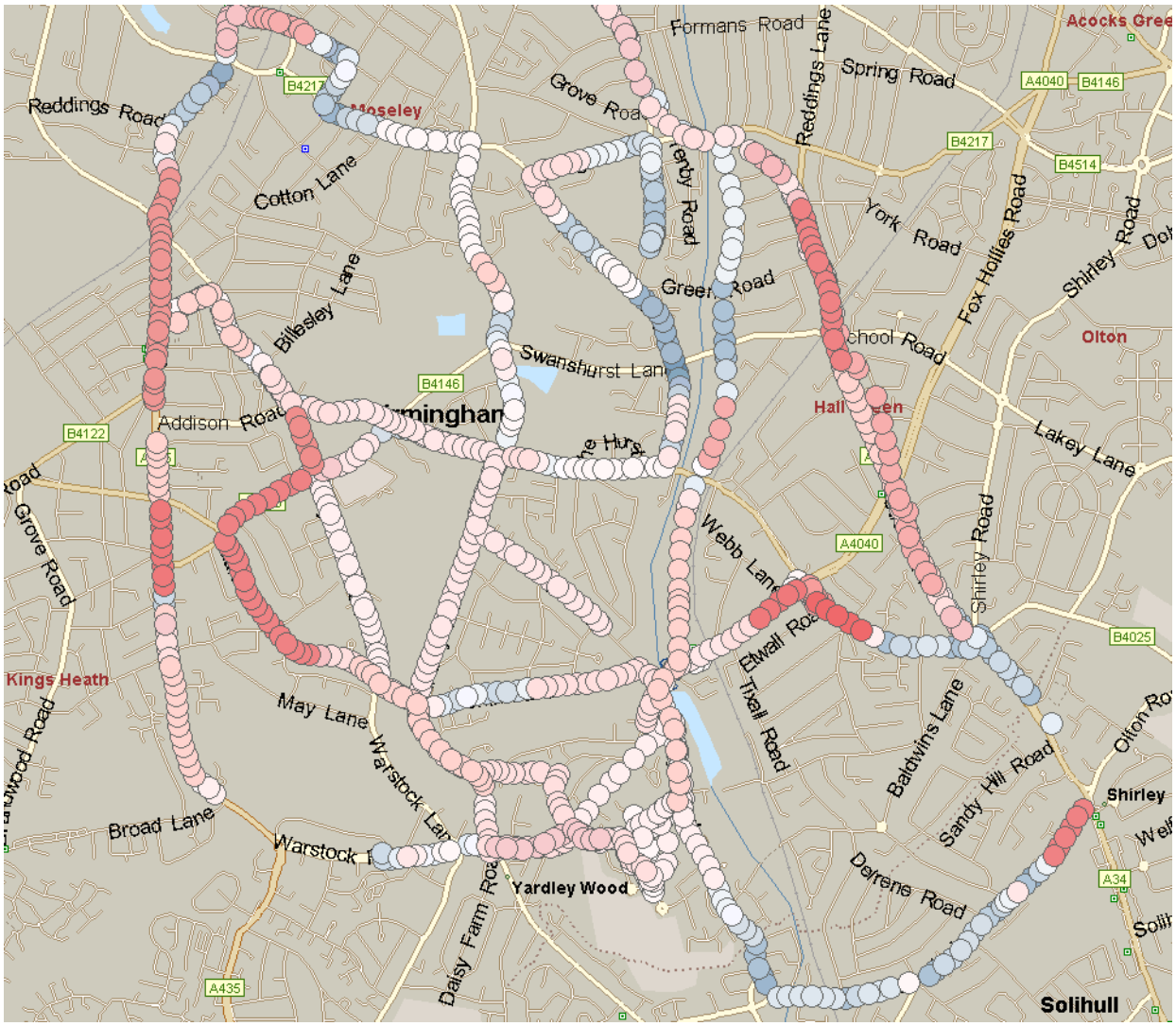

Figure 6.14 Fingerprints collected during Initial Mapping Stage

As introduced in Section 5.3.2, the CCS application allows the user to conduct the Initial Mapping Stage in each trial area in several step surveys in order to progressively build the database representing the BTS map. For each CCS experiment, the IMS can be stopped and resumed as long as the database is saved at the end of each IMS survey. In fact, the CCS application allows the user to save the estimated BTS landmark entries (BTS positions and

their associated lists of fingerprints) in a database file stored inside the phone's memory. The Network Localisation Stage is activated once the database obtained at the end of the IMS is deemed large enough to perform the EKF-SLAM process. Figure 6.15 shows the screenshots of the CCS application at the start of the IMS. Firstly, a GPS position fix is requested to initialise the state of the serving BTS as shown by the left side screenshot of Figure 6.15. The application then takes the GPS sample and combines it with the RSS measurement to form a fingerprint. Notice from the middle screenshot of Figure 6.14 the following:

- The RSS and the CID of the serving BTS are displayed under 'GSM Signal Information'.
- The GPS position fix obtained from the GPS module is displayed under 'GPS position' along with the speed and heading which are also measured using GPS.
- The initial estimate of the BTS landmark is displayed under the 'Initial Mapping Stage' next to the time instant and CID.

During the IMS survey, the mobile terminal travels while taking GPS samples, measuring the RSS and monitoring the CID to detect handovers to other base stations. Measurements are taken every 5 and 10 seconds in the driving and walking scenarios respectively. In the walking scenario, every measurement sample is taken manually using the CCS application command whereas in the driving scenario, the algorithm implementing the fingerprinting process uses a timer to take measurements every 10 seconds. The GPS monitor keeps track of the distance travelled in order to avoid taking several measurements while the smartphone is stationary. In fact, the fingerprinting process algorithm stops sending GPS position requests to the GPS monitor when the latter detects that the mobile terminal is not moving. The

regular GPS and fingerprint sampling is reactivated when a distance of 10 metres is travelled from the last stationary point.

As described in Section 5.3.2, each base station will be represented in the application by a Landmark object which encapsulates the BTS position, its CID and the list of fingerprint objects. All the landmark objects collected during the IMS can be saved in a database file at the end of every IMS survey by pressing the save command, as shown in the right side screenshot of Figure 6.15. In the next survey, the database can be accessed using the "Load" command as shown in the right screenshot of Figure 6.15. Loading an existing BTS map database allows the user to resume the IMS of ongoing SLAM experiments. As a result, more GPS samples can be taken to resume the initialisation process of existing BTS landmarks in the database, or to initialise newly observed landmarks whether in an existing trial area or a new unexplored area. The list of fingerprints associated to extracted or new BTS entries can therefore grow in preparation for the Network Localisation Stage.

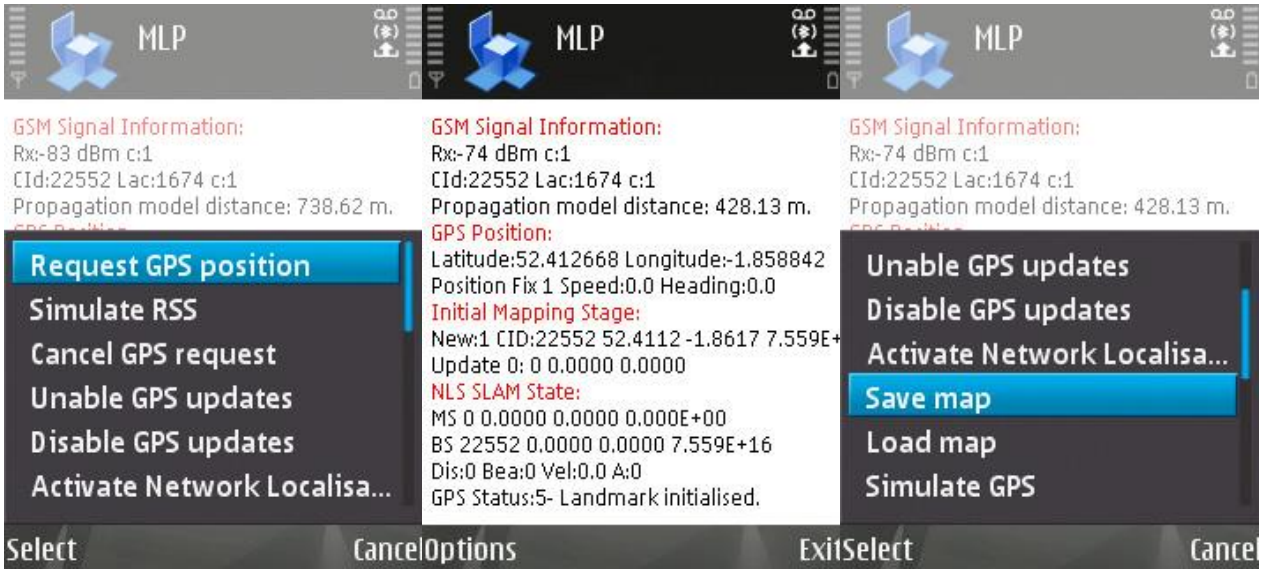

Figure 6.15. CCS Application Screenshots of the Initial Mapping Stage

It will be demonstrated in the next section that the accuracy of the CCS system strongly depends on the number of fingerprints collected during the IMS. On the other hand, the database is not loaded if the user wishes to start a new IMS survey and build an entirely new map of base stations.

Figure 6.16 consists of a graph showing the relationship between the number of fingerprints and the landmark accuracy which is again expressed in terms of rms distance error. The areas listed in Table 6.5 are numbered in Figure 6.16 and ordered according to the number of fingerprints. At first sight, the effect of the number of fingerprint on the landmark accuracy is not clearly apparent. Notice that areas 1, 2 and 3 have been surveyed whilst walking whereas areas 4, 5 and 6 have been surveyed while driving. If we separate the trial areas in the graph of Figure 6.15 into two groups according to the mobility scenario, we can notice in each group that the increase of the number of fingerprints leads to a decrease in the rms error and hence an improvement in the landmark estimation accuracy.

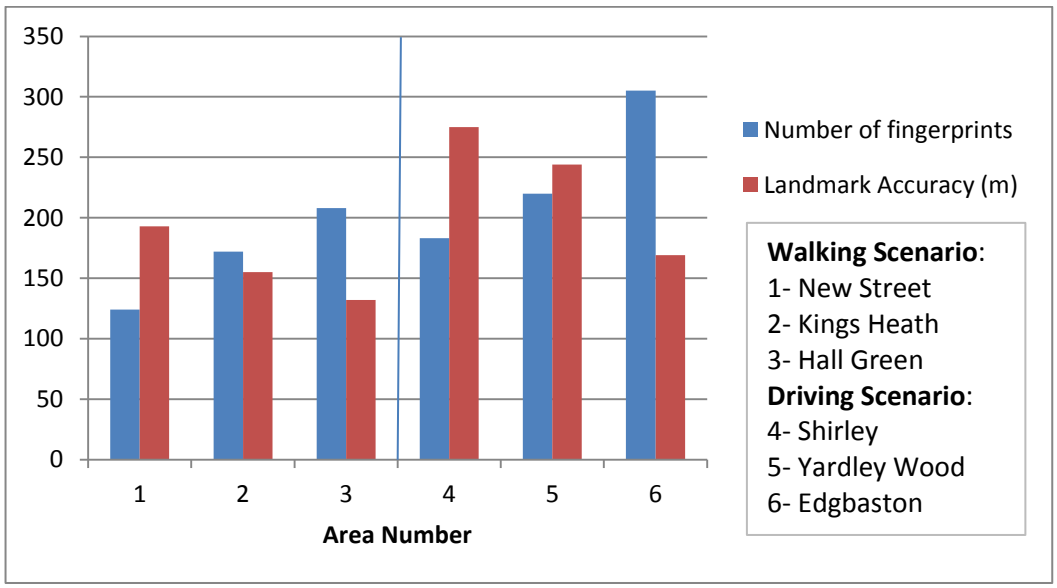

Figure 6.16 Landmark Initialisation Accuracy

Another important factor affecting the accuracy of landmark initialisation is the geometric dilution of precision (GDOP) which, in this case, consists of the displacements of GPS samples relative to the true position of the base stations. The accuracy of the landmark estimate improves if samples are taken from different directions relative to the true BTS position, especially if samples are taken in a circular manner around the true BTS position. However, the Initial Mapping Stage surveys have been conducted without taking into account the true positions of base stations. The surveys were rather focused on producing a fingerprint map of the highest possible resolution by taking GPS samples and RSS measurements along the major routes of each trial area, as shown in Figure 6.14.

Figure 6.17 provides an example of the estimation process of one of the base stations in the Yardley Wood area by showing the evolution of the BTS state estimates with respect to the true BTS position.

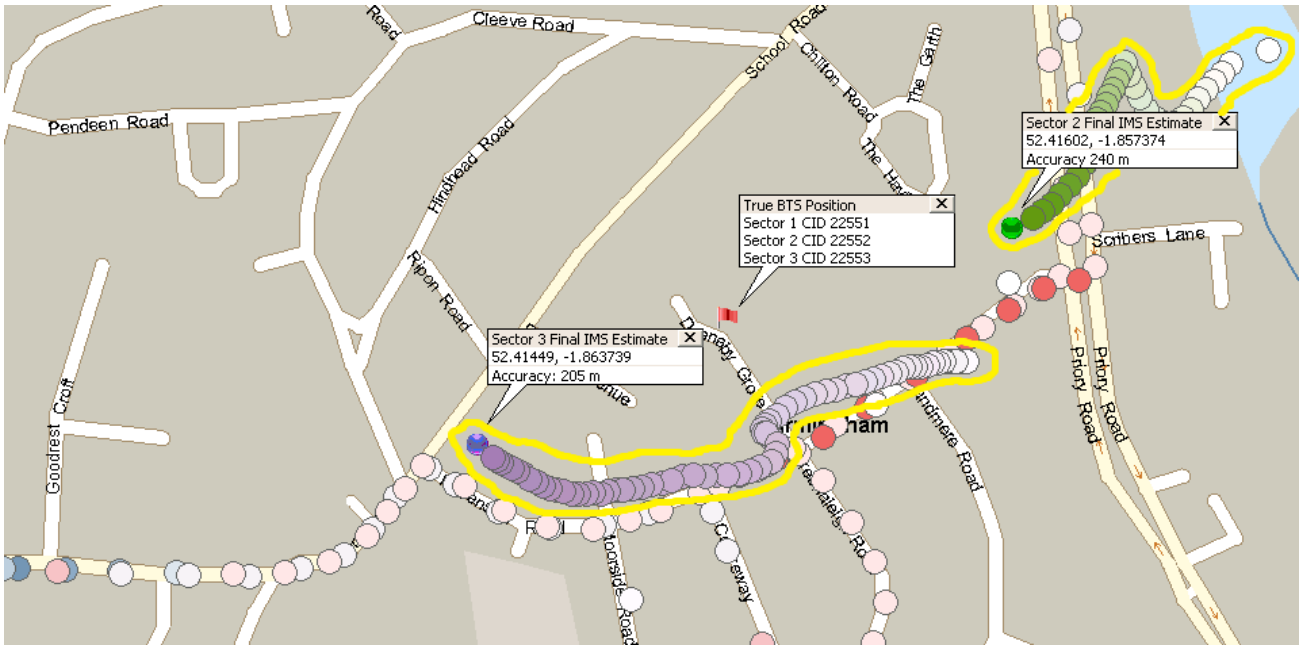

Figure 6.17 Evolution of landmark estimates during the Initial Mapping Stage.

In Figure 6.17, the true position of the surveyed BTS is denoted by the red flag whose label lists the three BTS sectors and their corresponding CID codes. The estimates of Sector 2 and Sector 3 produced by the BTS initialisation Model are mapped using the gradient coloured circles highlighted by the yellow line. Sector 2 and Sector 3 estimates are represented by the green and purple coloured circles respectively and only the final estimates resulting at the end of the IMS are labeled with their corresponding accuracy relative to the true BTS position. Note that the remaining circles that are not marked by the yellow line consist of the GPS samples/fingerprints, which are denoted using the same RSS-based colour scheme used in the map of Figure 6.14.

We can deduce from the evolution of landmark estimates shown in Figure 6.17 that the final landmark estimates produced by the BIM are not necessarily the most accurate positioning outcomes. While Sector 2 estimates converge towards the true BTS position, Sector 3 does not show this convergence. In fact, the accuracy of the landmark positioning outcome strongly depends on the path of the mobile terminal relative to the true BTS position, in other words, on the relative geometry between the MT GPS samples and the target BTS, which is defined by the Geometric Dilution of Precision (GDOP) [Fig10]. In the example experiment illustrated in Figure 6.17, the mobile terminal was travelling west making the Sector 3 estimates generally shift towards the west direction, as shown by the purple circles.

6.5.2 Network Localisation Stage Results and Evaluation

Once a trial area is surveyed as part of the Initial Mapping Stage, the Network Localisation Stage mode of the application is activated in order to start the EKF-SLAM positioning process. A path is chosen within the surveyed area making sure all the base stations that are hearable from any point of the chosen path have been mapped during the IMS. As stated in Chapter 4

and Chapter 5, if an unknown BTS is encountered during the NLS, the application returns to the IMS mode to initialise the position of this BTS and link fingerprints to it. When the NLS is activated by pressing the command shown in the left screenshot of Figure 6.18, the application starts the network monitoring process to constantly observe the received signal strength and the CID of the serving BTS in order to detect any handovers as soon as they occur.

Figure 6.18 CCS application screenshots during the Network Localisation Stage

Note from Figure 6.18 that the NLS has been activated after 71 fingerprints of base station ID 22552. Notice under the 'NLS SLAM State', the Mobile State (MS) position is specified in latitude and longitude next to the time instant to the left and the determinant of the MS covariance matrix to the right. Below the Mobile State, the Base station State (BS) is displayed which represents the state of the currently observed BTS. The BS position is displayed between the CID and the covariance matrix determinant associated with the BS. While focusing on the NLS SLAM state, notice in Figure 6.18 the difference between the middle and right-side screenshots. The middle screenshot shows the SLAM State after the initialisation of the first mobile state and BTS state while the right-side screenshot shows the SLAM State after 5 iterations.

As described in Section 4.5, the initial mobile position is produced by the database correlation algorithm after scanning the fingerprints associated with the observed BTS. The state of the mobile terminal is not updated until a change in the measured RSS or a handover to a different CID is detected. The a priori mobile state estimate is produced by the process model described in Section 4.5.2, which uses the displacement of the current mobile state relative to the new fingerprint extracted following a change in the network measurements (CID or RSS). Note from the screenshots of Figure 6.18 that the transition distance and bearing are displayed below the BTS state. As stated previously, GPS is used during the NLS solely for evaluation purposes. The accuracy of the mobile terminal position can therefore be monitored during the course of the experiment and is displayed next to the transition information along with the velocity, which is also measured using GPS.

Table 6.6 reports the positioning accuracy results of the CCS experiments for each of the mobile terminal and landmarks estimates. The details of the experimental setup associated with the NLS are listed in Table 6.6 as follows:

- *The number of observed base stations* which are first retrieved from the database representing the initial map and then integrated into the SLAM state vector in order to contribute to the EKF-SLAM estimation process.
- *The mobile accuracy* is the mean rms error between the estimated mobile position and the true mobile position.
- The landmark accuracy refers to the mean accuracy of all observed landmarks during the network localisation stage of the experiment. The accuracy of a landmark estimate consists of the rms error between the estimated landmark

position and the true position of the BTS which has been retrieved from Sitefinder for evaluation purposes only.

Table 6.6 Constrained Cellular SLAM experiments

Trial Area	Initial Mapping Stage					Network Localisation Stage		
	σ_{P_r} *(dB)*	Area (km^2)	Mobility	Number of Fingerprints	RSS Resolution (dB)	Observed BTS no	Mobile Accuracy (m)	Landmark Accuracy (m)
New Street ***(urban)***	8.6	3	Walking	124	23	5	281	160
Kings Heath ***(suburban)***	4.5	2.5	Walking	172	27	5	349	112
Hall Green ***(suburban)***	7.4	2	Walking	208	21	2	321	105
Shirley ***(suburban)***	5.9	5.5	Driving	183	28	3	283	237
Yardley wood ***(suburban)***	3.8	9	Driving	220	34	10	265	188
Edgbaston ***(mixed)***	7.7	10	Driving	305	36	7	297	157

Table 6.6 takes some elements of the Initial Mapping Stage reported in Table 6.5 in order to investigate the impact of the IMS on the Network Localisation Stage in terms of the accuracy of the mobile terminal and landmark estimates. Figure 6.19 is a graph illustrating the impact of the number of fingerprints collected during the IMS on the mobile and landmark accuracies at the end of the NLS.

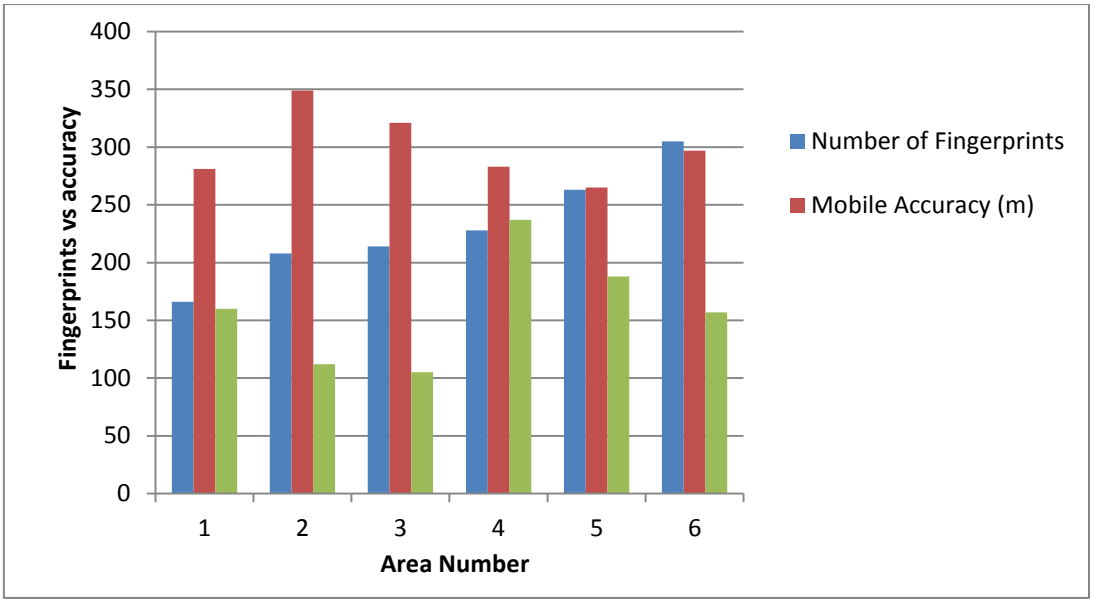

Figure 6.19 The impact of the fingerprinting process on mobile and landmark accuracies

Note that the suburban trials in areas 2 to 5 confirm that the accuracy of the mobile state estimates improves with the increase in the number of fingerprints. However, area 1 (New Street) and area 6 (Edgbaston) represent exceptions to this relationship as the increase in the number of fingerprints did not result in an improvement in the mobile accuracy. This may be due to the different nature of the environment in these urban areas. Despite a lower number of fingerprints, the New Street trial results are relatively accurate compared to the suburban trial results because it is a smaller area and with a similar resolution of signal strength measurements. This leads to more unique fingerprints in the BTS map database and hence improves the accuracy of the initialisation of the mobile state estimate, which is due to an enhanced performance of the database correlation algorithm described in Section 4.5.1. The results of the Edgbaston experiment are less accurate because the area is much larger with a similar RSS resolution, which does not improve the individuality or uniqueness of fingerprints.

On the other hand, the impact of the fingerprinting process on the landmark positioning outcome has already been demonstrated in the IMS surveys reported in the previous section. In this discussion however, we can evaluate the extent to which the EKF-SLAM process improves landmark accuracy after updating the augmented SLAM state vector during the Network Localisation Stage. As shown in Figure 6.20, the accuracy improvement is larger in trial areas with a well-fitted RSS model as defined by the calibration error standard deviation σ_{P_r}. The result of the New Street experiment is again an exception as its landmark accuracy appears to be relatively accurate compared to the suburban trials despite a larger RSS error standard deviation σ_{P_r}. Therefore, the characteristics of the fingerprinting process, namely the smaller urban area and high RSS resolution relative to the other trial areas, play a major role in the landmark estimation accuracy improvement.

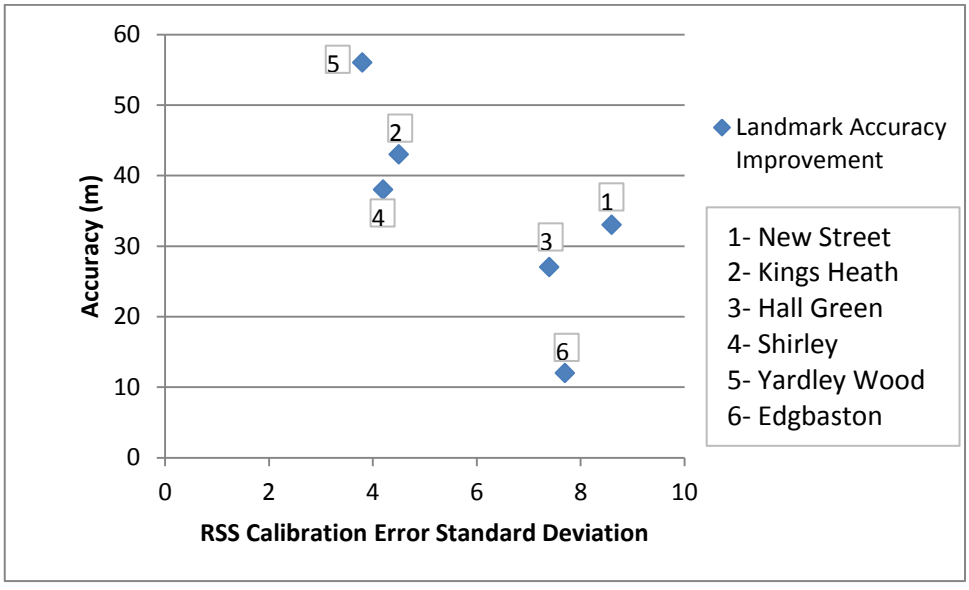

Figure 6.20 Impact of calibration error standard deviation on landmark accuracy improvement

Note from Table 6.6 that the mean accuracy of the mobile positioning outcomes from all the CCS trials is 299 metres. Compared to the Texas E-911 trial results shown in Table 6.4, the CCS accuracy is lower compared to U-TDOA and A-GPS/AFLT results. However, it is higher

than the A-GPS results within the 3G/UMTS networks in the 95th percentile. Compared to DCM methods in the literature, the accuracy achieved by CCS is lower because the size of the fingerprint map is considerably smaller in size and resolution compared to the maps constructed in DCM trials. It is however important to note that cellular DCM positioning received little interest in the literature compared to RSS fingerprinting methods for indoor WLAN positioning, which are characterised by high resolution fingerprint maps.

We can deduce from this discussion, that the Constrained Cellular SLAM can achieve higher accuracies than the reported mean accuracy of 300 m if the Initial Mapping Stage is conducted extensively. This would involve building a high resolution map of fingerprints, which is characterised by a large number of fingerprints as well as a high RSS measurement resolution. The accuracy of the mobile and landmark estimates would greatly increase if the path taken by the mobile leads to a high GDOP relative to the true locations of base stations.

6.5.3 CCS Positioning Experiment

This section provides a detailed outline of the Yardley Wood experiment in order to provide an example of a CCS trial, illustrate the positioning outcomes and demonstrate the convergence properties the SLMA state covariance matrix, which is fundamental in any EKF-SLAM system. Note from Figure 6.19 that this experiment represented by area 5 in the graph, achieved the most accurate mobile position estimate (265m). Conversely, this trial produced the second least accurate landmark positioning (224m).

6.5.3.1 Initial Mapping Stage

Figure 6.21 is a map showing the path taken during the Initial Mapping Stage of this trial area, which is approximately 27 Kilometers long covering an area of 9 Km^2.

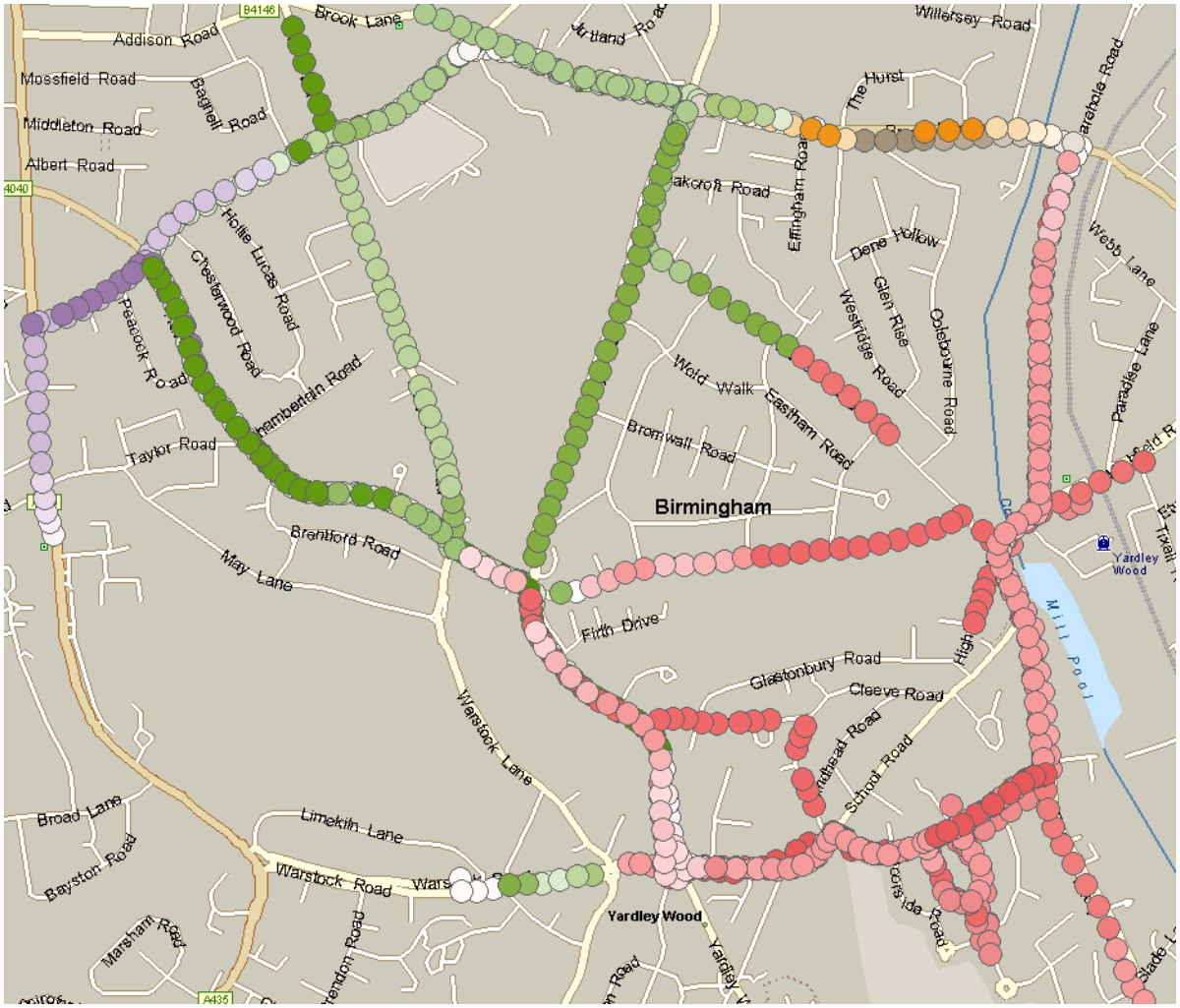

Figure 6.21 Fingerprints from Area 5 suburban CCS experiment (Initial Mapping Stage)

In this trial area, 5 distinct base stations have been identified from Sitefinder. Four of these BTS have three sectors according to the BTS identification process. As a result, a total of 13 individual antennas can be observed by the mobile terminal while travelling within this area. In Figure 6.21, the fingerprints are shown in a unique colour for each distinct base station and thus five colours can be distinguished. The gradient colour change from light to dark colour indicates the measured signal strength. The green coloured fingerprints from Figure 6.21, which belong to a single base station with three sectors, are redrawn in Figure 6.22. A different colour is now used to denote the fingerprints of different sectors.

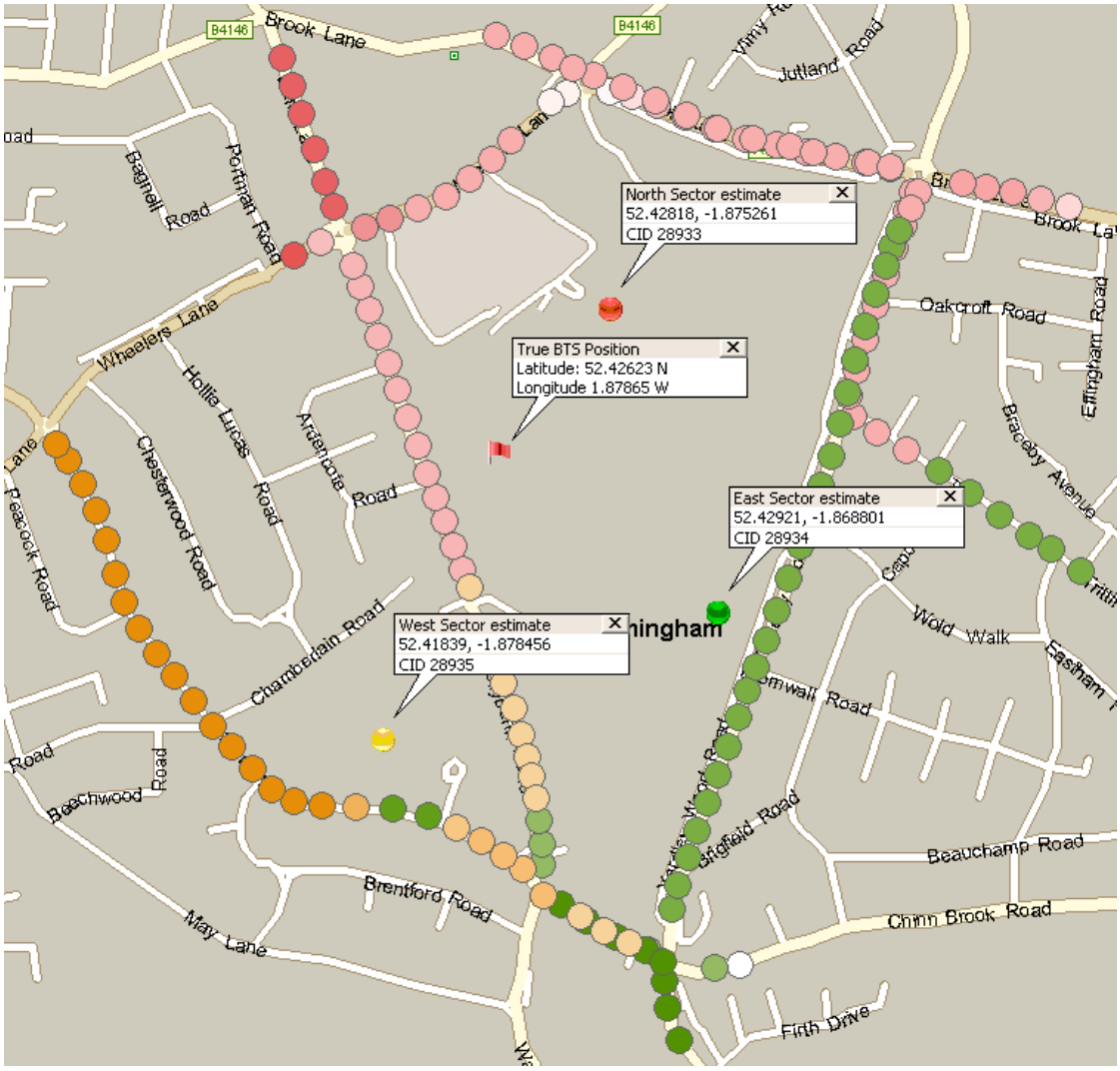

Figure 6.22 Fingerprints of individual BTS sectors and resulting landmark estimates

Figure 6.22 shows the true position of the surveyed BTS as well as the landmark estimates of each sector of the BTS produced by the BTS Initialisation Model. These landmark estimates are combined to their corresponding fingerprints and saved as part of the BTS map database constructed during this IMS survey.

6.5.3.2 Network Localisation Stage

As stated previously, the iterations of the EKF-SLAM algorithm during the NLS are determined by events detected by the network monitoring process of the CSS application, namely CID handovers and RSS variations. In this particular experiment, 49 iterations of the

EKF-SLAM algorithm were recorded by the application, which are listed in Table 6.7 along with the observed CID, the measured RSS and the resulting mobile position estimation accuracy.

Once the initial map of base stations has been constructed, the Network Localisation Stage is initiated to estimate the position of the mobile terminal as well as updating the initial BTS positions. In order to evaluate the accuracy of the EKF-SLAM positioning process, the true mobile terminal positions are retrieved by the CCS application from the built-in GPS module. The path taken by the MT during the NLS is shown in Figure 6.23. Starting from the bottom right corner of Figure 6.23, the trial consisted of driving around the loop in the anti-clockwise direction to return back to the starting position. Figure 6.23 denote the GPS evaluation samples using pushpins which are coloured according to the observed CID. Note that these colours were used to represent the same base station during the fingerprinting process of Figure 6.20.

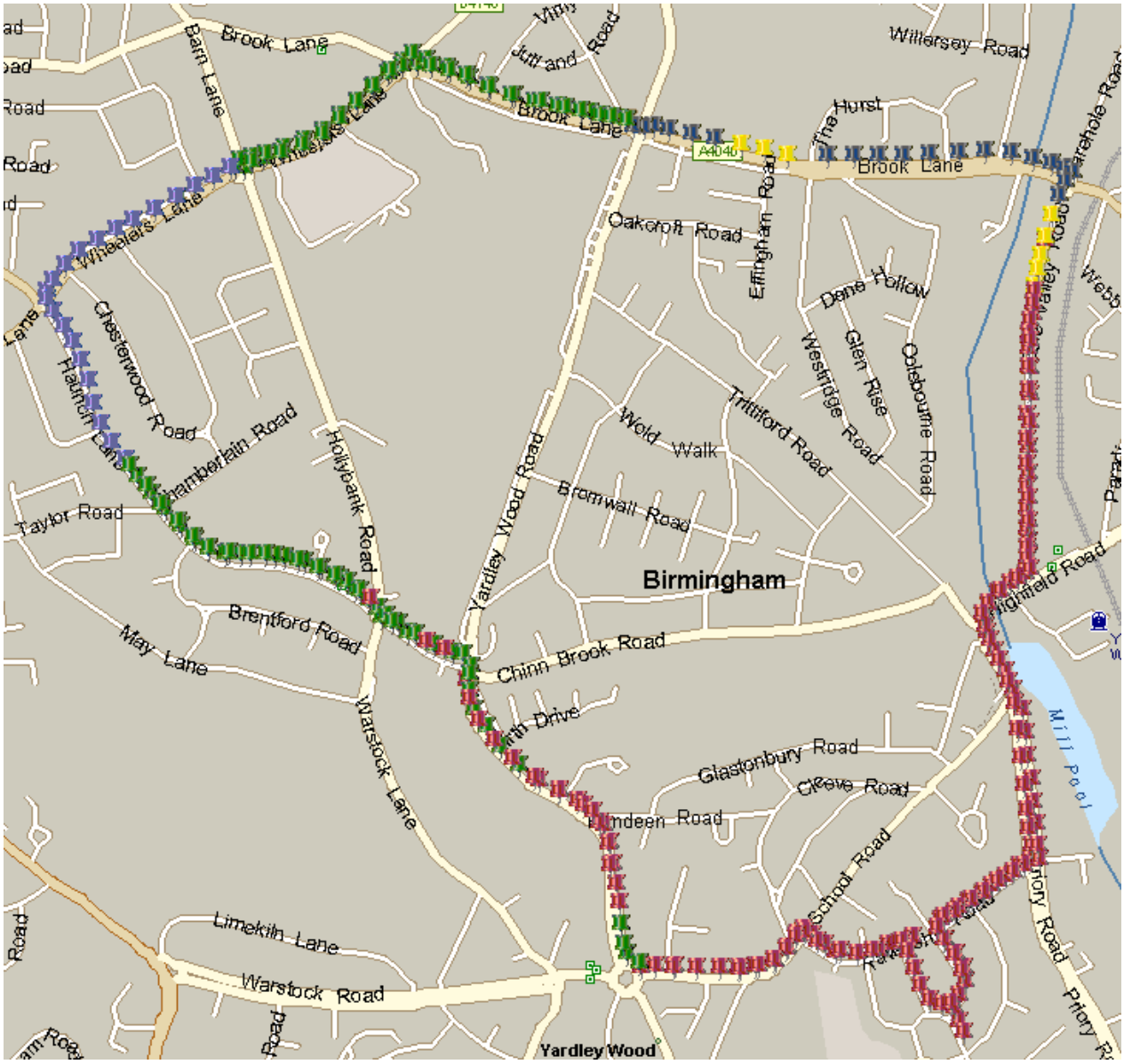

Figure 6.23 The true mobile terminal path taken during the Network Localisation Stage

Figure 6.24 is a graph showing the mobile state estimate accuracy at each EKF-SLAM iteration, which is denoted by time instant k. The mean accuracy of the mobile position estimate from k=1 to 49 is 265m. The estimated mobile terminal positions are illustrated by colour-coded circles in Figure 6.25. In order to show the chronology of mobile position estimates from time instant 1 to 49, Figure 6.25 uses gradient colour shading to denote the initial, intermediate and final estimates using the blue, white and red colours.

Table 6.7 Network Localisation Stage measurements and results

k	CID	Rss (dBm)	Latitude (degrees N)	Longitude (degrees W)	Accuracy (m)
1	22552	-82	52.41243	-1.858931	1
2	22552	-82	52.41252	-1.85875	14
3	22552	-82	52.4147	-1.858924	250
4	22552	-84	52.41523	-1.858474	312
5	22552	-79	52.41501	-1.858625	293
6	22551	-79	52.42287	-1.85955	332
7	22551	-82	52.42552	-1.858351	392
8	22551	-88	52.42563	-1.858258	398
9	22551	-85	52.42561	-1.858269	413
10	22551	-83	52.42468	-1.858195	524
11	22551	-84	52.42468	-1.85819	516
12	22551	-81	52.42525	-1.858354	451
13	29844	-81	52.42722	-1.861984	278
14	22079	-81	52.42983	-1.868058	322
15	22079	-77	52.42955	-1.868321	74
16	22079	-85	52.42961	-1.86583	277
17	28933	-85	52.43032	-1.869771	29
18	28933	-80	52.43027	-1.869932	23
19	28933	-75	52.43015	-1.870218	5
20	28933	-80	52.43008	-1.876313	163
21	28934	-80	52.42651	-1.876594	499
22	28934	-86	52.42648	-1.876608	502
23	28933	-86	52.4295	-1.874038	220
24	28933	-82	52.42953	-1.874019	219
25	28933	-80	52.42952	-1.874026	219
26	26597	-80	52.42765	-1.885479	196
27	26596	-80	52.4277	-1.886505	183
28	26596	-81	52.42777	-1.886447	293
29	26597	-81	52.42798	-1.885415	369
30	26597	-71	52.4277	-1.885546	380
31	26597	-82	52.42829	-1.884821	559
32	28935	-82	52.42562	-1.884802	265
33	28935	-71	52.42574	-1.885624	309
34	28935	-82	52.42353	-1.884538	420
35	22553	-82	52.41749	-1.873098	535
36	22553	-87	52.41738	-1.87296	550
37	28935	-87	52.41955	-1.876329	165
38	28935	-84	52.41968	-1.876571	145
39	28935	-71	52.41997	-1.87724	73
40	28934	-71	52.42027	-1.877279	128
41	22553	-71	52.41557	-1.871195	315
42	22553	-84	52.41406	-1.868322	166
43	28934	-84	52.41637	-1.871275	210
44	28934	-87	52.41537	-1.870555	167
45	22553	-87	52.41519	-1.871547	246
46	22553	-86	52.41498	-1.87198	246
47	22553	-82	52.41458	-1.87019	169
48	22553	-83	52.41374	-1.868305	113
49	22553	-89	52.41274	-1.868507	94

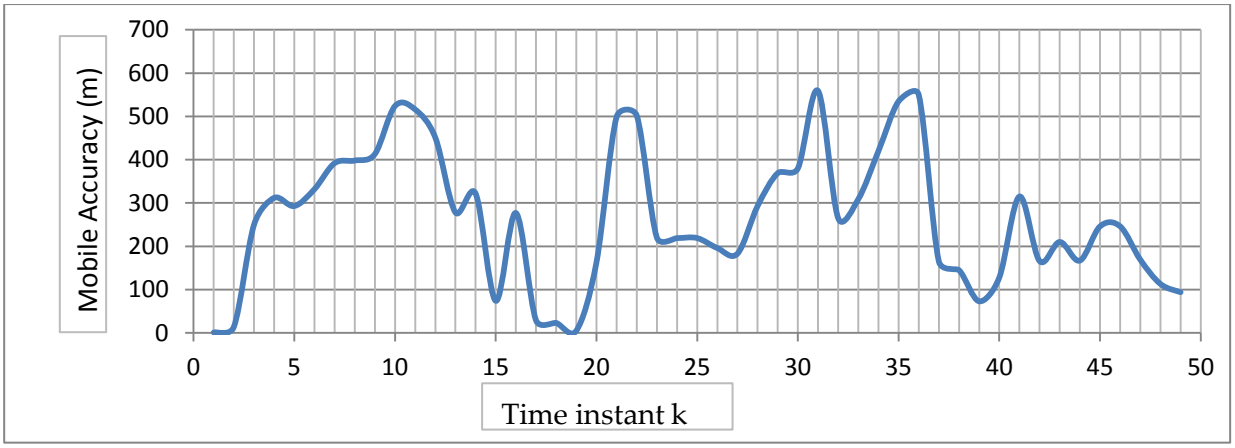

Figure 6.24 The mobile state estimate accuracy

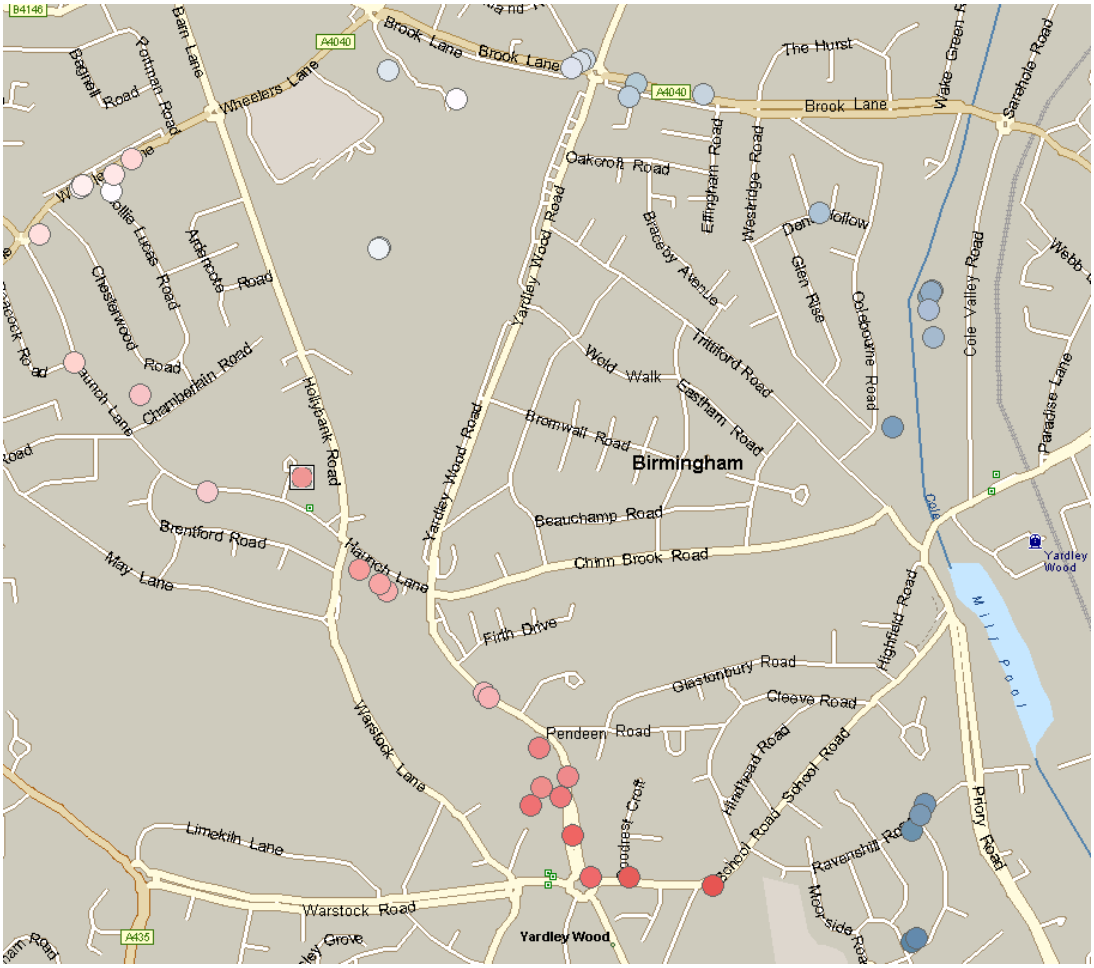

Figure 6.25 Map of mobile state estimates

Note from the map of mobile estimates of Figure 6.25 that there are displacement gaps between some estimates. These gaps illustrate the control inputs of the process model, namely the transition distance and bearing, which depend on the fingerprinting process and

the database correlation algorithm, as stated previously. The history of the transition distance is illustrated in Figure 6.26. Figure 6.27 shows the convergence property of the Mobile State (MS) covariance which is fundamental as far as the performance of the EKF-SLAM algorithm is concerned. As stated previously, the MS covariance can be defined by the determinant of the covariance matrix of the mobile state within the entire SLAM system covariance matrix.

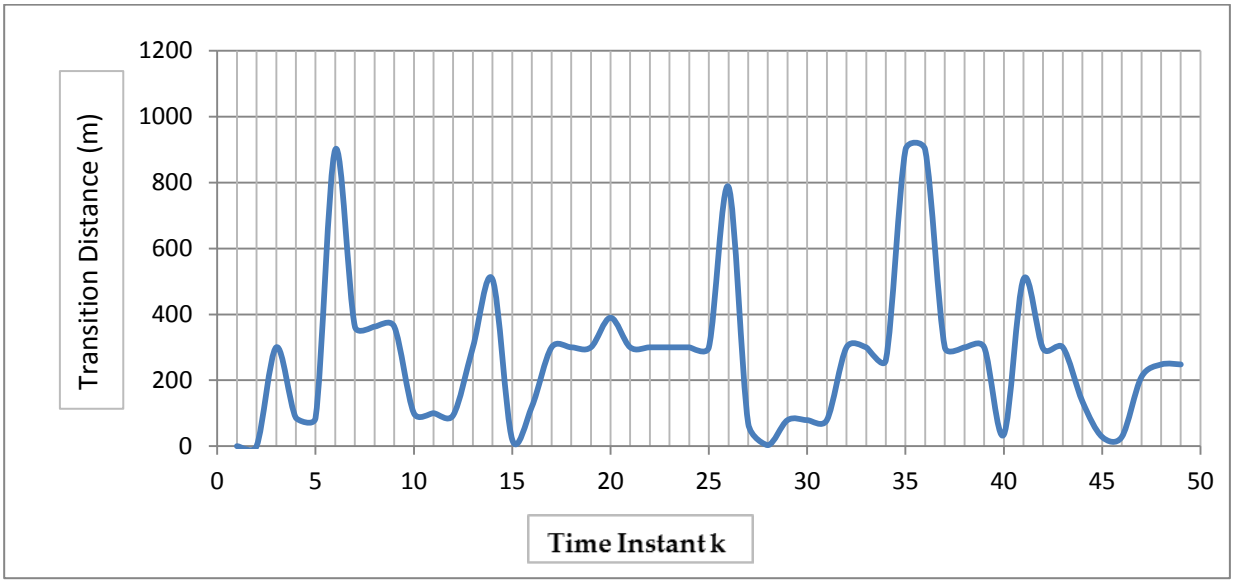

Figure 6.26 History of the transition distance

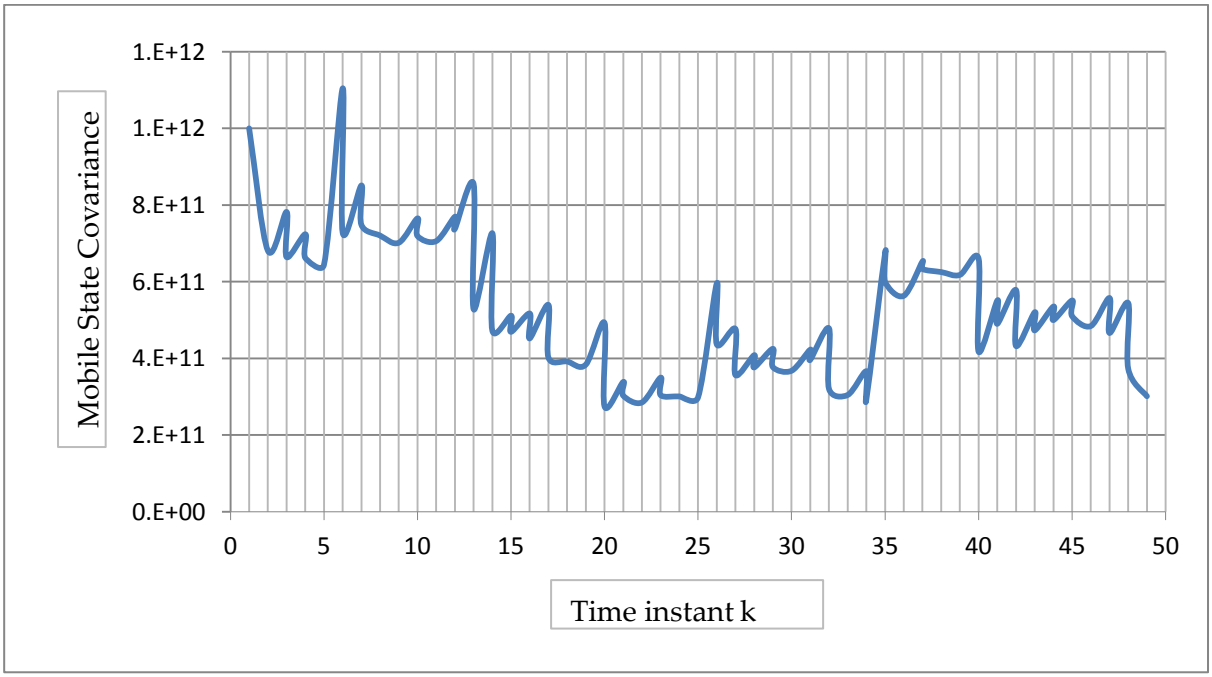

Figure 6.27 Evolution of Mobile State covariance

Like any EKF-based system, the length of the transition distance increases uncertainty in the prediction step of the EKF. This is illustrated in figure 6.27 by the increase in the mobile state covariance at the time instants where the transition distance is larger than 600 metres, as shown by the three peaks in Figure 6.26. The covariance increase is large enough to affect the overall convergence of the EKF-SLAM system as it remains visible after the update step of the EKF. However, it is clear that the system converges at each state update in line with the theoretical convergence property of EKF-SLAM.

Note from Table 6.7 that the iteration in which a handover occurred is shaded in red. The order in which each landmark is observed and for how long is important as far as the convergence of landmark covariance is concerned. For this reason, Table 6.8 is constructed to identify landmarks in terms of the order in which they have been observed using a Landmark Order ID.

Table 6.8 History of landmark observations

Landmark Order ID	K at Handover	CID	Observation Time Interval
1	1	22552	5
2	6	22551	7
3	13	29844	1
4	14	22079	3
5	17	28933	4
6	21	28934	5
7	26	26597	1
8	27	26596	2
7	29	26597	3
9	32	28935	3
10	35	22553	2
9	37	28935	3
6	40	28934	1
10	41	22553	2
6	43	28934	2
10	45	22553	5

Table 6.8 links the order ID to the CID of the landmark and specifies the time instant of the observation as well as the time interval during which the landmark has been observed. Notice in Table 6.8 that ten landmarks have been observed during the Network Localisation Stage of this trial. Table 6.8 also highlights the landmarks that are re-observed.

In support of Table 6.8, Figure 6.28 illustrates the history of landmark observations which consists of the time instants when new landmarks are observed following a handover and how long they are observed for. The red squares in this graph denote how long each landmark has been observed before the next handover occurs. The order ID of each landmark is shown in Figure 6.28 each red square.

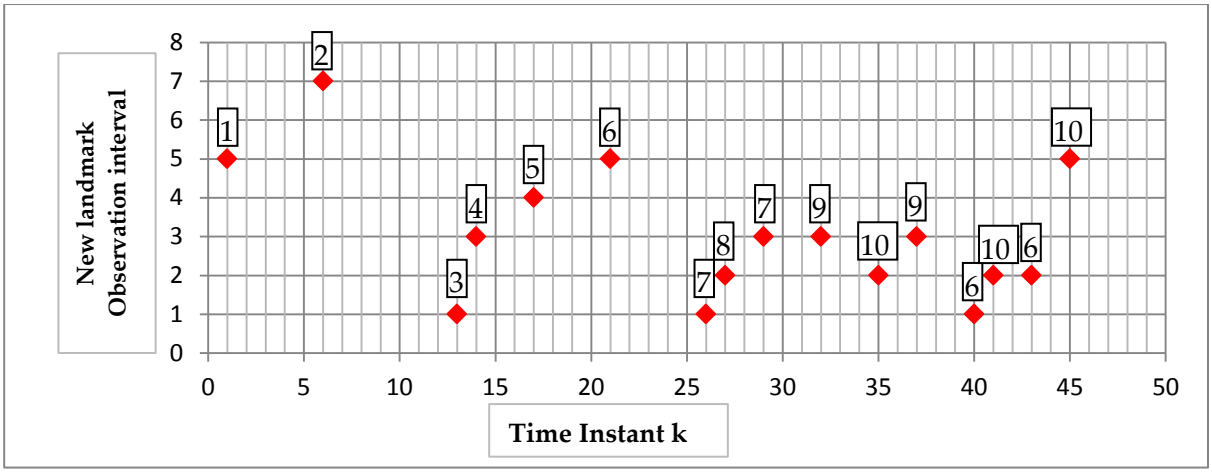

Figure 6.28 History of landmark observations

Figure 6.29 shows the history of the observed landmark covariance, which also illustrates when handovers occur. In fact, each increase in the determinant of the covariance matrix shows that a new landmark is being observed following a CID handover, at the same time intervals specified in Table 6.8 and Figure 6.28.

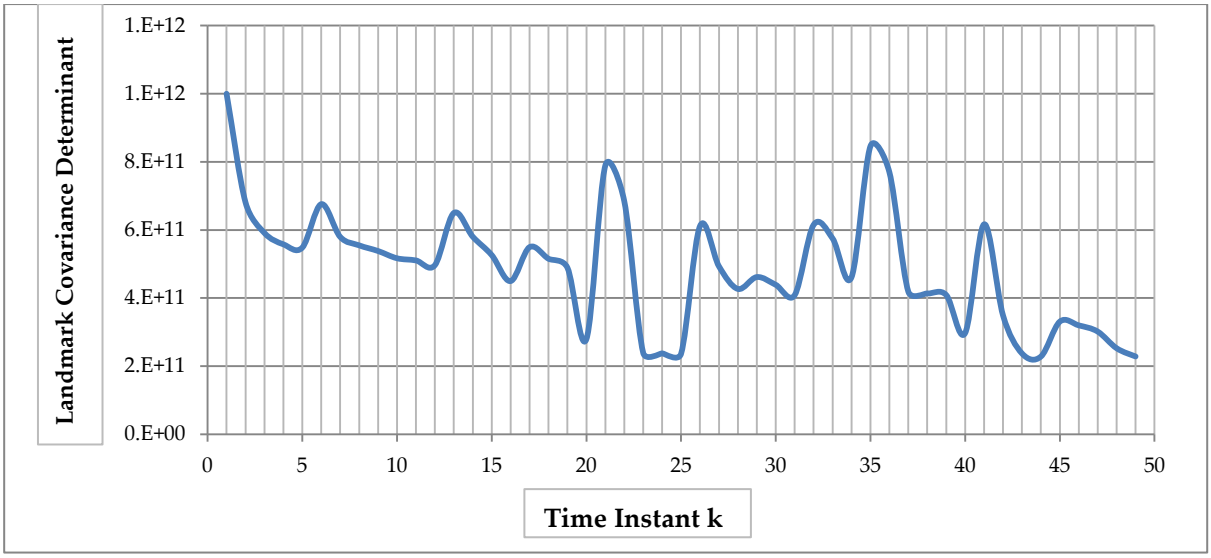

Figure 6.29 History of the observed landmark covariance

The evolution of the covariance associated with each landmark that was observed and integrated into the SLAM State vector is shown in Figure 6.30. The aim is to demonstrate the correlation between observed landmarks and existing landmarks whose states have been initialised and integrated into the SLAM augmented state vector. As stated previously this correlation is key to the convergence property of the map augmented state covariance matrix.

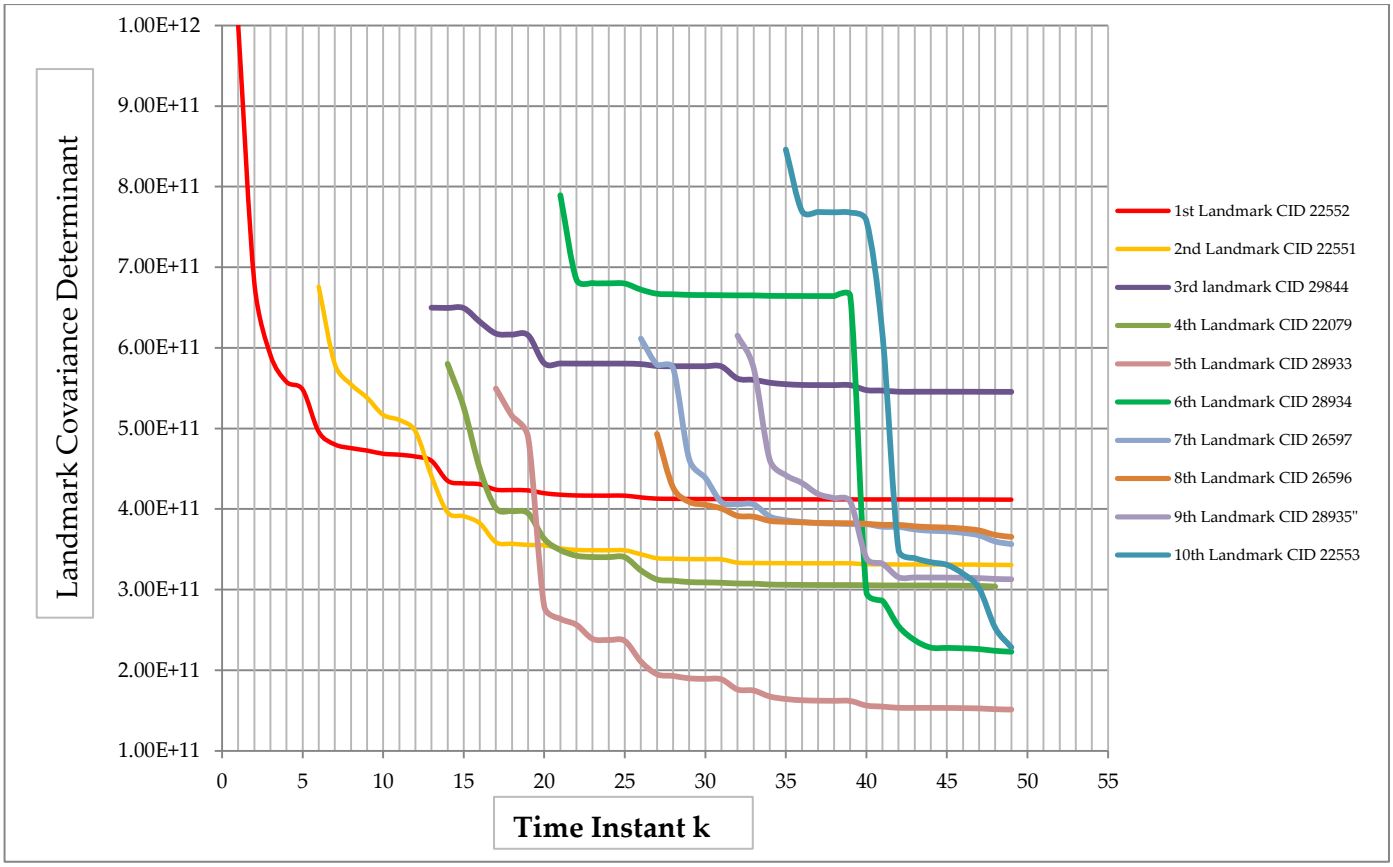

6.30 Evolution of each landmark covariance within the SLAM state covariance

Reading Figure 6.30 in conjunction with Figure 6.28, we can notice that:

- The 7th landmark (red, 26597) and 9th (orange, 28935) landmark were re-observed once at time instants 29 and 37 respectively.
- The 6th landmark (green, 28934) was re-observed twice at time instants 40 and 43.
- Similarly, the 10th landmark (blue CID 22553) was re-observed twice at time instants 41 and 45.
- Each re-observation of the landmarks stated above is reflected in the graph by a significant drop in the covariance matrix determinant associated with each of these landmarks.

Moreover,

- The 3rd landmark (purple, 29844) was observed only once and for a single time instance (k=13). Similarly, the 8th landmark (grey,26596) was observed once and for two time instants (27 and 28).
- This explains the slow reduction in the uncertainty associated with these landmarks. In fact, the slow convergence of the covariance determinant for each of these landmarks is due to the correlation of their estimates with the estimates of the other landmarks within the SLAM system.

Figure 6.31 is a map showing the evolution of the landmark estimates, which are retrieved from the map augmented SLAM state at each iteration. The true location of each BTS which was observed during the NLS survey is denoted in Figure 6.30 using a coloured triangle. In order to identify the base stations, the same colours as in Figure 6.23 are again used in Figure 6.30. The mean accuracy of all landmark estimates relative to their true BTS positions is 188 metres. Note that this accuracy has been reported in Table 6.6 as part of the Yardley Wood trial.

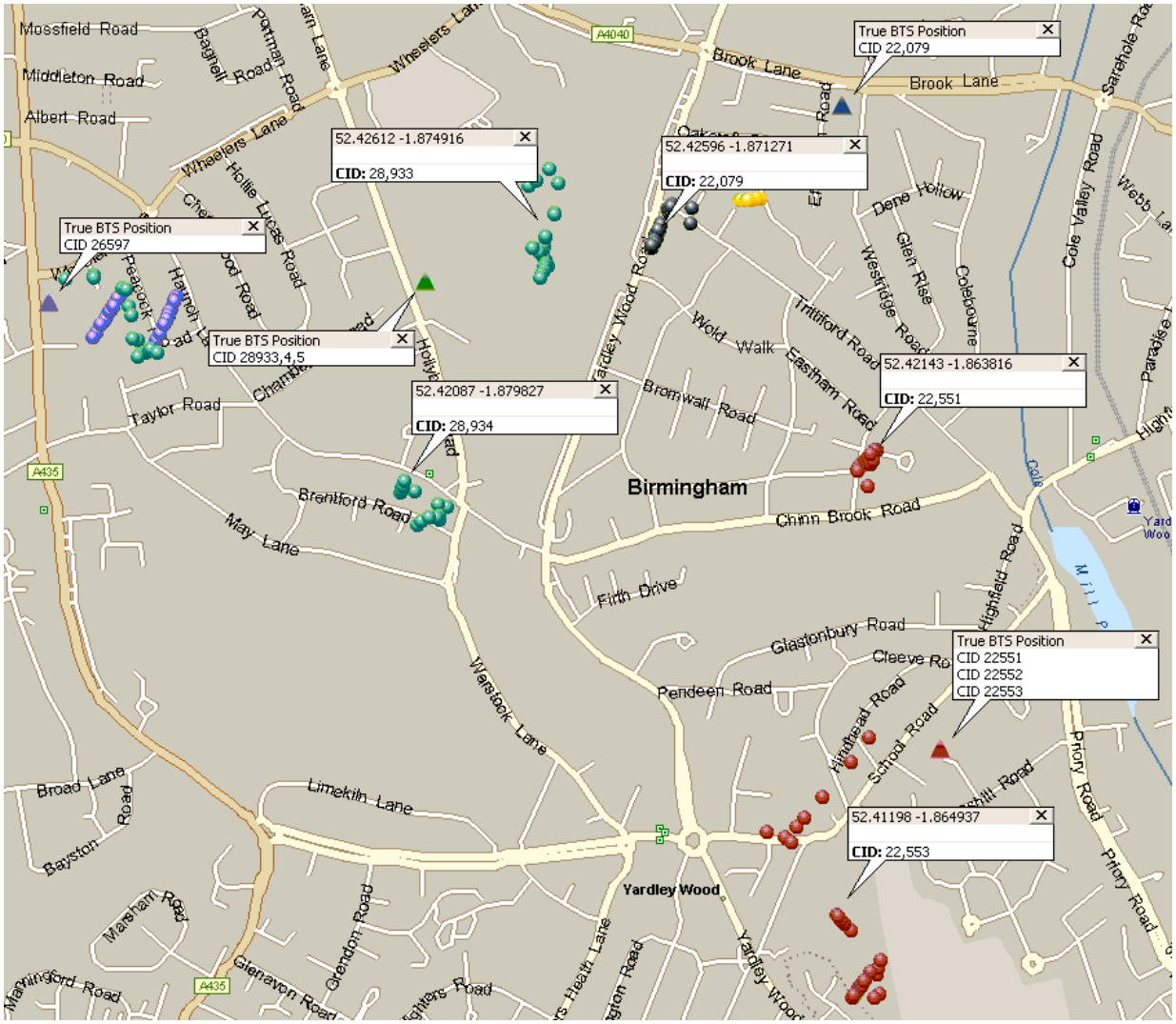

Figure 6.31 Evolution of BTS landmark estimates from the SLAM state vector

In order to show the convergence of landmark state estimates towards the true BTS position, Figure 6.32 considers one of the observed BTS landmarks shown in Figure 6.31. This landmark is denoted in the map of Figure 6.31 by the green triangle for its true position and by the green circles for its estimates. Figure 6.32 shows the evolution of the state estimates of each sector of this landmark using the same colour gradient shading that was used in Figure 6.22, as the latter illustrates the IMS estimation process of the same BTS. The evolution of covariance matrix determinant associated with each of these sectors has already been depicted in figure 6.30.

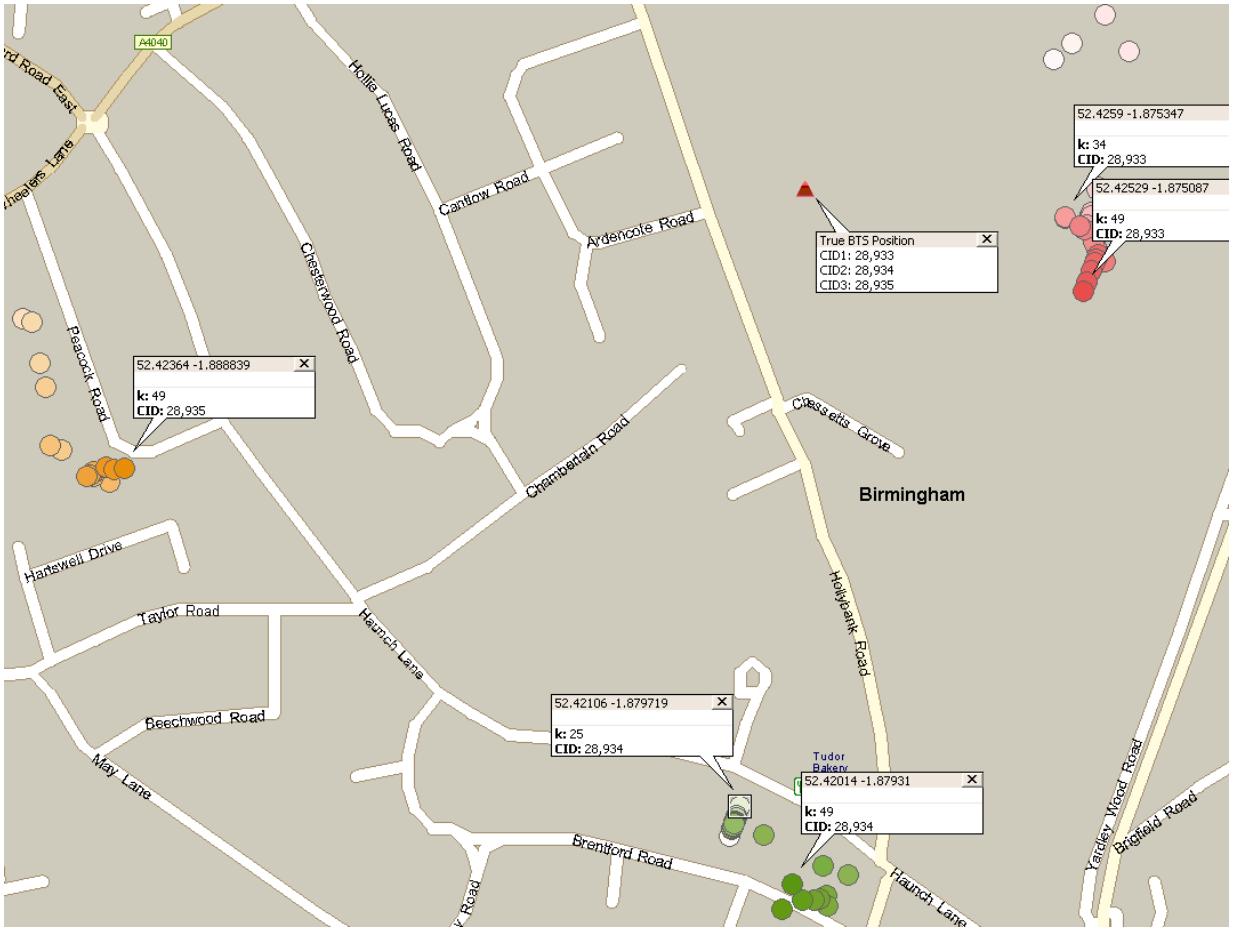

Figure 6.32 Convergence of landmark estimates associated with a 3 sectored BTS

Chapter 7 – Conclusion

As localisation systems depend on the infrastructure within which they operate, it is well known that a universal localisation method suitable for all types of applications simply does not exist. While critical location-based services such as the E-911 emergency service focus on the accuracy of the positioning system, other commercial and third party require less accurate positioning. In this work, we have focused on the development of pure software-based solutions to cellular positioning which takes advantage of the availability of signal strength measurements. The main advantage of using RSS rather than timing measurements is to overcome the need for synchronisation between base stations. In this thesis, we demonstrated through experimental evaluation that RSS-based static positioning can be performed using an Extended Kalman Filter model, and also, that Simultaneous Localisation And Mapping can be applied in the cellular positioning framework. The static EKF positioning system and the Constrained Cellular SLAM system were proposed in this thesis in Chapter 3 and Chapter 4 respectively. In order to evaluate their performance in real-world positioning trials, the proposed systems were designed and implemented as mobile software applications, which were referred to as the 'GSM Mobile Locator' and the 'CCS Application'. The design of these mobile applications was outlined in Chapter 5 while the experimental evaluation of the systems they implement was presented in Chapter 6.

7.1 The Static EKF Positioning System

The static EKF model described in Chapter 3 has been evaluated by conducting experiments in the same trial areas that have been surveyed to calibrate the adopted RSS-based propagation model. As reported in Section 6.4, 27 positioning trials were performed in 3 urban areas and 4 suburban areas. The static positioning trials were conducted using a network engineering tool to monitor the Network Measurement Report and the GSM Mobile Locator application to perform the positioning process. RSS measurements are entered in the application individually in order to operate the EKF algorithm sequentially and record the position estimate at each iteration.

In the Author's previous work [Ham06], a static EKF model was presented and the positioning outcomes were evaluated according to the generic propagation model that was used to convert RSS measurements to BTS-mobile terminal distance relationships. In this thesis, a new approach of extracting bearing measurements from BTS sectorisation information has been developed in order to extend the observation model to take into account bearing information. It has been demonstrated in Section 6.3 that adopting a range-bearing observation model leads to higher accuracies than adopting a range-only model.

Moreover, the use of a calibrated RSS model in the same area as the experimental setup improves the accuracy of the positioning process as opposed to using the Walfish-Ikegami model, which produced the most accurate positioning results among the other generic propagation models surveyed in [Ham06]. Furthermore, the accuracy improvement resulting from integrating bearing measurements into the EKF system is more important when the

calibrated propagation model is used to link the mobile state to the RSS measurement, as opposed to using the path loss equation of the WI model.

The static positioning trial results reported in Section 6.4 confirmed the impact on accuracy of the geometric dilution of precision (GDOP) and the number of reference base stations. Moreover, the results indicate that the goodness of the propagation model fitting process also affects the positioning outcome in similar environments. How well the model is fitted was defined using the RSS error standard deviation resulting from the calibration process. In fact, it was noticed that the goodness of the fit affected the positioning outcome in trials conducted in suburban areas of similar size.

Compared to U-TDOA and A-GPS results of real-life E-911 trials, our positioning results obtained using range-bearing EKF and the calibrated propagation model produced more accurate results. However, the accuracy of the A-GPS/AFLT combination in synchronised CDMA networks could not be matched by the proposed method. This was expected as time based methods in accurately synchronised networks outperforms RSS-based methods. Our static EKF system was therefore evaluated against another RSS-based and self-positioning method known as the Database Correlation Method, which has been applied in cellular positioning for the first time by Laitinen et Al [Lai01]. Compared to DCM, the proposed static EKF method is more accurate in suburban environments. One can argue that the fingerprinting process conducted as part of the data collection stage of DCM is more extensive in urban environments and thus produces high resolution fingerprint maps. In fact, the positioning accuracy achieved in the online estimation stage of DCM strongly depends on the size and resolution of the fingerprinting database. In addition to the availability of RSS measurements, another advantage of using DCM as a cellular positioning method is the fact

that it does not rely on a priori knowledge of base station locations. This is because the fingerprinting process in the offline stage produces all the required data for position estimation during the online stage.

7.2 The Constrained Cellular SLAM System

With the emergence of smartphones able to display maps and retrieve information based on the location of the user, the LBS community grew rapidly as they are given means to develop their own LBS applications. Many of these applications use databases of the WLAN access points and cellular base stations to complement GPS which has limited use indoors or in dense urban areas. Similarly to DCM, these databases are constructed using location fingerprinting. These LBS applications are available to smartphone with Wi-Fi connectivity and not available to basic feature phones. Moreover, third-party LBS developers have the choice of either using commercial databases which can be costly to obtain or using third-party databases collected by smartphone users themselves and are thus deemed unreliable.

The Constrained Cellular SLAM (CCS) methodology presented in Chapter 4 bears a similarity with DCM as it adopts the fingerprinting concept to overcome the need for a priori BTS location information. CCS extends this advantage by estimating the locations of base stations during the offline fingerprinting stage which will improve the position estimate during the online positioning stage. Therefore, CCS allows third-party developers to build their own map of base stations for use as reference location information required in LBS application development. Moreover, the CCS methodology is designed for low-cost mobile phones, which are still sold in higher numbers than state-of-the-art smartphones.

The Constrained Cellular SLAM system represents the main contribution of this thesis as SLAM has not previously been applied for cellular positioning. Some Visual-SLAM applications in the literature, such as [Kle09], used the built-in camera of mobile phones for mapping the environment, however, such applications should not be categorised within cellular positioning methods as they are not based on radiolocation. In fact, the location estimation process in Visual-SLAM applications that use camera phones do not take measurements on RF signals transmitted from cellular network base stations, which is fundamental in the definition of cellular positioning provided in this thesis. However, other RSS-based SLAM applications exist. They are classified as range-only SLAM approaches and have been developed for RFID and WSN applications. To the best of our knowledge, none of the range-only SLAM applications in the literature were used within the cellular positioning framework.

Our CCS approach has been designed to achieve autonomous cellular positioning for low-cost mobile phones without access to dead reckoning measurements. As described in Chapter 2, conventional feature-based SLAM approaches in the robotics literature rely on internal dead reckoning measurements to obtain knowledge on the robot's motion. External measurements relative to features in the environment are then used to initialise and update the locations of the observed features and thus build a map of the environment. Since dead reckoning measurements are not available to low-cost mobile phones, the proposed cellular SLAM system must rely on GPS in order to obtain information on the motion of the mobile which is necessary to build the map of the environment. Since GPS is an accurate self-

positioning method on its own, it should only be used during an initial data collection phase similar to that of Database Correlation Methods and RSS fingerprinting methods[28]. As a result, the estimation of the mobile position using cellular network observations, which is at the heart of any cellular positioning method, is delayed after the offline data collection phase. Therefore, in order to apply SLAM in this constrained cellular framework, the localisation of the target mobile has to be performed after an initial mapping task. In this thesis, we referred to the offline map building phase and the online cellular positioning stage as the Initial Mapping Stage (IMS) and Network Localisation Stage (NLS) respectively.

The IMS employed an EKF algorithm referred to as the BTS Initialisation Model (BIM) to estimate the position of the target BTS using GPS samples taken from the mobile terminal and the signal strength measurements during the IMS survey. Each GPS sample is linked to a RSS measurement to form the so-called fingerprint. Each collected fingerprint is associated with the initialised landmark estimate at the end of the IMS survey to produce a BTS Landmark Entry (BLE). As a result, the outcome of the IMS is a database of BLE's representing the initial map of the GSM network, which will be used as reference during the NLS. In order to compensate for the lack of dead reckoning measurements during the Network Localisation Stage, the fingerprints collected as part of the initial map of base stations are used by the EKF-SLAM process to predict the motion of the mobile terminal. The EKF-SLAM algorithm then receives new RSS measurements and associates them to existing landmarks within the map to integrate the newly observed landmarks into the map

[28] Unlike these DCM and other fingerprinting methods which construct a database of location-RSS fingerprints, the data collection phase of the CCS methodology is conducted to build a map of base stations, in which each BTS entry includes a list of mobile location-RSS tuples representing the fingerprints.

augmented state vector (SLAM state). The EKF update stage can then use the measurements to update the estimate of the mobile terminal state as well as all the landmark state estimates that are part of the augmented SLAM state.

The experimental evaluation of the Constrained Cellular SLAM system has been presented in Section 6.5. Six trials have been conducted using the CCS smartphone application in suburban, urban and mixed environments within areas that have been surveyed to identify base stations for evaluation purposes and to calibrate the propagation model to be used as the observation model for the EKF-SLAM algorithm. The evaluation of landmark initialisation accuracy has been performed at the end of the Initial Mapping Stage for each CCS trial. At the end of the IMS, it was noted that the landmark estimates produced by the BIM do not always converge towards the true BTS positions. In fact, the accuracy of the landmark initialisation strongly depends on the Geometric Dilution of Precision (GDOP) defining the relative geometry between the measured mobile positions and the target BTS. At the end of the NLS of each CCS trial, the mean accuracy of the mobile terminal estimates has been reported which less than 300 metres. As expected, it was noted that positioning accuracy strongly depends on the number of fingerprints collected during the IMS especially in suburban areas. The urban experiments produced results which highlighted the importance of the signal strength measurement resolution. As it defines the individuality of fingerprints, the RSS resolution affects the performance of the database correlation algorithm employed to extract fingerprints from the database and thus affects the positioning accuracy.

Finally, the mean accuracy of CCS trials was evaluated against the cellular positioning methods which were standardised for E-911 positioning. The reported accuracy outperformed A-GPS results reported in real life E-911 trials conducted within 3G UMTS

networks but could not match that of A-FLT/A-GPS trials within CDMA networks. Therefore, we can conclude that a Cellular SLAM method is not only feasible for implementation as a software application for low-cost smartphones but also can achieve positioning results that can be more accurate than A-GPS. We can also deduce that the Constrained Cellular SLAM can achieve higher accuracies than the reported mean accuracy of 300 m if a high resolution map of fingerprints is constructed during the Initial Mapping Stage. The map should be not only large in terms of the number of fingerprints but should also be characterised by a high individuality of fingerprint RSS measurements as well as a high GDOP associated with the relative geometry between the fingerprint locations and the true locations of base stations.

7.3 Prospective Work

As far as the static positioning system is concerned, a prospective work consists of the application of the system in indoor environments. Further experimentation is required in order to evaluate the performance of the system indoors and compare the results with WLAN localisation systems. The GSM Mobile Locator application can also be modified for deployment on new smartphones that are able to monitor the network measurement report and thus overcome the need to use a separate network monitoring tool. Moreover, the application would become more attractive to the user because of the intuitive touch screen interface of state-of-the-art smartphones.

The lack of dead reckoning measurements represents the main observational constraint which prevented the implementation of the full SLAM methodology in the cellular framework. Without this constraint, a conventional EKF-SLAM approach can be applied to achieve autonomous cellular positioning. Therefore, the proposed cellular SLAM

methodology can be improved to exploit the capability of state of the art smartphones, which are equipped with built-in accelerometers and gyroscopes. Dead reckoning measurements would be retrieved by the smartphone application implementing the system in order to be used in the prediction stage of the EKF-SLAM process. Moreover, the performance of the EKF-SLAM update stage can be improved by obtaining measurements relative to more than one BTS from a single mobile position. In order to enable multiple RSS measurements, the mobile platform on which the smartphone application is deployed would need to provide the developer with the software development kits required to access the Network Measurement Report. By exploiting the connectivity of state-of-the-art smartphone, the methodology can also be extended to combine WLAN and cellular positioning in one application. Furthermore, a method based on Visual-SLAM can be developed to extend the scope of the cellular positioning framework. In addition to BTS locations initialised using RSS measurements, the camera of the smartphone could be used to identify and extract other features from the environment such as streets and buildings.

REFERENCES

[Abi05] Kenneth Hyers, "Location Based Services-Analysis of Carrier Spending, Subscribers Devices, and Application for Handset-Based and Telematics Services", ABI Research, 2005.

[Abi11] Dominique Bonte, Kevin Burden, "Trueposition Whitepaper", Research report, ABI Research, July 14, 2011.

[Alh06] Mona Al Hallak, Dr.Mohamed Said Safadi, "Mobile Positioning Technique Using Signal Strength Measurement method with the aid of Passive Mobile Listener Grid'', IEEE Information and Communication Technologies, 2006.

[And06] Ian Anderson, Henk Muller, "Exploring GSM Signal Strength Levels in Pervasive Environments'', Proceeding of the 20th International Conference Information Networking and Appliances (AINA'06), IEEE 2006.

[Aup06] Andreu Urruela Planas, " Signal Processing Techniques for Wireless Locationing", PhD Thesis, Technical University of Catalonia, April 2006.

[Bai02] Tim Bailey, "Mobile Robot Localisation and Mapping in Extensive Outdoor Environments", PhD Thesis, Australian Centre for Field Robotics, Department of Aerospace, Mechanical and Mechatronic Engineering, The University of Sydney, August 2002.

[Ban91] K.M. Banks, "Datatrak: Automatic Vehicle Location System in Operational Use in the UK", Vehicle Navigation and Information Systems Conference, IEEE, 1991

[Bau06] J.Baumann, D.Zimmermann, M.Layh, F.M.Landstorfer, "Accuracy Estimation of Location Determination Based on Database Correlation", Vehicular Technology Conference, IEEE 2006.

[Bil06] Olof Billstrom, Lars Cederquist, Magnus Ewerbring, Ggunnar Sandergren and Jan Uddenfeldt, "Fifty Years With Mobile Phones From Novelty to no.1 Consumer Product ", Ericsson Review No.3,2006.

[Bla02] Nathan Blaunstein, J. Bach Andersen, "Multipath Phenomena in Cellular Networks", Artech House, 2002.

[Bul09] Jeffery F. Bull, "Wireless Geolocation –Advantages and Disadvantages of the Two Basic Approches for E-911'', IEEE Vehicular Technology Magazine 2009.

[But11] Margaret Butler, "Android: Changing the Mobile Landscape", Pervasive Computing, Volume 10, IEEE, 2011.

[Caf98] James j. Caferry, Jr . and Gordon L. Stuber , "Overview of Radiolocation in CDMA Cellular Systems'', IEEE Communication Magazine, April 2005.

[Che10] Xun Chen, Z. Jane Wang, "Reliable Indoor Location Sensing Technique Using Active RFID", 2nd International Conference on Industrial Mechatronics and Automation, 2010.

[Cso97] Michael Csorba, "Simultaneous Localisation and Map Building", PhD Thesis, University of Oxford, 1997.

[Dju05] Joseph Djugash, Sanjiv Singh, George Kantor and Wei Zhang, "Range-Only SLAM for Robots Operating Cooperatively with Sensor Networks" IEEE International Conference on Robotics and Automation, May, 2006, pp. 2078 - 2084.

[Dju08] Joseph Djugash, and Sanjiv Singh, "A Robust Method of Localization and Mapping Using Only Range". International Symposium on Experimental Robotics, July, 2008.

[Dis01] M. W. M. Gamini Dissanayake, Paul Newman, Steven Clark, Hugh f .Durrant-Whyte, M. Csorba, "A Solotion to the Stimultaneous Localization and Map Building (SLAM) Problem'', IEEE Transactions on Robotics and Automation,Vol. 17, NO. 3, June2001.

[Dra98] Christopher Drane, Malcolm Macnaughtan, and Craig Scott, "Positioning GSM Telephones'', IEEE Communication Magazine, April 1998.

[Duf96] P. J. Duffett-Smith, "High Precision CURSOR and Digital CURSOR: the real alternatives to GPS", Landnav Proceedings, 1996.

[Dur06] Hugh Durrant-Whyte, Fellow, Tim Bailey, "Simultaneous Localisation and Mapping (SLAM): Part I The Essential Algorithms", Robotics and Automation Magazine, June 2006.

[Far05] Tom Farley , "Mobile Telephone History'', Telectronik, 2005.

[Fig10] João Figueiras, Simone Frattasi, “Mobile Positioning and Tracking: From Conventional to Cooperative Techniques”, Wiley, 2010.

[Fig69] W. G. Figel and N.H. Shepherd, “Vehicle Location by a Signal Attenuation Method”, IEEE Vehicular Technology Conference, San Francisco, 1969.

[Fil11] R. Filjar, K. Vidovic, P. Britvic and M. Rimac, “eCall: Automatic notification of a road traffic accident”, Proceedings of the 34th International Convention, MIPRO, 2011.

[Fre10] Richard h. Frenkiel, “Creating Cellular: A History of The Amps Project (1971–1983)”, IEEE Communications Magazine, September 2010.

[Gui02] Jose E. Guivant, “Efficient Simultaneous Localization and Mapping in Large Environement” ,PhD Thesis, the University of Sydney,2002.

[Gul03] Ranjay Gulati, Mohanbir S. Sawhney, Anthony Paoni, “Kellogg on Technology & Innovation”. John Wiley & Sons, Hoboken, New Jersey, 2003.

[Gus05] Fredrik Gustafsson , Fredrik Gunarsson, “Mobile Positioning Using Wireless Networks’’, IEEE Signal Processing Magazine, July 2005.

[GXu03] Guochang Xu, “GPS: Theory, Algorithms and Applications”, Springer, 2003.

[Ham06] S.Hamani and M.Oussalah, “Mobile Location System using Netmonitor and Mappoint Server”, PG Net 2006 Proceedings, the 6th annual Postgraduate Symposium on The Convergence of Telecommunications, Networking & Broadcasting, Liverpool John Moores University, 26-27 June 2006.

[Ham07] S.Hamani, M.Oussalah and P.Hall, “Combination of GSM and GPS signals for Mobile Positioning and Location Service Using Kalman Filter”, World Congress of Engineering 2007, Imperial College, London 2-4 July 2007.

[Ham08] S.Hamani, M.Oussalah and P.Hall, “GSM Mobile Positioning Using Kalman Filter For Sector Antennas”, IEEE SMC UK & Ireland Chapter Conference, London 7-8 September 2008.

[Ham09] S.Hamani and M.Oussalah, “SLAM Based Approach for Mobile Positioning”, , IEEE Systems, Man & Cybernetics Society UK-RI Chapter Conference 2009, The University Of Birmingham, 9-10 September 2009.

[Has91] Homayoun Hashemi, “Pulse Ranging Radiolocation Technique And Its Application To Channel Assignment In Digital Cellular Radio”, 41st IEEE Vehicular Technology Conference, Gateway to the Future Technology in Motion, 1991.

[Hel99] Martin Hellebrandt ,Rudolf Mathar, “Location Tracking of Mobiles in Cellular Radio Networks”, IEEE Transactions on Vehicular Technology , VOL.48, NO.5, September 1999.

[Hil00] Oliver Hilsenrath, Mati Wax, “Radio Transmitter Location Finding For Wireless Communication Network Services And Management”, US Patent 6026304, 15 February 2000.

[Hub09] Denis Huber, “Background Positioning for Mobile Devices - Android vs. iPhone” Joint Conference of IEEE computer & communication Socities, 2011.

[Kae05] Kamol Kaemarungsi, “Design of Indoor Positioning Systems Based on Location Fingerprinting Technique”. PhD thesis, University of Pittsburgh, 2005.

[Kan02] George Kantor, Sanjiv Singh, “Preliminary Results in Range-Only Localization and Mapping”, International Conference on Robotics 8 Automation, IEEE 2002.

[Keh06] Ath. Kehagias, J. Djugash, S. Singh, “Range-Only SLAM with Interpolated Range Data”, tech. report CMU-RI-TR-06-26, Robotics Institute, Carnegie Mellon University, May, 2006.

[Kim04] SungJoon Kim, “Efficient Simultaneous Localisation and Mapping - Algorithms using Submap Networks”, PhD Thesis, Massachsetts Institue Of Technology, June 2004.

[Kle09] Georg Klein, David Murray, “Parallel Tracking and Mapping on a Camera Phone”, 8th IEEE International Symposium on Mixed and Augmented Reality 2009 (ISMAR 2009), 19-22 Oct. 2009.

[Kos00] Hiroaki Koshima, Joseph Hoshen. “Personal locator Services Emerge”, IEEE Spectrum February 2000.

[Kup05] Axel Kupper, "Location-based Services Fundamentals and Operation'', WILEY, 2005.

[Kur04] Derek Kurth, "Range-Only Robot Localization and SLAM with Radio", CMU-RI-TR-04-29, May 2004.

[Lai01]Heikki Laitinen,Jaakko Lahteenmaki,Tero Nordstrom, "Database Correlation Method for GSM Location", IEEE Vehicular Technology Conference, 2001 .

[Lai07] Heikki Laitinen, Suvi Juurakko, Timo Lahti, Risto Korhonen, and Jaakko Lahteenmaki, "Experimental Evaluation of Location Methods Based on Signal-Stength Measurments", IEEE Transactions on Vehicular Technology ,VOL.56, NO.1, January 2007.

[Lau07] Erin-Ee-Lin-Lau,Wan-Young Chung, "Enhansed RSSI-based Real-time User Location Tracking System for Indoor and Outdoor Environments", International Conference on Convergence Information Technology, 2007.

[Leb96] Frederick LeBlan, "System and method for updating a location databank", US Patent 5570412, October 29, 1996.

[Lin05] Ding-Bing Lin, Member, IEEE, and Rong-Terng Juang, "Mobile Location Estimation Based on Differences of Signal Attentions For GSM Systems'', IEEE Transactions on Vehicular Technology, July 2005.

[Lop99] L Lopes, E Villier and B Ludden, "GSM Standards Activity on Location'', The Institute of Electrical Engineers, 1999.

[Men09] Emanuele Menegatti, Andrea Zanella, Stefano Zilli, Fancesco Zorci, Enrico Pagello, "Range-only SLAM with a Mobile Robot and a Wireless Sensor Networks", IEEE International Conference on Robotics and Automation, 2009.

[Mer10] L. Merino, F. Caballero and A. Ollero, "Active Sensing for Range-Only Mapping Using Multiple Hypothesis", The 2010 IEEE/RSJ International Conference on Intelligent Robots and Systems, Taipei, Taiwan, October 18-22, 2010.

[Mkc04] Kenneth M.K. Chu, Karl R.P.Leung, Joseph Kee-Yin Ng, Chun Hung Li, "Locating Mobile Stations With Statistical Directions Propagation Model'', Proceeding of the 18th

International Conference on Advanced Information Networking and Application (AINA'04), IEEE 2004.

[Mot01] Motorola Inc, "Overview of 2G LCS Technologies and Standards", 3GPP Workshop TSG SA2 LCS, London, January 2001.

[Mut09] Kavitha Muthukrishnan, "Multimodal Localisation". PhD Thesis, University of Twenty, 2009.

[New03] P. Newman, J. Leonard, "Pure Range-Only SubSea SLAM", proceeding of IEEE Conference on Robotics and Automation, 2003.

[New99] Paul Michael Newman, "On The Structure and Solution of the Simultaneous Localisation and Map Building Problem", PhD Thesis, The University of Sydney, March 1999.

[Nyp02] Trond Nypan ,Oddvar Hallingstad, "A Cellular Positioning System Based on Database Comparison –The Hidden Markov Model Based Estimator Versus the Kalman Filter", 5th Nordic signal processing symposium on board hurtigruten Norway. October 4-7,2002.

[Ofc10] Steve Methley, Chris Davis, Nigel Wall, "Locating Wireless Devices: Methods for locating devices in areas where GPS is unavailable - Final report", Ofcom, May 2010.

[Ofc12] Mobile Phone Base Station Database, Ofcom, Independent regulator and competition authority for the UK communications industries, URL: http://www.sitefinder.ofcom.org.uk.

[Ols04] Edwin Olson, John Leonard, and Seth Teller, "Robust Range-Only Beacon Localization", IEEE journal of oceanic engineering.oct 2006.

[Pat05] Pubudu N Pathirana Nirupama Bulusu Andrey, V Savkin, Sanjay Jha, "Node Localization Using Mobile Robots in Delay-Tolerant Sensor Networks", IEEE Transactions On Mobile Computing, 2005.

[Pat91] I.J. Paton, E.W Crompton, J.G. Gardiner, J.M. Noras, "Terminal Self-Location In Mobile Radio Systems ", Sixth International Conference on Mobile Radio and Personal Communications, 1991.

[Per09] Tommi Perala, Simo Ali-Loytty and Robert Piche, " A Comparative Survey of WLAN Location Fingerprinting Methods", Proceeding of The 6th Workshop on Positioning , Navigation and Communication ,2009.

[Rap96] T. S. Rappaport, J . H. Reed, and B. D. Woerner, " Position Location Using Wireless Communications on Highways of the Future'', IEEE Communication Magazine, October 1996.

[Rit77] Stephen Riter, "Automatic Vehicle Location – An Overview", IEEE Transactions On Vehicular Technology, vol. vt-26, no. 1, February 1977.

[Sag93] Willian E. Sagey, "Cellular Telephone Service Using Spread Spectrum Transmission", US Patent, no 52186188, Jun , 1993.

[Sau07] Simon R. Saunders, Alejandro Aragon-Zavala, ''Antennas and Propagation for Wireless Communication Systems'', WILEY 2007.

[SCC90] R. Smith, M. Self, and P. Cheeseman, "Estimating Uncertain Spatial Relationships

in Robotics", Autonomous Robot Vehicles, Springer Verlag, 1990.

[Sco93] Tony Scorer, "Vehicle Location and Fleet Management Systems", IEE Colloquium on Date of Conference, 8 Jun 1993.

[Sch04] Jochen H. Schiller, Agnès Voisard, "Location-Based Services", Elsevier, 2004.

[She10] Sidney Shek, "Next-generation Location-based Services for Mobile Devices", CSC Grants, February 2010.

[She91] Eliezer A. Sheffer, "Vehicle Location System", United States Patent, no 5055851, Oct 8, 1991.

[Sil96] Marko I. Silventoinen and Tim0 Rantalainen, "Mobile Station Emergency Locating in GSM", ICPWC, IEEE, 1996.

[Sir07] Niilo Sirola, "Mathematical Methods for Personal Positioning and Navigation", PhD Thesis, Tampere University of Technology, October 2007.

[Sol00] Samir Soliman , Parag Agashe, Ivan Fernandez, Alkinoos Vayanos, Peter Gaal and Milan Olijaca, "A Hybrid Position Location System'', IEEE Sixth International Symposium on Spread Spectrum Techniques and Applications ,2000.

[Son94] Han-Lee Song, "Automatic Vehicle Location in Cellular Communications Systems", IEEE Transactions On Vehicular Technology, vol. 43, no. 4, November 1994.

[SSC90] R. Smith, M. Self, and P. Cheeseman. "Estimating uncertain spatial relationships in robotics", Autonomous Robot Vehicles, pages 167-193, Springer-Verlag, 1990.

[Sva90] S.C. Svales, M.A. Beach, "Direction Finding In The Cellular Land Mobile Radio Environment", Fifth International Conference on Radio Receivers and Associated Systems, 23-27 Jul 1990.

[Swa90] S.C. Swales, M.A. Beach, "Direction Finding in the Cellular Land Mobile Radio Environment", Fifth International Conference on Radio Receivers and Associated Systems, 1989.

[Swa99] S.C. Swales, J.E. Maloney, J.O. Stevenson, "Locating Mobile Phones & The Us Wireless E-91i Mandate", The Institute of Electrical Engineers, London, 1999.

[Tak07] Claude Takenga, Tao Peng, kyandoghere Kyamakya, "Post-processing of Fingerprint Localisation Using Kalman Filter and Map-matching Techniques", The 9th International Conference on Advanced Communication Technology ,2007.

[Tay05] Mayank Tayal, "Location Services in the GSM and UMTS Networks", IEEE International Conference on Personal Wireless Communications, 2005.

[Vak11] Michael Vakulenko, Stijn Schuermans, Andreas Constantinou, Matos Kapetanakis, "Mobile Platforms: The Clash of Ecosystems", Vision Mobile, November 2011.

[Van05] Arnold-Kees Van Rongen, "The Necessity For An EU-Wide 112 Emergency Wireless Location Service", European Journal Of Navigation, Volume 3, Number 4, 2005.

[Vau09] S.J. Vaughan-Nichols, "Will Mobile Computing's Future Be Location, Location, Location?", Computing & Processing, Volume 42, p14-p17, IEEE Computer Society, 2009.

[Ven04] Saipradeep Venkatraman, "Wireless Location In Non-Line-Of-Sight Environments", PhD Thesis, Department of Electrical and Computer Engineering and Computer Science, The University of Cincinnati, 2004.

[Wan00] S. S. (Peter) Wang, Marilynn Green, and Maged Malkawi, "E-911 Location Standards and Location Commercial Services", Emerging Technologies Symposium: Broadband, Wireless Internet Access, IEEE, 2000.

[Wan06] Wei Wang, Yanling Hao and Bing Xue, " Study on Positioning Algorithm For Navigation Signal Based on Improved Kalman Filter'', International Conference on Manchester and Automation Proceeding of the IEEE,2006.

[Web99] John G. Webster, "The Measurement, Instrumentation, and Sensors Handbook", Springer, 1999.

[Wei03] Anthony J. Weiss, "On The Accuracy of a Cellular Location System Based on RSS Measurements'', IEEE Transactions on Vehicular Technology, VOL.52, NO. 6, November 2003.

[Wij08] Pushpika Wijesinghe,Dileeka Dias, "Novel Approach for RSS Calibration in DCM-Based Mobile Positioning using Propagation Models", 4th International Conference on Information and Automation for Sustainability, 2008.

[Wil01] Stefan Bernard Williams, "Efficient Solutions to Autonomous Mapping and Navigation Problems", PhD Thesis, The University of Sydney, September 2001.

[Win11] Beth Winkowski, "HopStop Adds Skyhook Location Technology To Android App", Skyhook Wireless Press, July 14, 2011.

[Zan09] Paul A Zandbergen, "Accuracy of IPhone Locations: A Comparison of Assisted GPS, WiFi and Cellular Positioning", Transactions in GIS Volume 13, Issue Supplement 1s, pages 5–25, June 2009.

[Zha00] Yilin Zhao, "Mobile Phone Location Determination and Its Impact on Intelligent Transportation Systems", IEEE Transactions on Intelligent Transportation Systems,Vol.1, No.1, March 2000.